SKB

TECHNICAL REPORT 94-03

Reassessment of seismic reflection data from the Finnsjön study site and prospectives for future surveys

Calin Cosma[1], Christopher Juhlin[2], Olle Olsson[3]

1 Vibrometric Oy, Helsinki, Finland
2 Section for Solid Earth Physics, Department of Geophysics, Uppsala University, Sweden
3 Conterra AB, Uppsala, Sweden

February 1994

SVENSK KÄRNBRÄNSLEHANTERING AB
SWEDISH NUCLEAR FUEL AND WASTE MANAGEMENT CO
BOX 5864 S-102 40 STOCKHOLM
TEL. 08-665 28 00 TELEX 13108 SKB S
TELEFAX 08-661 57 19

REASSESSMENT OF SEISMIC REFLECTION DATA FROM THE FINNSJÖN STUDY SITE AND PROSPECTIVES FOR FUTURE SURVEYS

Calin Cosma[1], Christopher Juhlin[2], Olle Olsson[3]

1 Vibrometric Oy, Helsinki, Finland
2 Section for Solid Earth Physics, Department of Geophysics, Uppsala University, Sweden
3 Conterra AB, Uppsala, Sweden

February 1994

REASSESSMENT OF SEISMIC REFLECTION DATA FROM THE FINNSJÖN STUDY SITE AND PROSPECTIVES FOR FUTURE SURVEYS

FEBRUARY 1994

CALIN COSMA
VIBROMETRIC OY
HELSINKI, FINLAND

CHRISTOPHER JUHLIN
SECTION FOR SOLID EARTH PHYSICS
DEPARTMENT OF GEOPHYSICS
UPPSALA UNIVERSITY, SWEDEN

OLLE OLSSON
CONTERRA AB
UPPSALA, SWEDEN

ABSTRACT (English)

Reprocessing of data from the seismic reflection survey performed at Finnsjön in 1987 show that reflection seismics is a viable technique for mapping fracture zones in crystalline rock. Application of state of the art processing algorithms clearly image a gently dipping fracture zone located in the depth interval 200-400 m. In addition, several other reflectors were imaged in the reprocessed section, both gently and steeply dipping ones. Correlations with borehole data indicate that the origin of these reflections are also fracture zones. The data acquisition procedures used at the Finnsjön survey were basically sound and could, with minor modifications, be applied at other sites. The results indicate that both sources and receivers in future surveys should be placed in boreholes a few meters below the ground surface.

Keywords: seismic reflection, fracture zone, static corrections, Image Point Transform, velocity analysis, migration.

ABSTRACT (Swedish)

Omprocessering av data från en seismisk reflektionsmätning utförd i Finnsjön 1987 har visat att reflektionsseismik är en användbar teknik för att lokalisera sprickzoner i kristallint berg. En svagt lutande sprickzon på 200-400 m djup avbildades tydligt genom användning av moderna processeringsalgoritmer. Ytterligare reflektorer kunde identifieras i seismogrammet, både med flacka och branta stupningar. Jämförelse med borrhålsdata visade att dessa reflektioner också orsakats av sprickzoner. Den teknik som använts vid insamlingen av data i Finnsjön har visat sig vara i grunden riktig och kan med mindre ändringar användas också på andra platser. Resultaten visar att både signalkällor och mottagare bör placeras i borrhål några meter under markytan.

SUMMARY AND CONCLUSIONS

In 1987 the Swedish Nuclear Fuel and Waste Management Co (SKB) funded shooting of a 1.7 m long high resolution profile over the Finnsjön study site. The site is located approximately 140 km North of Stockholm and the host rocks are mainly granodioritic.

Data were collected using a SERCEL 348 telemetry system. Field parameters included 10 m shot and geophone spacing, with 100 m near offset and 60 channels recorded per shot. A total of 151 shots were fired, most of them in holes drilled down to bedrock.

One of the objectives of the profile was to image a known fracture zone with high hydraulic conductivity dipping gently to the West at depths of 100 to 400 m. The initial processing of the data failed to image this fracture zone. However, a steeply dipping reflector was imaged indicating that the field data were of adequate quality and that the problem lay in the processing. These data have now been reprocessed by two different groups, Uppsala University and Vibrometric OY, using two different approaches. Both approaches resulted in clear images of the fracture zone in the depth interval 200-400 m. In addition, several other reflectors were imaged in the reprocessed sections, both gentle and steeply dipping ones. Correlations with borehole data indicate that the origin of these reflections are also fracture zones.

The main reason for failure of the initial processing was that geophone static corrections were not applied. Seismic wavelengths of the signal correspond to about 10 ms cycles (50 m) which are on the same order as the corrections applied using refraction statics in the reprocessed data. Under these conditions, destructive interference will be common when stacking the data.

A study has also been made to evaluate what factors control data quality in crystalline rock environments and how a survey could be optimized with respect to data quality and cost. Based on this study it is clear that sources and receivers should be placed in boreholes reaching a few meters below the water table or a few meters down into bedrock. Explosives detonated in the boreholes are the preferred source. Vertical component geophones placed in boreholes should be used as receivers. It is considered most efficient to drill the boreholes required for the survey in advance of any data acquisition.

Data should be collected using an end-on spread where the boreholes are first used for geophones and then for shots. This procedure will minimize the number of boreholes required.

Data recording should be done with a system with a dynamic range of at least 16 bits. The recommended number of channels for a 10 m geophone spacing is 96.

Data collected along a main survey line will provide a two-dimensional image of the geologic features present along the line. To obtain information on the dip and strike of these features it is necessary to collect additional data which provide some three-dimensional information. This is done most cost effectively by placing geophones along short cross-lines perpendicular to the main survey line at regular intervals (e.g. every 500 m). The length of the cross-lines should be about 230 m.

If a target area for detailed investigations has been identified it is feasible to perform a full 3-D survey over a limited area (500 x 500 m) at a reasonable cost. A total of 250 shotpoints and geophone points will give good coverage.

Application of seismic reflection surveys at potential deep repository sites is recommended to start by measuring two perpendicular lines, crossing approximately in the center of the site. The length of each line is tentatively set to 4 km. The survey should include recording of short cross-lines to provide information on dip and strike of the identified reflectors. Regional geology and airborne geophysics will provide the necessary information for positioning the lines.

Finally we conclude that the reprocessing of the Finnsjön data and the subsequent analyses show that reflection seismics is a viable technique for mapping fracture zones in crystalline rock. The data acquisition procedures used at the Finnsjön survey were basically sound and could, with minor modifications, be applied at other sites. The results indicate that both sources and receivers in future surveys should be placed in boreholes a few meters below the ground surface.

CONTENTS

		Page
	ABSTRACT (English)	i
	ABSTRACT (Swedish)	i
	SUMMARY AND CONCLUSIONS	ii
	CONTENTS	iv
	LIST OF FIGURES	vii
	LIST OF TABLES	xi
1	INTRODUCTION	1
1.1	BACKGROUND	1
1.2	EXAMPLES OF SEISMIC SURVEYS IN CRYSTALLINE ROCK	2
1.3	OBJECTIVES AND PROJECT OUTLINE	3
2	THE FINNSJÖN STUDY SITE	4
3	DATA ACQUISITION	8
4	REPROCESSING BY UPPSALA UNIVERSITY	9
4.1	PROCESSING SEQUENCE	9
4.2	CRITICAL PROCESSING STEPS	15
4.2.1	Comparison with earlier processing	15
4.2.2	Quality control	21
5	REPROCESSING BY VIBROMETRIC OY	22
5.1	BACKGROUND	22
5.2	PRELIMINARY PROCESSING	22
5.3	STACKING	32
5.4	PRE-STACK MIGRATION	32
5.5	TAU-P FILTERING OF THE STACKED PROFILES	32
6	DISCUSSION ON REPROCESSING	39
6.1	COMPARISON OF PROCESSING RESULTS	39
6.2	SIMULATION OF OTHER FIELD PARAMETERS	42
6.3	REFLECTION PROPERTIES OF FRACTURE ZONES	46
6.4	ANISOTROPY CONSIDERATIONS	50

6.5	BOREHOLE SEISMIC DATA FROM FINNSJÖN	50
7	COMPARISON WITH GEOLOGIC INFORMATION	54
7.1	FRACTURE ZONE 2	54
7.2	DEEPER ZONES	56
7.3	MIGRATION VELOCITY	56
8	GEOPHONE AND SHOT COUPLING ANALYSIS	57
8.1	INTRODUCTION	57
8.2	DATA PROCESSING	57
8.2.1	Theory	57
8.2.2	Parameters	58
8.3	RESULTS AND DISCUSSION	59
8.3.1	Charge profile	59
8.3.2	Shot response	59
8.3.3	Geophone response	64
8.3.4	Frequency response	67
8.3.5	Estimating the attenuation factor, Q	71
9	THEORETICAL STUDIES OF FIELD PROCEDURES	73
9.1	INTRODUCTION	73
9.2	MODELLING	74
9.2.1	Model layout	74
9.2.2	Discussion of modelling results	75
9.2.3	Receiver arrays	82
9.3	SEISMIC SOURCES	84
9.3.1	Explosive sources	84
9.3.2	Measuring while drilling	84
9.3.3	Other sources	85
10	3-D DATA ACQUISITION	86
10.1	3-D ACQUISITION IN GENERAL	86
10.2	APPLICATIONS IN COAL PRODUCTION	86
10.3	OTHER 3-D OPERATIONS	87
10.4	BASIC ACQUISITION STRATEGY	87
10.5	POTENTIAL EXAMPLE FOR AN SKB STUDY SITE	92
10.5.1	Acquisition parameters	92
10.5.2	Time and cost considerations	92
10.6	BASIC PROCESSING STRATEGY	93

11	PROPOSED APPLICATION OF SEISMIC REFLECTION SURVEYS AT SKB STUDY SITES	94
11.1	LIMITED 3-D SURVEY	94
11.2	COST CONSIDERATIONS	95
12	CONCLUSIONS	99
12.1	RECOMMENDATIONS FOR SEISMIC SURVEYS IN CRYSTALLINE ROCK ENVIRONMENTS	99
12.2	A SUGGESTED STRATEGY FOR SITE INVESTIGATIONS	101
	ACKNOWLEDGEMENT	102
	REFERENCES	103
	APPENDICES	106
A	STATIC CORRECTIONS USED BY UPPSALA UNIVERSITY	106
B	VELOCITY FIELD USED BY UPPSALA UNIVERSITY	107
C	SHOT-HOLE DATA	108

LIST OF FIGURES

		Page
Figure 2-1	Location map and major lineaments in the vicinity of the Finnsjön study site (after Ahlbom et al., 1992).	5
Figure 2-2	Profile location and fracture zones in its vicinity. Numbers along the profile refer to station location (multiply by 10 to get the length coordinate used by Vibrometric).	7
Figure 4-1	Shot gather from the beginning of the profile (a) without static corrections and (b) with refraction static corrections.	11
Figure 4-2	Final stack after processing up to point 14 in Table 4-1. Station numbers correspond to those shown in Figure 2-2.	12
Figure 4-3	Final stack in Figure 4-2 after coherency filtering (point 15 in Table 4-1). Station numbers correspond to those shown in Figure 2-2.	13
Figure 4-4	Final stack shown in Figure 4-3 after migration (point 16 in Table 4-1). Station numbers correspond to those shown in Figure 2-2.	14
Figure 4-5	Initial stack using processing parameters given in Table 4-2. Station numbers correspond to those shown in Figure 2-2.	17
Figure 4-6	Same processing as in Figure 4-5 but with a 90 Hz low cut filter before stack. Station numbers correspond to those shown in Figure 2-2.	18
Figure 4-7	Same processing as in Figure 4-6, but using the refraction statics given in Appendix A. Station numbers correspond to those shown in Figure 2-2.	19
Figure 4-8	Same processing as in Figure 4-7, but using the velocity function given in Appendix B. Station numbers correspond to those shown in Figure 2-2.	20
Figure 5-1	Original shot-gather data, record number 60.	25
Figure 5-2	Band-pass filtered shot-gather data, record number 60.	26
Figure 5-3	NMO-corrected and CMP-stacked data section.	27
Figure 5-4	Characteristic shot delays for each shot (record numbers vertically) and each receiver (numbers horizontally).	28
Figure 5-5	Computed characteristic delays for each shot-receiver pair.	29
Figure 5-6	Static corrected and amplitude equalized (AGC) shotgather data.	30
Figure 5-7	Two-way Image Point transformed shotgather data, record number 60.	31
Figure 5-8	NMO-corrected and CMP-stacked data from Image Point processed shotgathers.	33
Figure 5-9	NMO-corrected and CMP-stacked data from amplitude equalized (AGC) and Image Point processed shotgathers.	34
Figure 5-10	Pre-stack migrated shotgather data, record number 60, aperture ±45°, velocity 5500 m/s.	35
Figure 5-11	Stack of migrated shotgathers.	36

Figure 5-12	Tau-P processed CMP stacked data, apparent dips between -25° and +25°.	37
Figure 5-13	Tau-P processed pre-stack migrated data, apparent dips between -25° and +25°.	38
Figure 6-1	Migrated stack obtained after processing by Uppsala University (same as Figure 4-4).	40
Figure 6-2	Final migrated stack obtained after processing by Vibrometric (same as Figure 5-11).	41
Figure 6-3	Similar processing as in Figure 4-3, but including only the first 30 channels. Station numbers correspond to those shown in Figure 2-2.	43
Figure 6-4	Similar processing as in Figure 4-3, but including only channels 31-60. Station numbers correspond to those shown in Figure 2-2.	44
Figure 6-5	Similar processing as in Figure 4-3, but including only every fifth shotpoint. Station numbers correspond to those shown in Figure 2-2.	45
Figure 6-6	a) Velocity model for Zone 2 and b) travel time curves for P and S waves including direct waves and reflections off the top and bottom of the fracture zone.	47
Figure 6-7	(a) P and S wave velocities at intact/fractured interface where Poisson's ration in the fracture zone 0.25, the same as in the intact rock. Density were set 2.65 g/cm^3 and 2.60 g/cm^3 in layer 1 and layer 2, respectively. (b) P and S wave reflection coefficients as a function of angle of incidence for the model in (a). Corresponding channel intervals for angles of incidence are based on the geometry shown in Figure 6-6.	48
Figure 6-8	(a) P and S wave velocities at intact/fractured interface where Poisson's ratio in the fracture zone 0.4, considerably higher than in the intact rock. (Density were set 2.65 g/cc and 2.60 g/cc in layer 1 and layer 2, respectively. (b) P and S wave reflection coefficients as a function of angle of incidence for the model in (a). Corresponding channel intervals for angles of incidence are based on the geometry shown in Figure 6-6.	49
Figure 6-9	Sonic velocity log for borehole BFi02. The upper boundary of Zone 2 is interpreted to be at 204 m.	52
Figure 7-1	Final stack shown in Figure 4-3 after migration (point 16 in Table 4-1). Information about known fracture zones from nearby boreholes have been mapped onto the section.	55
Figure 8-1	a) Bandpass (120-360 Hz) spherical divergence corrected shot gathers before shot scaling has been applied, b) same gathers after application of shot scaling.	60
Figure 8-2	Profile of the shots included in the analyses. The station numbers do not exactly correspond to those given in Sections 3 through 7 since shots were not fired at all stations.	61
Figure 8-3	P and S-wave scaling factors along the profile. A high scaling factor implies a relatively weak shot and a low scaling factor implies a relatively strong shot.	62

Figure 8-4	P-wave scaling factor versus depth into bedrock. A negative depth implies that the shot was fired in the overlying peat or till.	63
Figure 8-5	P-wave scaling factor versus depth.	63
Figure 8-6	S-wave scaling factor versus depth.	64
Figure 8-7	Geophone response scaling factors along the profile and depth of overburden. A high scaling factor implies that the signals recorded are weaker than the average signal level.	65
Figure 8-8	Geophone response scaling factor for P-wave energy versus cover thickness.	66
Figure 8-9	Geophone response scaling factor for S-wave energy versus cover thickness.	66
Figure 8-10	Shots used in the frequency analyses. a) shots fired in bedrock below the water table, and b) shots fired into bedrock above the water table and tamped with sand.	68
Figure 8-11	Shots used in the frequency analyses. a) shots fired at shallow depth (less than or equal to 1 m), and b) shots fired above bedrock.	69
Figure 8-12	Frequency content of shots shown in Figures 8-10 and 8-11 in the P-wave window.	70
Figure 8-13	Frequency content of shots shown in Figures 8-10 and 8-11 in the R-wave window.	70
Figure 8-14	Observed amplitude decay curves (*) of first arrivals and theoretical decay curves for selected values of Q.	72
Figure 9-1	Shot gathers for a) 5 m overburden, shot at 3 m depth, b) 1 m overburden, c) 3 m overburden, d) 5 m overburden, for figures b) through e) shots are placed at ground surface.	77
Figure 9-2	Shot gathers with random noise added for a) 5 m overburden, shot at 3 m depth, b) 1 m overburden, c) 3 m overburden, d) 5 m overburden, e) 10 m overburden, for b) through e) shots placed at ground surface.	78
Figure 9-3	Shot gathers for shots at 3 m depth and a) 1 m overburden, b) 3 m overburden, c) 5 m overburden, and d) 10 m overburden. Normalized traces.	79
Figure 9-4	Shot gathers with random noise added for shots at 3 m depth and a) 1 m overburden, b) 3 m overburden, c) 5 m overburden, and d) 10 m overburden. Normalized traces.	80
Figure 9-5	Shot gathers for 5 m overburden and shot depths of a) 1 m, b) 2 m, c) 3 m, d) 4 m, and e) 6 m. Normalized traces.	81
Figure 9-6	a) Processed data (AGC) with strong surface waves, b) processed data (AGC) with surface converted energy.	82
Figure 9-7	a) Signal from a geophone placed at the bottom of a hole and b) signal from a geophone placed at 3 m depth in the overburden.	83
Figure 10-1	Two shot points, geophone line and corresponding common midpoints. The light squares indicate that no traces have been binned to that area while the dark squares indicate that a trace has been binned to that area.	88

Figure 10-2 Total CDP area that is covered by one shot line and one geophone line. The shaded area comprises a set of darkened squares as shown in Figure 10-1. 89

Figure 10-3 As Figure 10-2, but a second geophone line has been added resulting in increased coverage where the two areas overlap. 90

Figure 10-4 As Figure 10-3, but now there are 5 shot lines and 5 geophone lines. It data are recorded from each shot on all lines then the coverage will be as high as 25 in the central portions of the area under investigation. 91

Figure 11-1 Proposed layout of survey lines for a seismic reflection survey at a potential deep repository site. Short cross-lines are included to provide 3-D information. 95

LIST OF TABLES

		Page
Table 3-1	Acquisition parameters for the seismic reflection survey at Finnsjön performed in May 1987.	8
Table 4-1	Processing steps used by Uppsala University.	10
Table 4-2	Processing steps used by Dahl-Jensen and Lindgren (1987).	15
Table 5-1	Processing steps used by Vibrometric OY.	23
Table 9-1	Parameters for model.	75
Table 11-1	Estimated costs for data acquisition and processing for three different survey configurations.	98

1 INTRODUCTION

1.1 BACKGROUND

One of the basic tasks in characterization of a potential site for final disposal of spent nuclear fuel is to detect and to determine the orientation, extent, and character of fracture zones. Knowledge of the geometry and properties of fracture zones is essential for evaluation of the suitability of a site for final disposal of hazardous waste and for determining a layout of a repository that makes optimal use of a site. Experience from characterization of fracture zones in crystalline rocks now exist from more than 10 study sites in Sweden and a number of sites in other countries (e.g. SKB RD&D Programme 1992). Characterization techniques that can be applied from boreholes and underground excavations have been developed and applied in several underground laboratories, e.g. Stripa and Äspö in Sweden, URL in Canada, and Grimsel in Switzerland. The initial phase of the Äspö Hard Rock Laboratory Project, which is currently in progress, was aimed specifically to verify the predictive capabilities of site characterization methods (Wikberg et al., 1991).

The general experience from these investigations shows that there are several surface methods which are effective in detecting and characterizing steeply dipping fracture zones. With respect to detection of semi-horizontal fracture zones from surface surveys the situation is different. In this case the only method with sufficient resolution and depth penetration appears to be reflection seismic profiling. During the past 15 years, seismic reflection surveys have been applied at a few potential repository sites in crystalline rock with varying degrees of success.

To meet the requirements for characterization of potential repository sites, the reflection seismic method has to provide data on fracture zone geometry from the ground surface down to depths of 1000-1500 m The need for seismic reflection data on rock properties from the upper 50 meters is of limited interest as there are several other geophysical methods which provide useful data in this depth interval. In addition, steeply dipping fracture zones can generally be detected by several other characterization techniques, their outcrops identified, and their dips estimated. Hence, the main targets for reflection seismic surveys are semi-horizontal or moderately dipping fracture zones. For investigations in the site scale (several km^2) the targets for the seismic surveys can be constrained to major fracture zones, i.e. zones with a thickness in excess of 5-10 m.

1.2 EXAMPLES OF SEISMIC SURVEYS IN CRYSTALLINE ROCK

In 1980 Green and Mair (1983) performed a seismic reflection survey at the WNRE site near Pinawa, Manitoba, Canada with the objective of characterizing fracture zones within a granitic batholith. They used a Mini-Sosie (vibrator) seismic source and receiver arrays of nine 40 Hz geophones. Data in the frequency interval 65-120 Hz were used for the stacked sections (seismic images). Comparatively clear indications of fracture zones were obtained after relatively elaborate processing made to suppress surface waves. The seismic data showed reasonable agreement with fracture zone data from boreholes.

Seismic reflection work surveys have been performed at Finnsjön (Dahl-Jensen and Lindgren, 1987) and Äspö (Plough and Klitten, 1988, Olsson, 1992) as a part of the SKB program. The results from these surveys have so far not been very convincing. The results from the Finnsjön survey failed to detect a major semi-horizontal fracture known to exist in the depth interval 200-300 m. The data from Äspö collected by Plough and Klitten have been processed by three different institutions which produced three essentially different results (Juhlin, 1990a). The data from the survey at Äspö in 1991 (Olsson, 1992) had such a poor signal to noise ratio that it was not possible to assess if the seismic sections contained any geologic information. In this survey a light weight vibrator source was used which evidently did not input enough energy into the bedrock.

A survey made to investigate sub-horizontal fracture zones at a potential gas storage site at Slöinge, Sweden also provided results which lacked any distinct reflectors (Stenberg and Triumf, 1990). The poor results were partly attributed to interference by surface waves generated by the explosive sources applied at the ground surface. In a seismic survey made to study the depth of the contact zone between Dala Sandstone and the underlying crystalline bedrock Juhlin et al. (1991) observed a high amplitude reflection at a depth of about 700 m which originated from a fracture zone in the crystalline basement. In this survey shots were generally fired in 4 m deep shotholes drilled into the till overburden.

Positive results from seismic reflections surveys in crystalline rock have also been obtained from a number of surveys made within the framework of the LITHOPROBE project in Canada (Milkerit et al., 1992a, 1992b). In these surveys the seismic source consisted of two vibrator trucks and 240 receiver channels were recorded. The same data collection equipment and procedures have also been successfully used to map geologic structure at two mine sites (Spencer et al., 1993, Milkerit et al., 1992c) in crystalline rock.

1.3 OBJECTIVES AND PROJECT OUTLINE

SKB has recognized the need for an efficient method to detect sub-horizontal fracture zones from the surface without the need to drill deep boreholes. In view of the variable quality of results obtained from surveys in crystalline rock it is evident that further development of the method is required before it can be applied as a standard tool in characterization of potential repository sites in crystalline rock.

The main aim of the project is to develop the reflection seismic method into a standard tool that can be applied in future characterization of potential repository sites.

The project will address the following issues.

- identify the critical factors for collecting data of sufficient quality at potential sites in Sweden.
- identify appropriate processing algorithms and schemes.

To resolve these issues the project is planned to include the following activities:

1 Reprocessing of seismic reflection data collected at Finnsjön by Dahl-Jensen and Lindgren (1987).
2 Theoretical studies to support planning of surveys in crystalline rock environments for application at potential repository sites.
3 Field test of proposed field procedures followed by processing of data.

This report presents results from the first and second steps of the project. The reprocessing of the Finnsjön data was made by two different organizations; the Department of Geophysics at Uppsala University and Vibrometric OY. This was followed by a closer analysis of the factors which determined the quality of the Finnsjön data and theoretical studies to optimize field surveys based on experience from the Finnsjön results.

2 THE FINNSJÖN STUDY SITE

The Finnsjön study site is located in central Sweden about 140 km north of Stockholm (Figure 2-1). Finnsjön was selected as a study site in 1977 and site characterization work has since then been performed intermittently until 1992. The results of these comprehensive investigations are summarized by Ahlbom et al. (1992). A brief review of the geology relevant to interpretation of the seismic profile is given here based on this summary.

The Finnsjön site is located in a region of low topographical relief. Although outcrops are common, the exposed rock make up about 15% of the total area. The overburden is up to a few meters thick and composed of Quartenary sediments, mainly moraine and peat.

The site is located in the Svecokarelian (also referred to as the Svecofennian) domain of rocks of mainly granodioritic composition which were intruded into the surrounding volcanic rocks about 1.85 Ga ago in conjunction with the Svecokarelian orogeny. These rocks were deformed at the later stages of the orogeny and have present day gneissic character with foliation at N50-60°W and steeply dipping to the NE. About 1.7 Ga ago, granites intruded the bedrock resulting in brecciation and thermal alteration near contacts. Pegmatite, basic and aplite dikes are also present and are generally less than a meter thick with a predominantly vertical orientation.

Two sets of major lineaments have been identified in the area (Ahlbom and Tiren, 1991), one with a NNE trend and the other with a NW trend. The blocks within the lineaments are tilted up to 2° indicating listric faults at depth. The Finnsjön site is located north east of the intersection of a N trending and a NW trending lineament (Figure 2-1), with dips to the E and NE, respectively.

Three major sets of fracture groups have been identified in the area, a steeply dipping NE trending set, a steeply dipping NW trending set and a flat lying or gently dipping set with dips to the SW. The fracture frequency is high in the area with an average of 3 fractures/m in outcrops and in some boreholes, however, other boreholes have lower fracture frequencies of 1 fractures/m. No decrease in fracture frequency with depth in the boreholes has been observed.

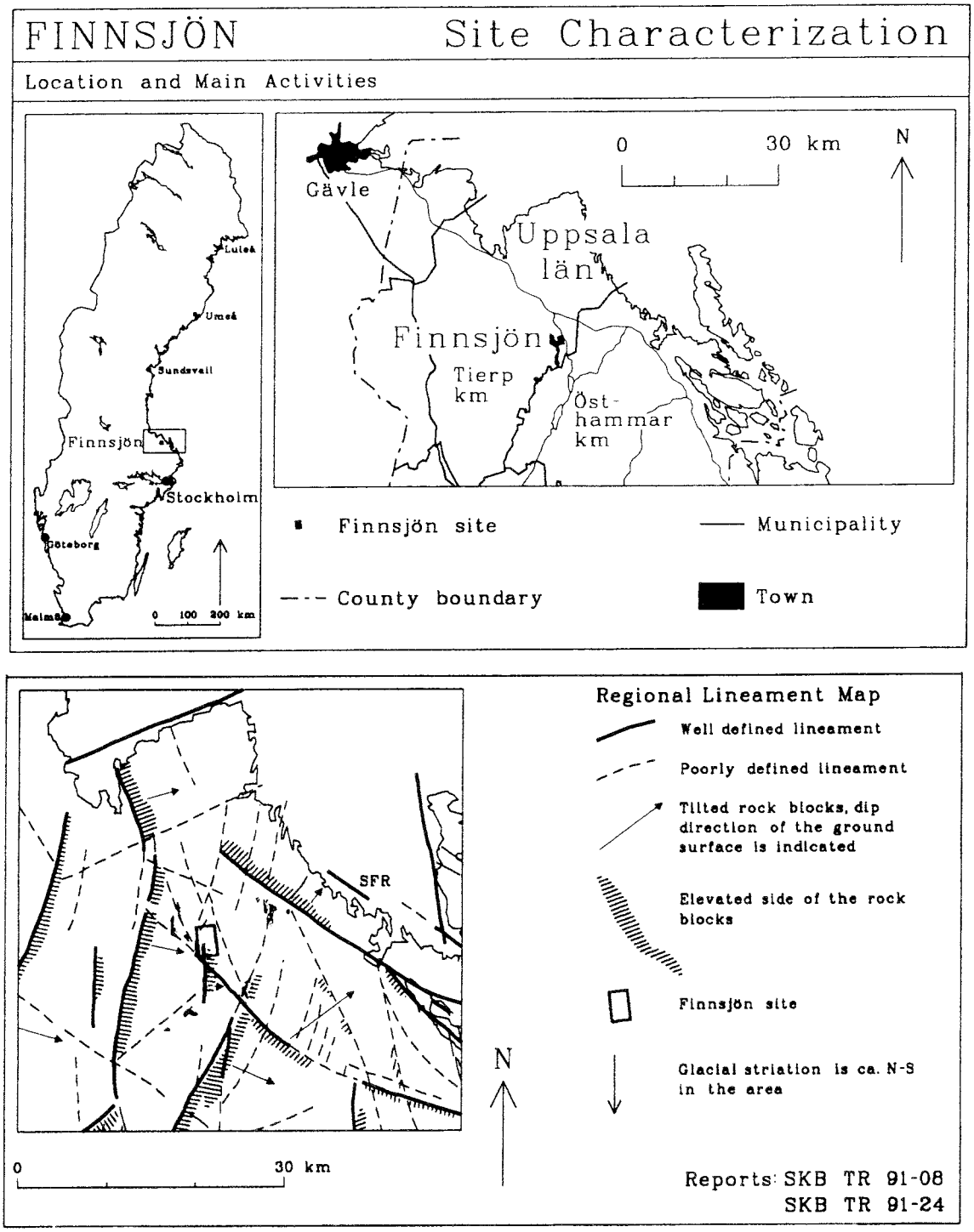

Figure 2-1 Location map and major lineaments in the vicinity of the Finnsjön study site (after Ahlbom et al., 1992).

Fourteen fracture zones have been identified at the study site. The ones near or crossing the seismic profile on the surface are shown in Figure 2-2. Zone 1 (the Brändan zone) crosses the profile near its beginning and dips to the SE implying that it is not possible to image it given the location of the profile. Zone 1 has been classified as certain using the nomenclature of Bäckblom (1989). Zones 5, 6, and 8 dip at about 60° and zone 10 about 85° to the SW with zone 5 being classified as probable and the other zones as possible. All these zones are probably too steep to be imaged by standard seismic processing methods. Zones 12 and 14 are near vertical and also classified as possible, although zone 14 may be correlated with the NW trending lineament since movement has occurred on it and may have a listric form with depth. Zone 9 has recently been interpreted to have shallow dip of 15° to the SW and it should be possible to image it if it has sufficient impedance contrast compared to the host granodiorite. The most important zone observed in the area is zone 2 which does not have a surface expression, but which has been intersected in most of the boreholes drilled in the depth range 100-400 m. It is characterized by a significantly higher hydraulic conductivity and is well defined east of borehole BFi01 (Figure 2-2). The borehole data indicate it to dip about 15° to the SW and that it is non-planar in part. The gentle dip and the high hydraulic conductivity make it an ideal target for the seismic reflection method.

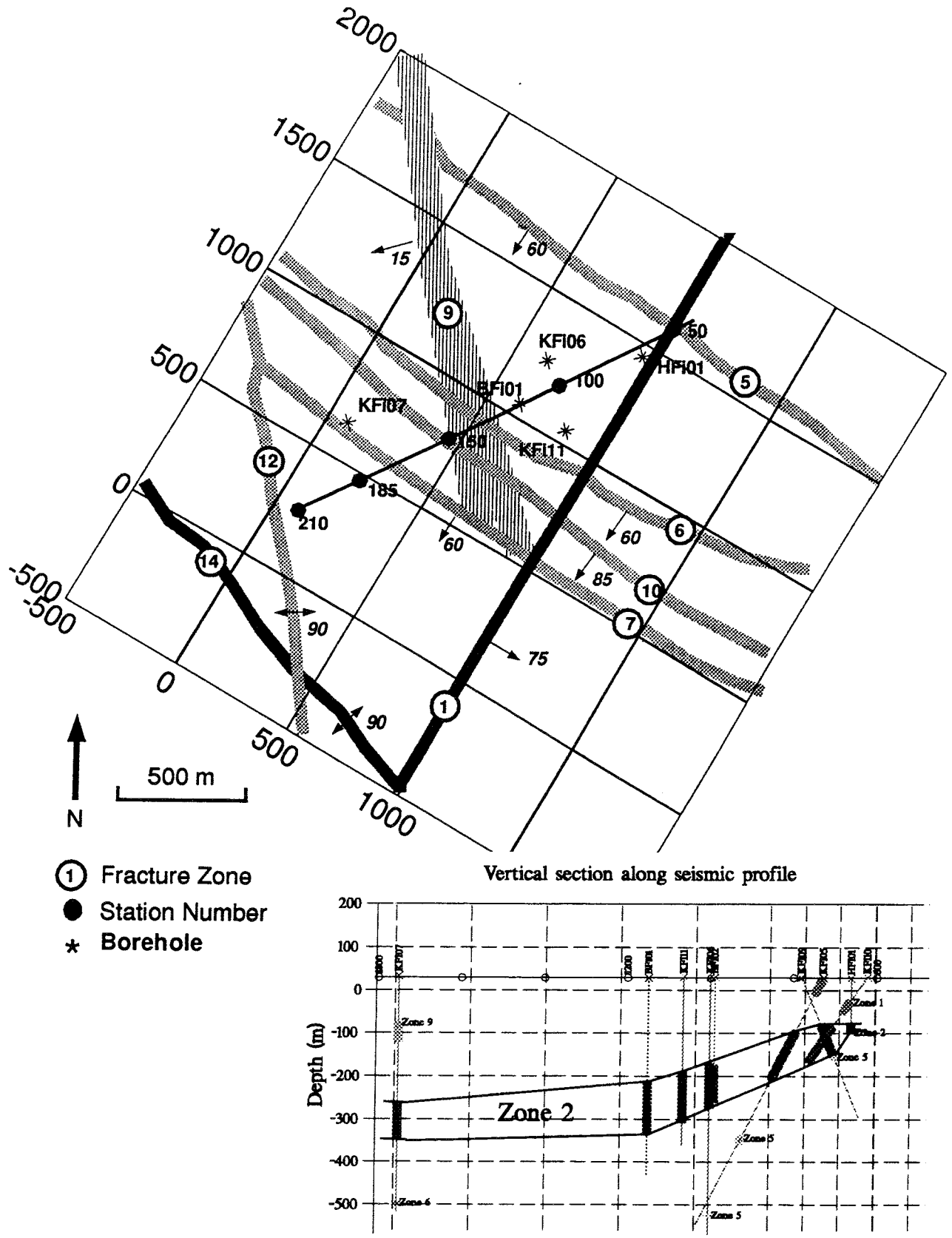

Figure 2-2 Profile location and fracture zones in its vicinity. Numbers along the profile refer to station location (multiply by 10 to get the length coordinate used by Vibrometric).

3 DATA ACQUISITION

The seismic reflection data were collected in May 1987 by the Section for Solid Earth Physics at Uppsala University using a SERCEL 348 telemetry system. Field parameters are given in Table 3-1. The SERCEL 348 has a dynamic range close to 120 dB and data are transferred digitally from the recording point to the recording system. The seismic line ran approximately perpendicular to the gently dipping zone 2 with the first shot-point at station 36 and the first geophone point at station 47 (Figure 2-2). The total profile length was about 2200 m with a total subsurface Common Depth Point (CDP) coverage of about 1700 m. A total of 151 shots were fired, most of them in holes drilled down to bedrock. Data quality were variable along the profile with 3 areas giving poorer quality data; stations 80-100, 115-130 and shotpoints 181-188.

Table 3-1 Acquisition parameters for the seismic reflection survey at Finnsjön performed in May 1987.

Spread type	End-on
Number of channels	60
Near offset	100 m
Geophone spacing	10 m
Geophone type	28 Hz single
Shot spacing	10 m
Charge type	50 g dynamite
Nominal charge depth	2 m in bedrock or 4 m in soil
Nominal fold	30
Recording instrument	SERCEL 348
Sample rate	1 ms
Field low cut	Out
Field high cut	250 Hz
Record length	2 seconds

4 REPROCESSING BY UPPSALA UNIVERSITY

4.1 PROCESSING SEQUENCE

Initial processing of the data (Dahl-Jensen and Lindgren, 1987) showed only one steeply dipping reflector in the final stacked section. The sub-horizontal fracture zone, Zone 2, was not visible at all. Inspection of a shot gather (Figure 4-1a) at the beginning of the profile clearly shows the reflection from a steeply dipping zone. Indications of a reflection from a more shallow zone can also be seen in the shot gather. However, inspection of the first arrivals show great variation in the geophone statics. These statics are not due to topography since the total elevation difference along the entire profile is less than 10 m, implying that local variations near the geophone stations play an important role in the time delays observed on the shot gathers. After application of refraction statics, the reflection from zone 2 appears as a coherent event (Figure 4-1b) along with other deeper events.

Application of refraction static corrections along with the other processing parameters (Table 4-1) give a much improved image over the earlier processing of Dahl-Jensen and Lindgren (1987). Four steps were shown to be of significant importance in obtaining the final image. These were

- Refraction statics
- Velocity analyses
- Editing and muting
- Bandpass filtering

The final stack is shown in Figure 4-2 where the upper 500 ms of data have been displayed. The stack shows several prominent events. The reflection from Zone 2 can be followed relatively clearly from near the eastern end of the profile at station 45 at 40 ms two way travel time (TWT) to about station 160 at 130 ms TWT. To the west of station 160 it is not clear if zone 2 continues. There are also a number of clear steeply dipping events. In order to position these correctly in space the data need to be migrated. Several migration tests were performed and it was observed that application of a coherency filter prior to migration (Figure 4-3) improved the migrated section. The migration algorithm used is based upon the scheme described by Loewenthal et al (1991) since it will even migrate steeply dipping reflectors to their correct spatial positions if the velocity of the media is known. The need for migration is obvious since reflectors which were crossing one another in the time section may not do so in the depth section (Figure 4-4). Note that the easterly dipping high amplitude event on the eastern end of the profile between stations 50 and 80 at 200 to 300 ms TWT

(Figure 4-2) is migrated from being below the more gently western dipping reflector in the time section to above it in the depth section (Figure 4-4). The migration velocity used was 5000 m/s. In this figure Zone 2 appears as a clear sub-horizontal reflector between stations 50 and 150 at a depth which increases from 150 m at station 50 to about 300 m at station 150.

Table 4-1 Processing steps used by Uppsala University.

1.	Demultiplex and gain restoration
2.	Spherical divergence correction, v=5500 m/s, t_0=10 ms
3.	Notch filtering, 50 Hz and 150 Hz
4.	Bandpass filter 90-270 Hz, 120 dB/octave
5.	CDP sort
6.	Refraction statics, Pass 1
7.	Trace amplitude balancing, 50 ms window
8.	Trace editing and surgical mute
9.	Velocity analysis
10.	Refraction statics, Pass 2
11.	NMO
12.	Stack
13.	Trace amplitude balancing, 200 ms window
14.	Bandpass filter 50-150 Hz, 60, 120 dB/octave
15.	Coherency filter 1 ms/trace over 11 traces
16.	Reverse time migration, 5000 m/s

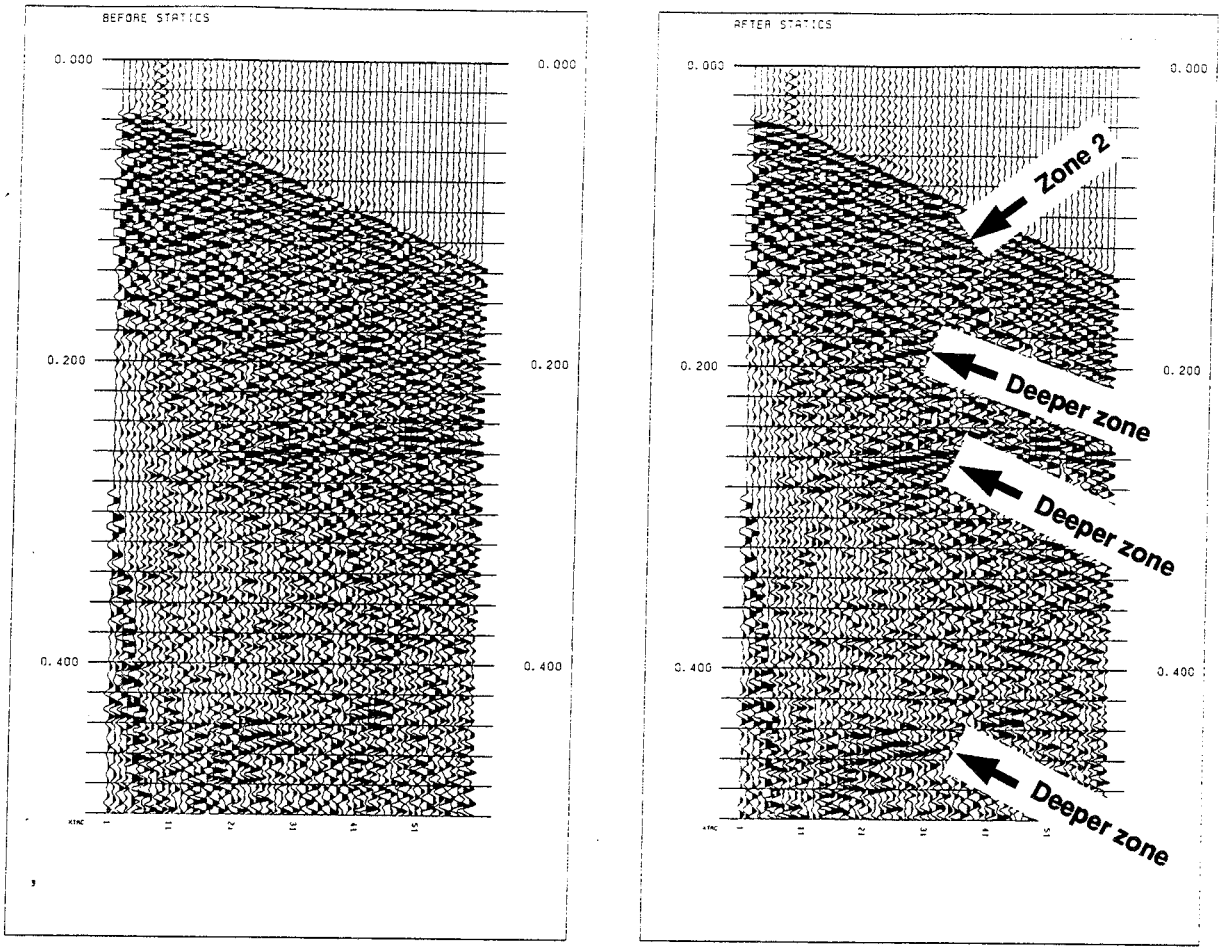

Figure 4-1 Shot gather from the beginning of the profile (a) without static corrections and (b) with refraction static corrections.

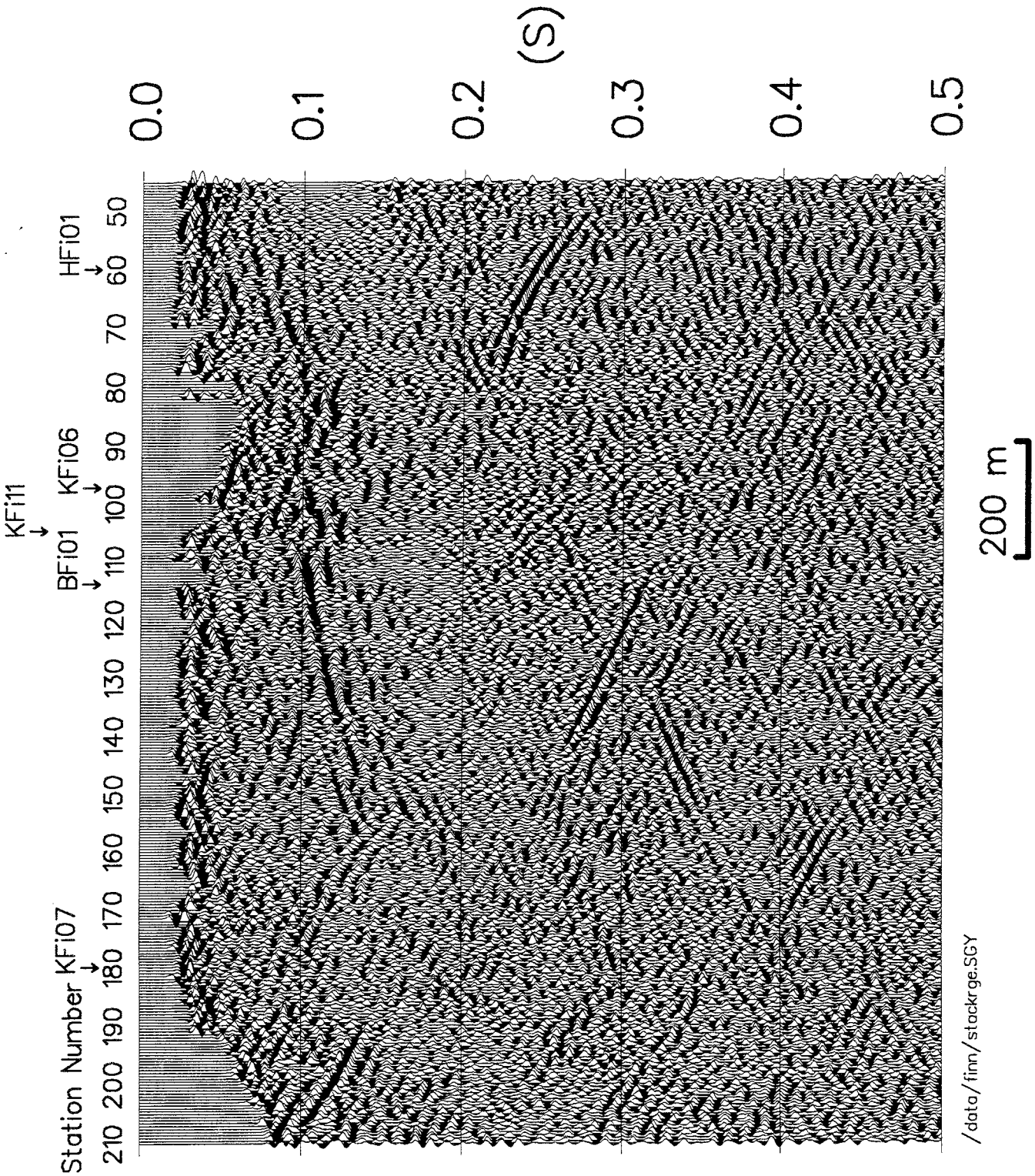

Figure 4-2 Final stack after processing up to point 14 in Table 4-1. Station numbers correspond to those shown in Figure 2-2.

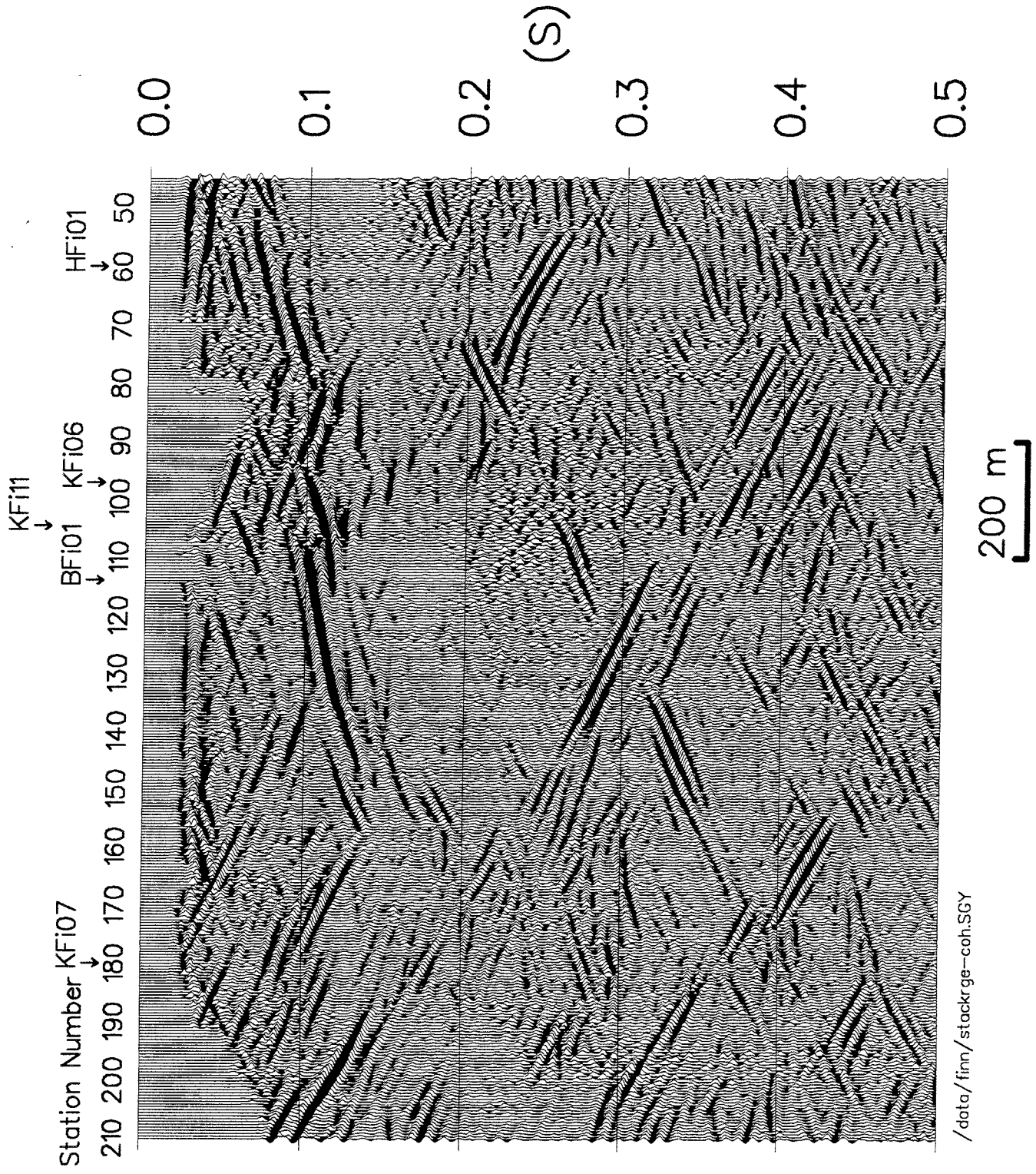

Figure 4-3 Final stack in Figure 4-2 after coherency filtering (point 15 in Table 4-1). Station numbers correspond to those shown in Figure 2-2.

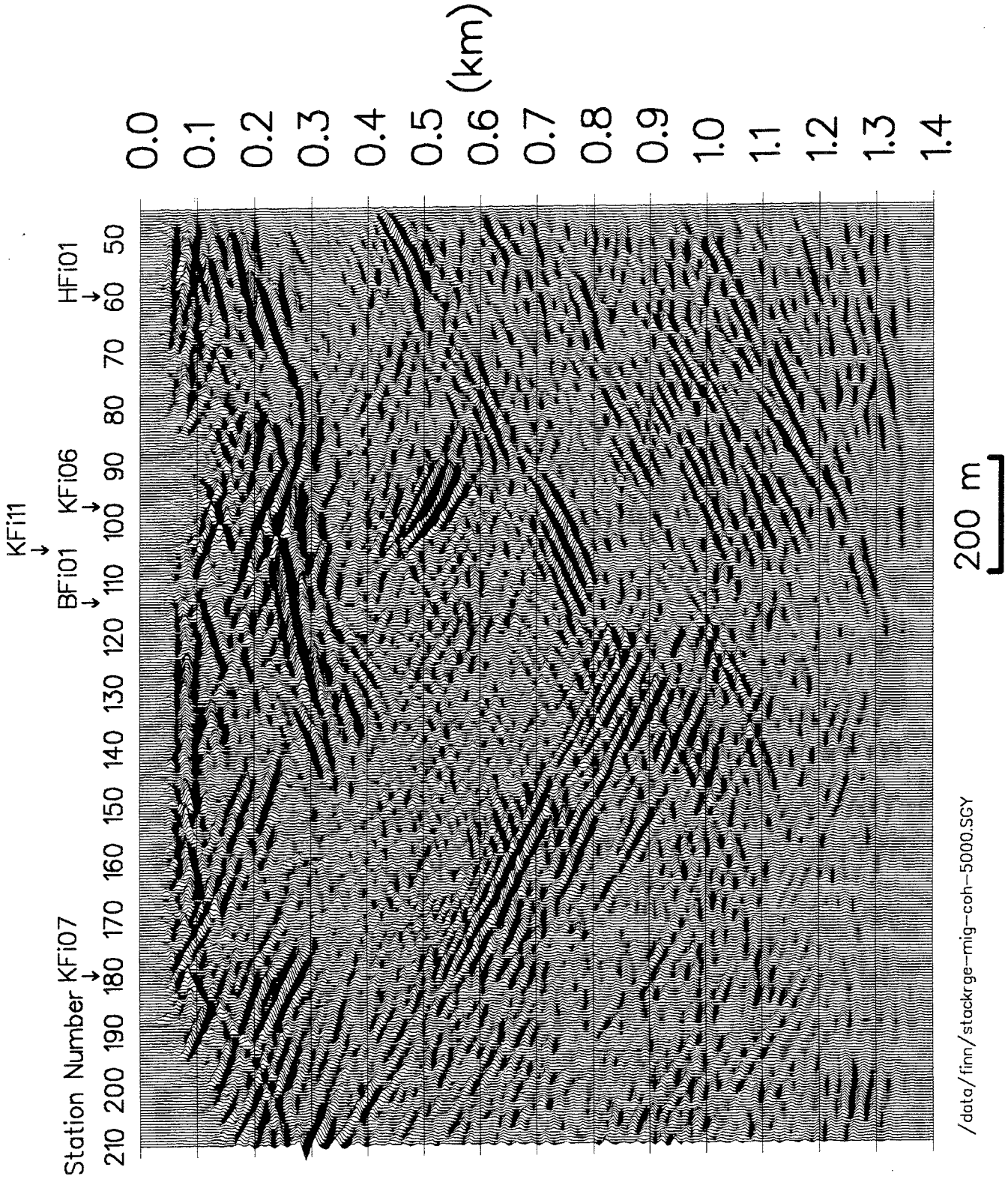

Figure 4-4 Final stack shown in Figure 4-3 after migration (point 16 in Table 4-1). Station numbers correspond to those shown in Figure 2-2.

4.2 CRITICAL PROCESSING STEPS

4.2.1 Comparison with earlier processing

The reprocessing has resulted in a seismic image which is considerably more useful than the previous processing. We will now attempt to show how the application of various processing steps affect the image obtained. It is not possible to exactly reproduce the result of Dahl-Jensen and Lindgren (1987) due to a new computer system, new processing software and lack of documentation. A section of reasonable similarity (Figure 4-5) may be obtained using the processing steps listed in their report and given in Table 4-2. Note, however, that the time section now begins much earlier (≈20 ms or 50 m depth) than in the work of Dahl-Jensen and Lindgren (1987) due to careful muting of the first arrivals. This time section shows very little of interest. A few steeper easterly dipping zones can be perceived through the lower frequency surface waves and ground roll. It is clear that application of a higher low cut frequency filter would improve matters.

Table 4-2 Processing steps used by Dahl-Jensen and Lindgren (1987).

1.	Demultiplex and gain restoration
2.	Notch filtering 150 Hz and 250 Hz
3.	Mute
4.	Bandpass filter 40-250 Hz
5.	RMS normalization
6.	CDP sort
7.	NMO, velocity 5200 m/s @ 0 s, 6000 m/s @ 1.5 s
8.	Stack
9.	AGC

Application of a 90 Hz low cut filter before stack results in considerable improvement (Figure 4-6). Most of the ground roll has been eliminated and several of the steeper dipping events are now clearer. Zone 2 is still not obvious, but is imaged somewhat better than before the low cut filter was applied.

The application of refraction statics results in zone 2 standing out on that part of the section east of station 150 (Figure 4-7). Further refinement of the section (Figure 4-8) is possible by applying the same velocity functions as used in the processing of Figure 4-2. These velocities result in the steeper dipping reflectors being imaged more clearly. The static corrections improve mostly the image of zone 2 while the velocity analyses result in a better image of the deeper steeply dipping zones. This is to be expected since the

original velocity function chosen by Dahl-Jensen and Lindgren (1987) is a reasonable estimate of the true velocity in the rock column and sub-horizontal reflectors should stack constructively, while steeper ones require a higher velocity be used to stack constructively

Figure 4-8 forms the basis for producing the final section shown in Figure 4-2. Additional passes of refraction statics and trace editing are the main differences in the processing of the two sections. Although these additional processing steps lead to definite improvements, most of the main features of the Figure 4-2 may be seen in Figure 4-8.

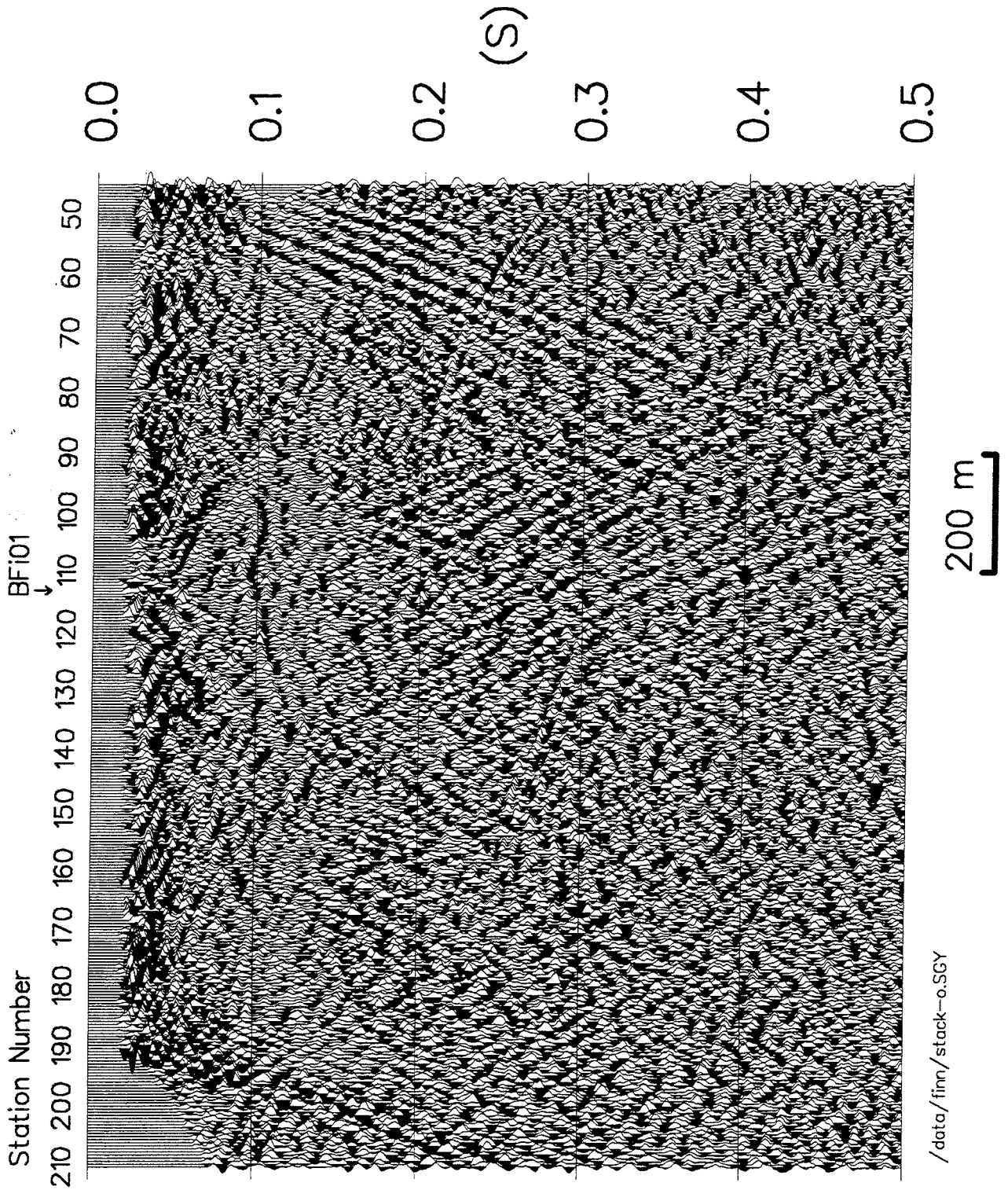

Figure 4-5 Initial stack using processing parameters given in Table 4-2. Station numbers correspond to those shown in Figure 2-2.

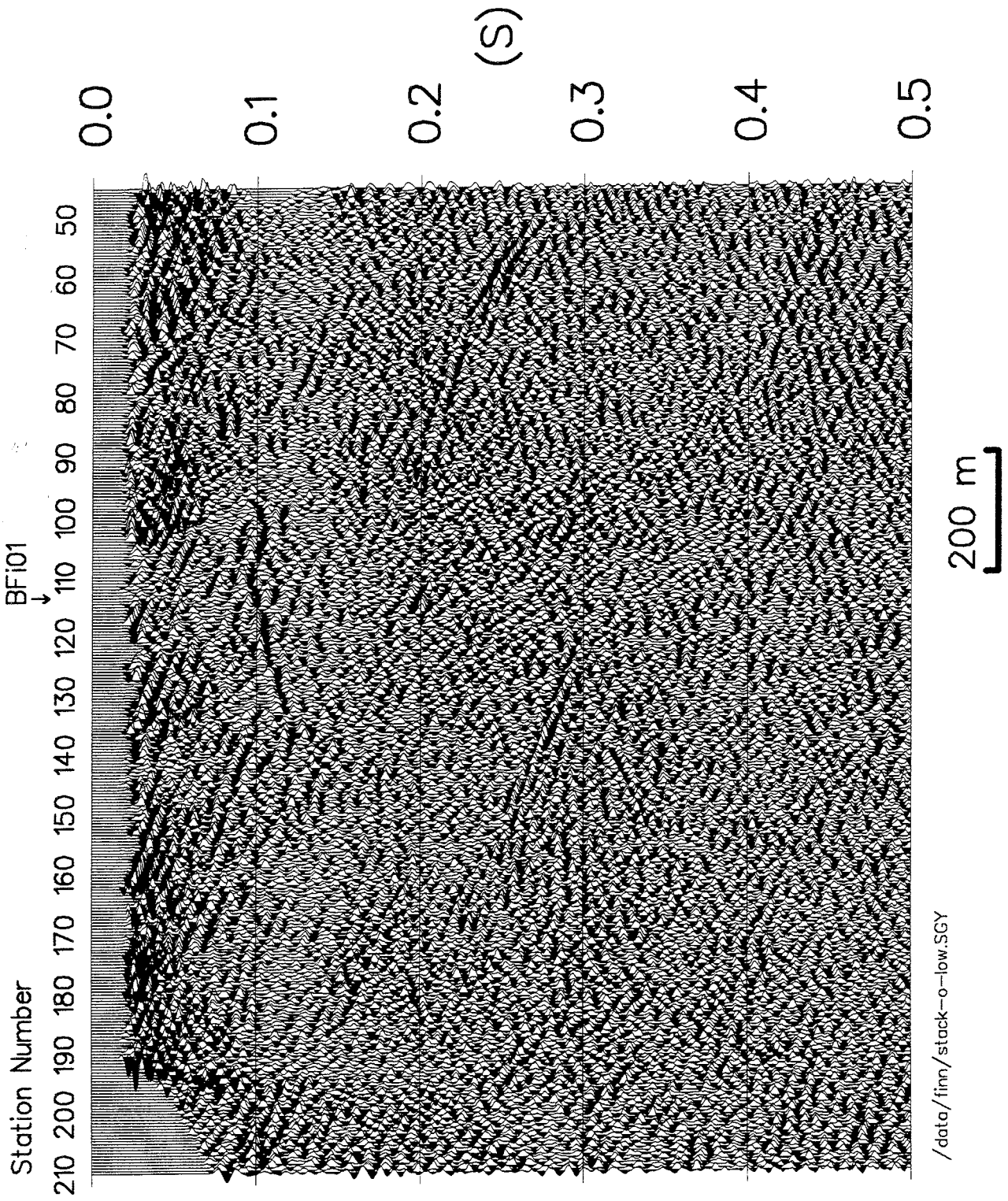

Figure 4-6 Same processing as in Figure 4-5 but with a 90 Hz low cut filter before stack. Station numbers correspond to those shown in Figure 2-2.

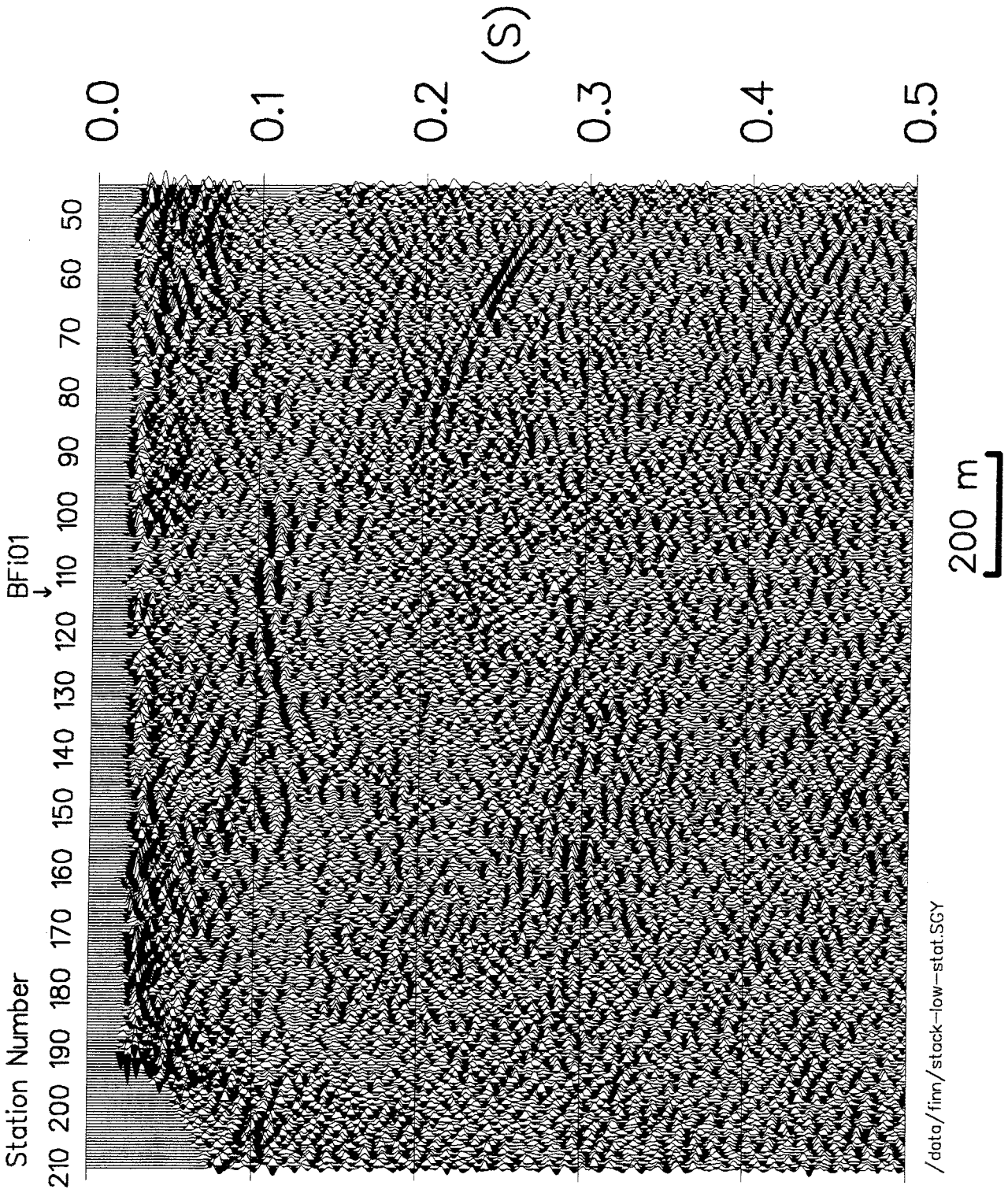

Figure 4-7 Same processing as in Figure 4-6, but using the refraction statics given in Appendix A. Station numbers correspond to those shown in Figure 2-2.

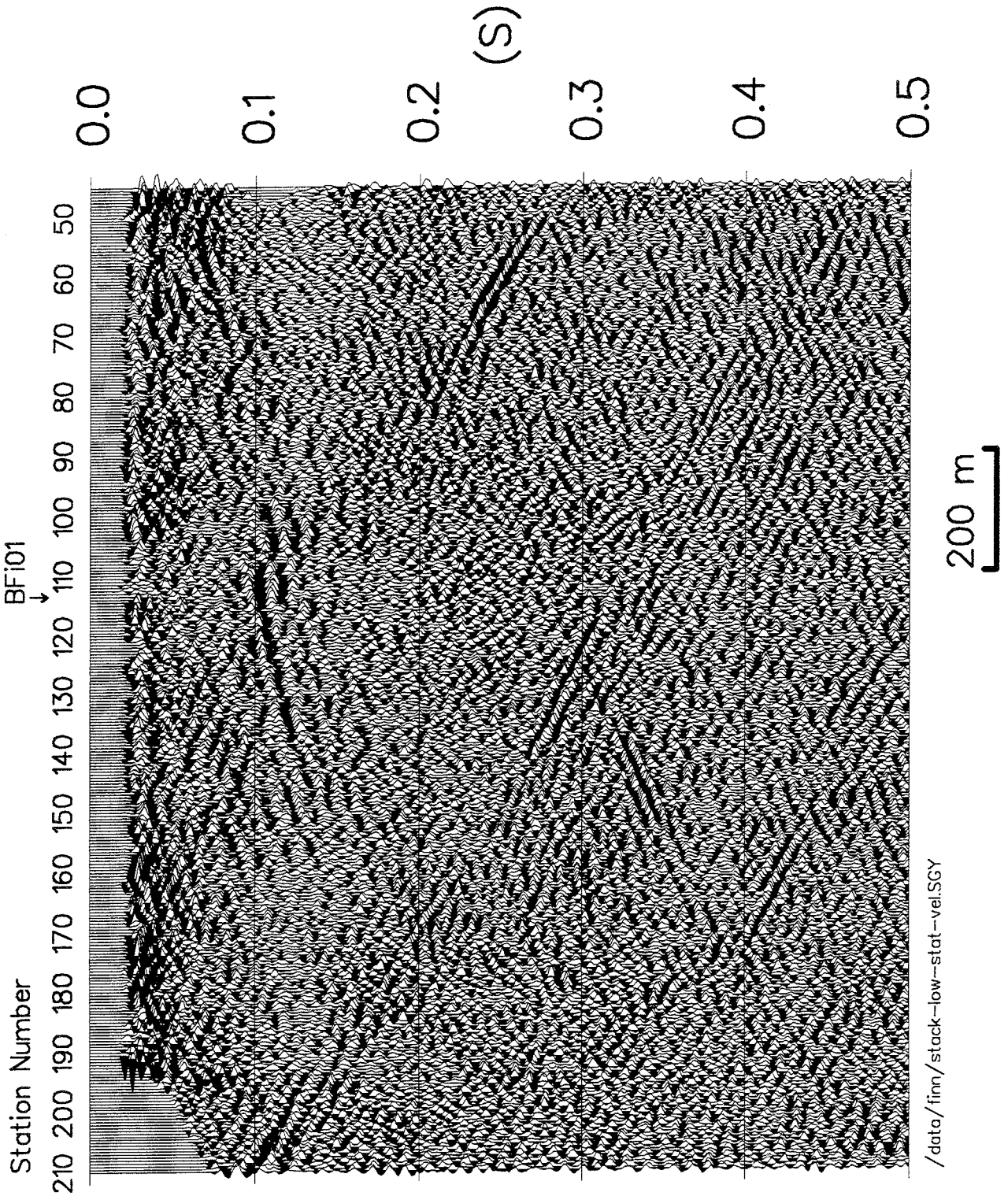

Figure 4-8 Same processing as in Figure 4-7, but using the velocity function given in Appendix B. Station numbers correspond to those shown in Figure 2-2.

4.2.2 Quality control

An obvious question which arises is whether the section displayed in Figure 4-2 could have been produced without knowing about the existence of zone 2 from the drilling, that is, has the reflection been "fabricated" rather than processed. Given the conflicting results from previous reprocessing of seismic data from Äspö (Juhlin, 1990a) the question is valid. There are several lines of evidence showing that the reflection is real and would have been produced even without any information about the drilling results:

- The event is visible on the shot sections (Figure 4-1). This was not the case at Äspö.

- Refraction statics are independent of the reflectors since the first arrivals are aligned rather than events arriving from the reflectors themselves. The refraction statics would be the same regardless of what is known about the subsurface.

- The reflections stack in at "reasonable" velocities based upon experience from other crystalline rock areas. Zone 2 stacks in at about 5300 m/s where it is clearly visible and consistent with refraction velocities.

There is no evidence that any of the reflections observed in Figure 4-2 are "artifacts" of the processing, but some of them may be from out of the plane of the profile. To determine their true geometrical position will require 3-D data acquisition.

5 REPROCESSING BY VIBROMETRIC OY

5.1 BACKGROUND

The conventional processing techniques applied by Dahl-Jensen and Lindgren (1987) did not yield any certain reflection events which could be attributed to geological features in the rock. To see if better results could be obtained with other processing techniques it was decided to test the processing approach based on the Image Point (IP) Transform on the Finnsjön data set. The IP approach has been extremely successful with Vertical Seismic Profiling (VSP) surveys in crystalline rock (e.g. Cosma et al., 1991, Blümling et al., 1990). A first attempt to apply the IP approach to surface reflection data was carried out on the second data set from Äspö (Heikkinen et al., 1992). The seismic sections obtained with the IP approach produced a number of coherent reflectors and indicated the capability of the IP approach also for processing of surface reflection data.

Due to the low initial expectations that further processing of the Finnsjön data set would produce better results and to the very laborious computation needed for further processing using the IP approach, it was decided to test the IP approach only on a part of the available data set. A number of 69 shot-gathers, from record 52 to record 120 were included in the reduced data set (Figure 2-2). Lower numbers for shot-gathers were eliminated due to the too shallow position of Zone 2 under them, in relation with the shot offset (100 m to 790 m). The initial intention was to include also the shot-gathers from 121 to 152, but this idea was abandoned because the shooting geometry starts to vary towards the end of the profile, the signal-to-noise ratio is extremely poor for some of the shots in the same area and, finally, because it was considered more useful to apply a more extensive processing scheme to a smaller data set.

The processing steps applied to the data are listed in Table 5-1 and described in the following sections.

5.2 PRELIMINARY PROCESSING

The band-pass filtering was performed using a 4-pole Butterworth minimum phase filter with the cut-off limits 150 Hz and 600 Hz. The high-cut limit was set somewhat optimistically, but it was made with to avoid any risk of cutting of higher frequencies, needed for resolving events near the ground surface. For the same reason, the data was interpolated, resulting in a

Table 5-1 Processing steps used by Vibrometric OY.

1.	Preliminary processing - Band-pass filtering (150 Hz - 600 Hz) and resampling to 0.5 ms. - Arrival time picking - Static corrections - Amplitude equalization (AGC) - Two-way Image Point transform
2.	Stacking - NMO corrections - CMP stack
3.	Pre-stack migration - Migration of the shot-gathers - Stacking of migrated shot-gathers
4.	Tau-P filtering of the stacked profiles

sampling rate of 0.5 ms instead of 1 ms, used in acquisition. An example of original data is given in Figure 5-1 and the corresponding filtered shot-gather is shown in Figure 5-2. It can be seen that the surface waves and the noise bursts are partly removed. Some faint reflection patterns seem to develop, but are difficult to follow due to the inconsistency of the phase. One can also observe that the first onsets are not positioned on a straight line, being sometimes offset by more than a full period with respect to the neighboring traces.

A first attempt to proceed directly to the CMP stack produced the result shown in Figure 5-3. This attempt was purely academic and results are comparable to those shown in Figure 4-5. Not much was expected without correcting for statics.

For static corrections, the travel times were picked by a two-step procedure. Firstly, the picking was done by an automatic routine based on maximum likelihood. This routine proved to be very efficient even with noisy signals but in some cases it picked a negative half cycle and in other cases a positive one to be the first onset. An attempt was made to change the routine to keep track of phase, but then the accuracy of the pick became poor. It was decided to keep the picks as they were, and then refine them by applying a cross-correlation routine to turn all of them in phase.

The arrival times obtained by this double pick were used in time-term analysis, to determine the characteristic delays for each shotpoint and each receiver. For each shot-receiver pair the traveltime can be written as:

$t_{(i,j)} = (d_{(i,j)} / V) + t_{1(i)} + t_{2(j)}$

where i is the shot number, j the receiver number, d is the shot-receiver distance, V is the mean velocity and t_1, t_2 are the characteristic delays for shots and receivers, respectively. V, t_1 and t_2 are determined by a least squares procedure. In Figure 5-4, the receiver number runs horizontally and the record number vertically. The picked travel times are plotted as a function of shot number and receiver number and the existence of characteristic shot delays shows itself by the vertical coherency. The horizontal coherency, due to receiver characteristic delays, manifests itself by consistent vertical shifts, which can also be observed.

In Figure 5-5, the quantity plotted is:

$\Delta t_{(i,j)} = t_{1(i)} + t_{2(j)}$

which are the computed characteristic delays for each shot-receiver pair. The travel times were corrected by subtracting Δt from each trace.

The frequency filtering did not reduce sufficiently the surface waves and an automatic gain operator (AGC) with a window length of 100 ms had to be applied to avoid problems in the subsequent multi-channel processing. Figure 5-6 shows the shotgather from Figure 5-2, after offset correction and AGC. It can be seen that the first onsets line up regularly. The pre-arrival noise has been muted using a 20 ms ramp.

Reflection events now became much more visible than in the previous stage, due to the improvement of the phase consistency.

The Image Point filtering procedure was applied independently for each shot and receiver gather. The effect of the procedure can be seen in Figure 5-7. The shotgather became very "clean" and one can safely assume that the remaining coherent patterns are P-wave reflections. The difficulty of interpreting these results is well known from VSP surveys. It is characteristic for crystalline rock that reflectors with different orientation produce criss-crossing events, quite difficult to follow. With VSP surveys it is normal to filter the profiles by isolating the strongest events and presenting them separately in different classes according to their orientation. In the present study, processing proceeded with the shotgathers as they were to the stacking stage, the enhancement of certain classes of reflectors remaining to be done on the stacked profiles.

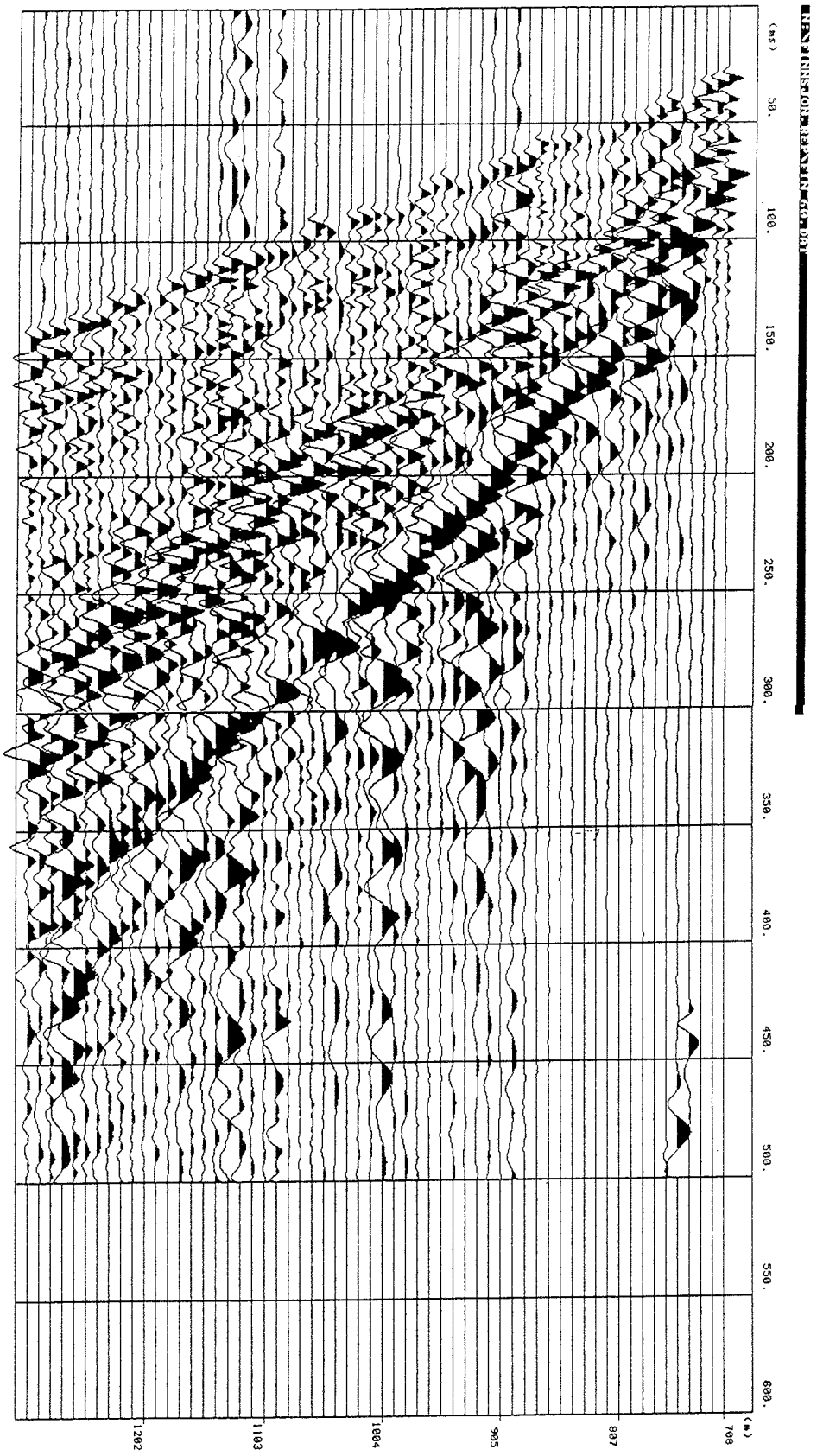

Figure 5-1 Original shot-gather data, record number 60.

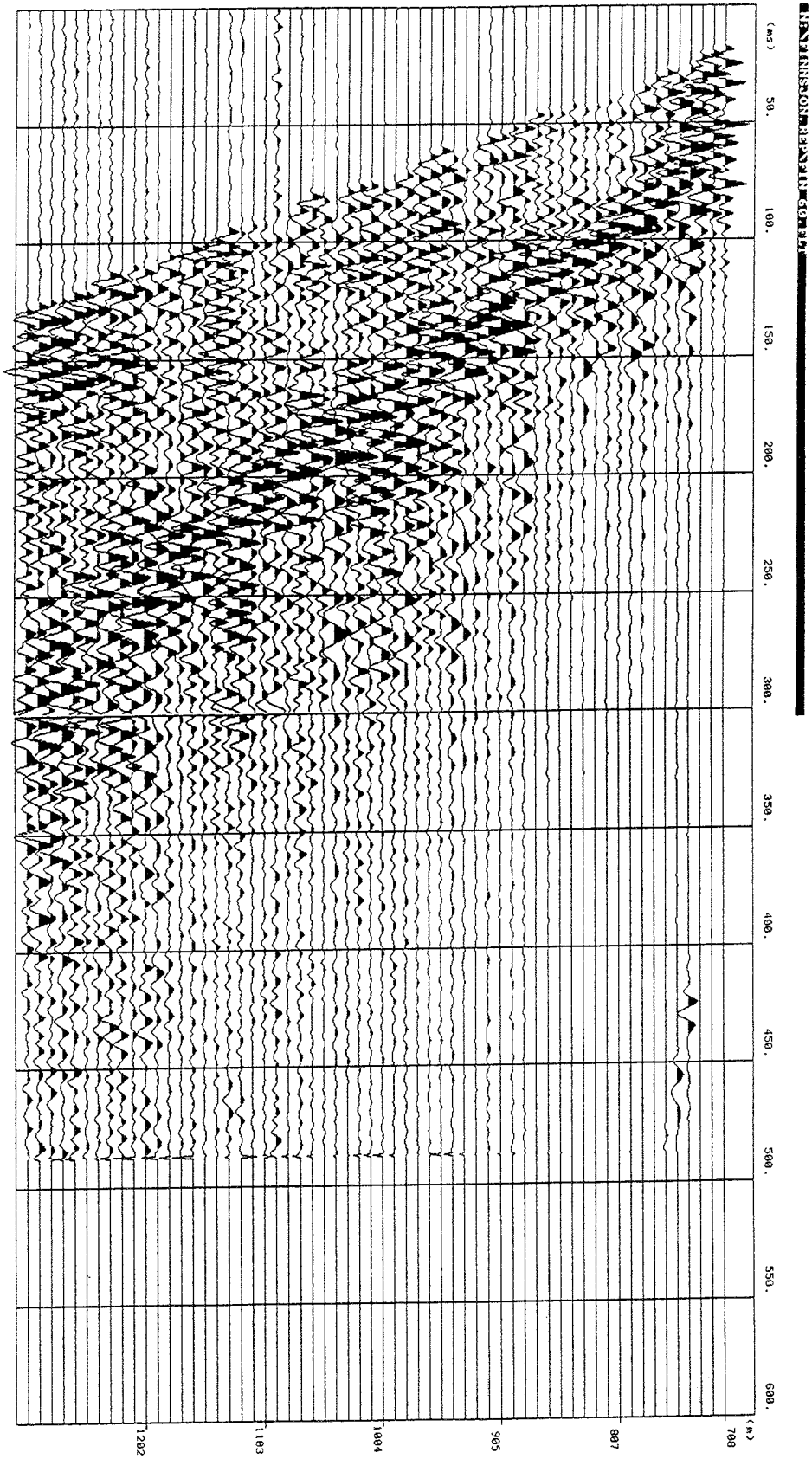

Figure 5-2 Band-pass filtered shot-gather data, record number 60.

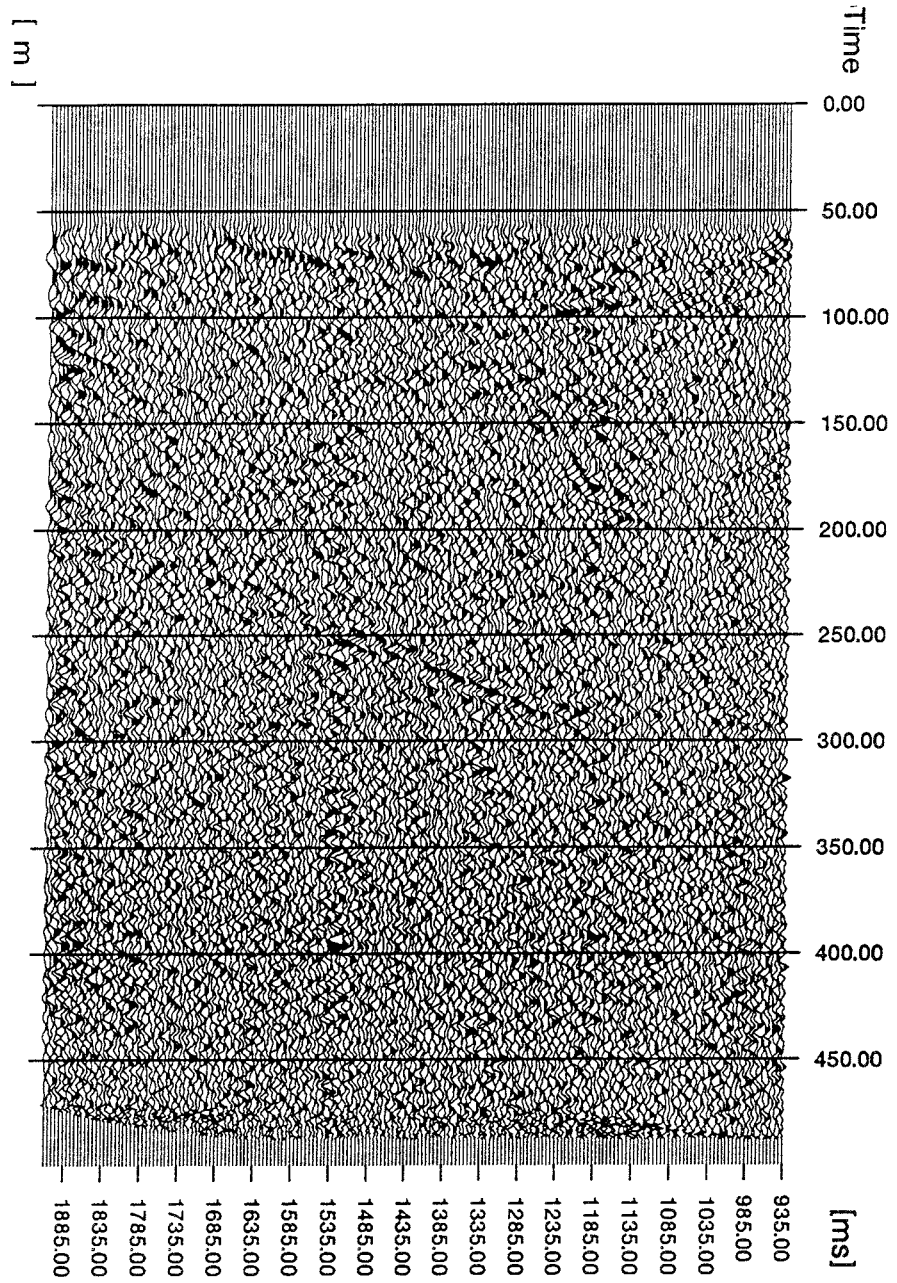

Figure 5-3 NMO-corrected and CMP-stacked data section.

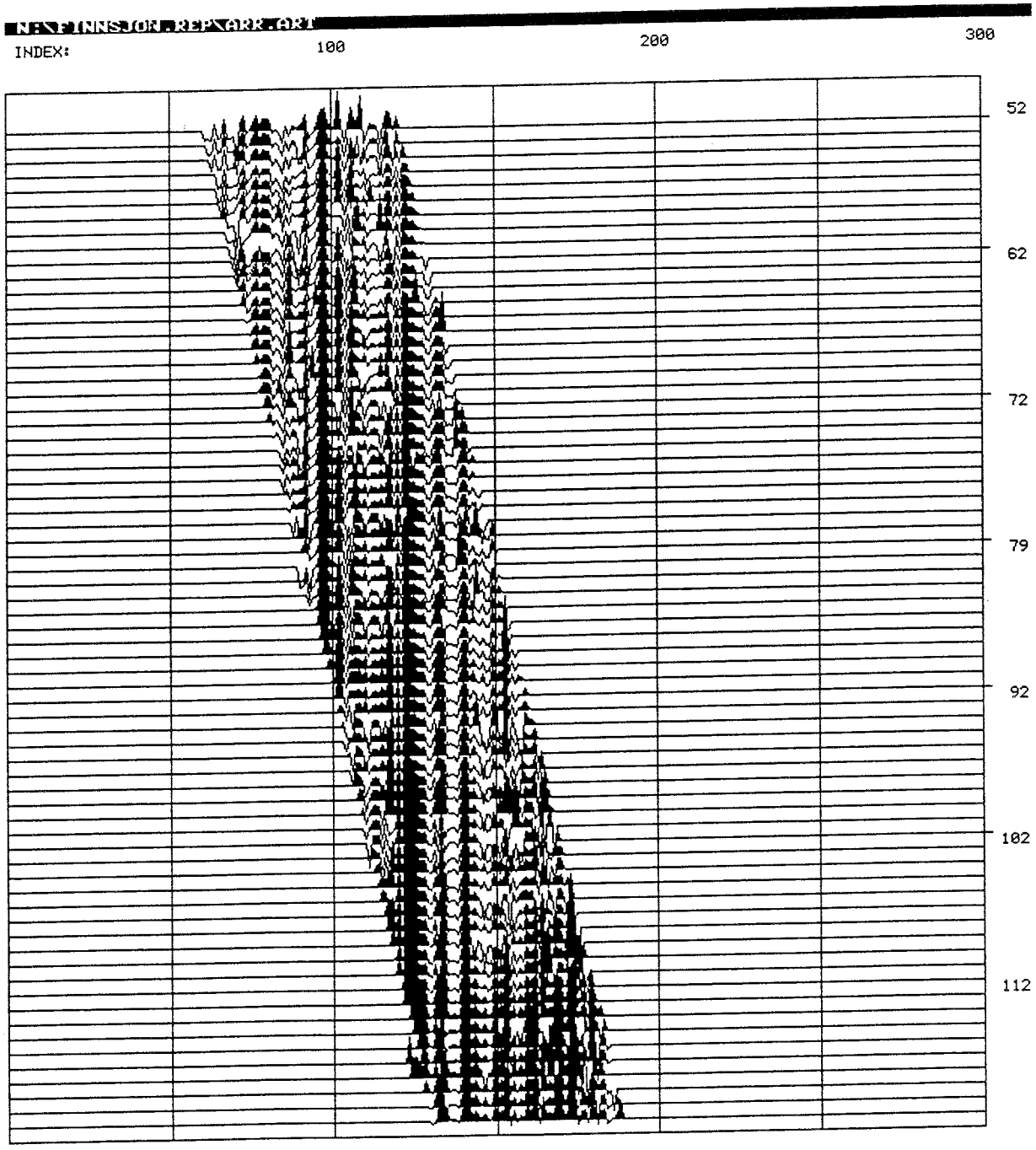

Figure 5-4 Characteristic shot delays for each shot (record numbers vertically) and each receiver (numbers horizontally).

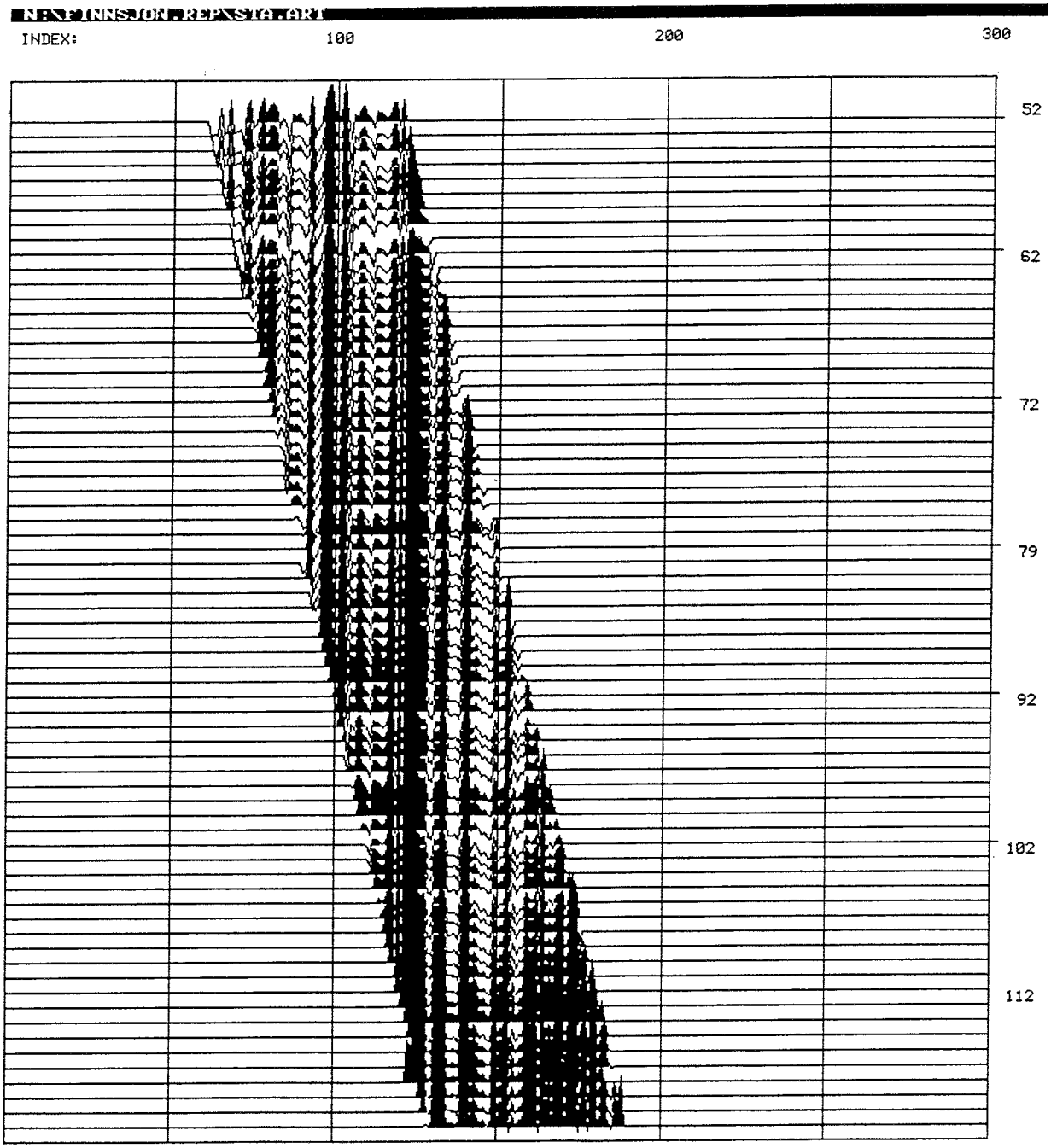

Figure 5-5 Computed characteristic delays for each shot-receiver pair.

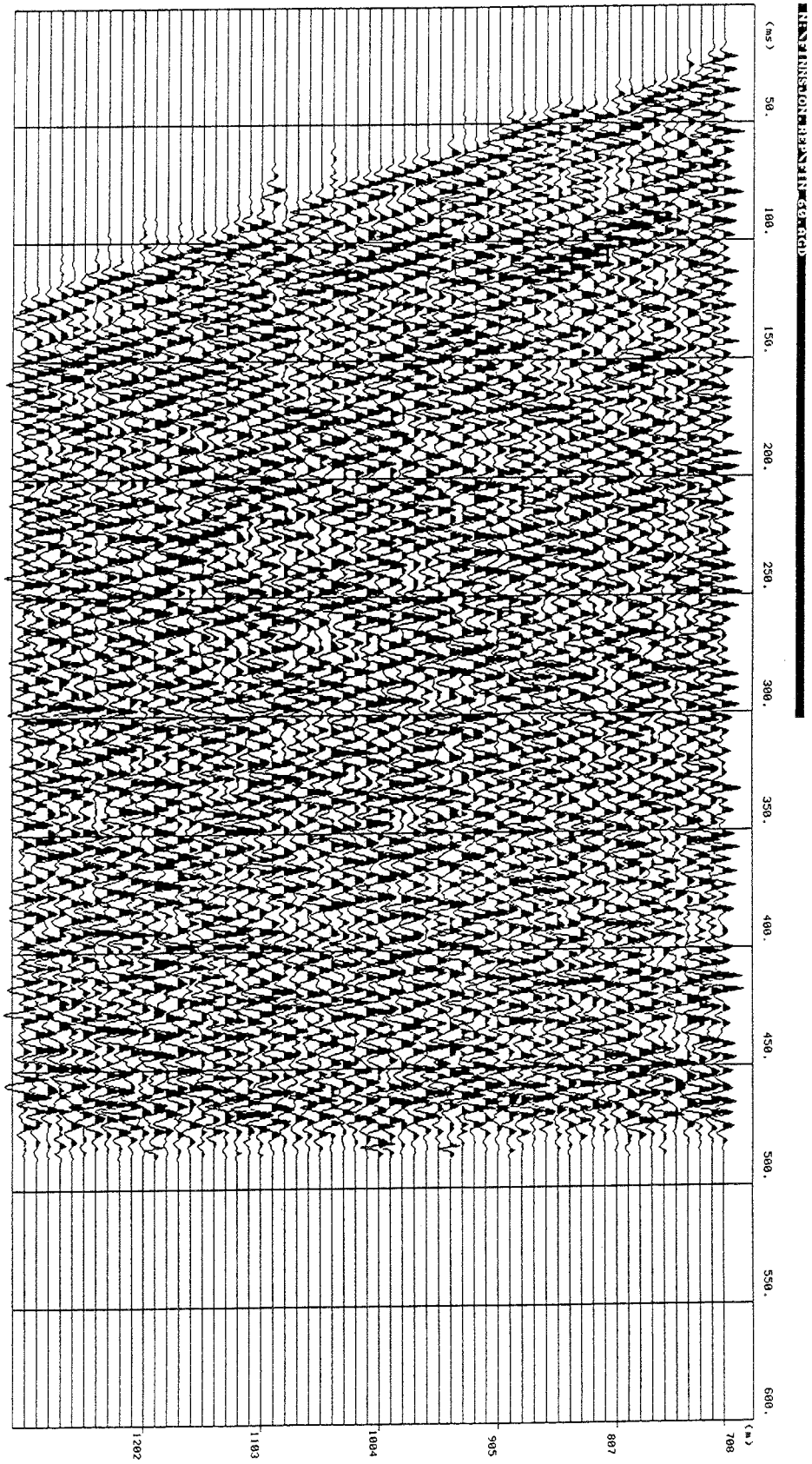

Figure 5-6 Static corrected and amplitude equalized (AGC) shotgather data.

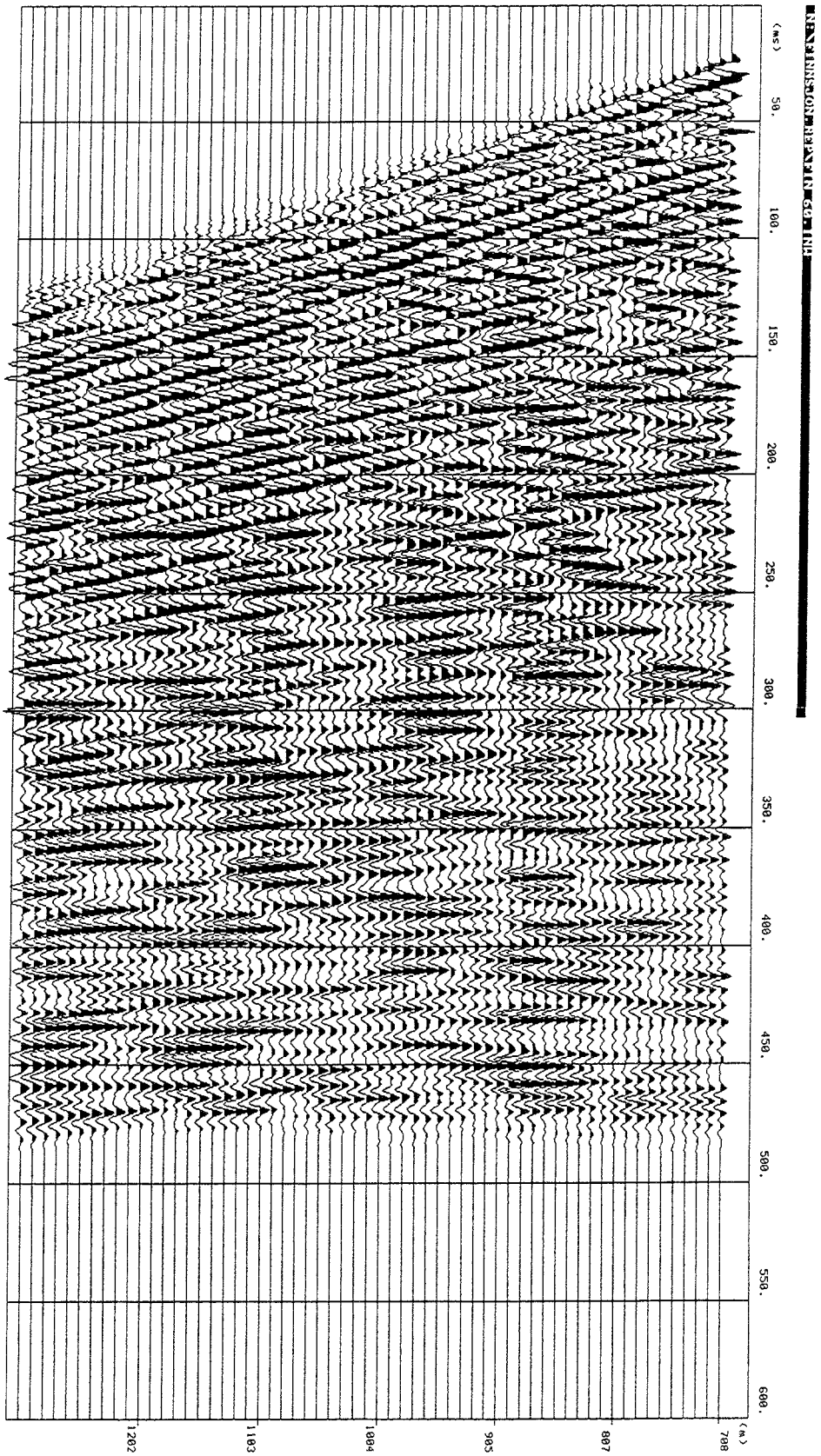

Figure 5-7 Two-way Image Point transformed shotgather data, record number 60.

5.3 STACKING

Here, the processing flow branches. One line goes directly to the CMP stack presented in Figures 5-8 and 5-9. The other line proceeds through the pre-stack migration presented in section 5.4. In the stacked profiles, the distance is marked in meters from the beginning of the measuring line, as shown in Figure 2-2. The difference between Figures 5-8 and 5-9 resides in the way the amplitude decay is compensated. Figure 5-8 was obtained by least squares fit of the function:

$$\acute{A}_{(t)} = A_{(t)}\, e^{\alpha}\, e^{\beta}$$

which conserves the amplitude ratio between adjacent cycles. In Figure 5-9, the 100 ms sliding window AGC was applied. It is arguable which way the result is better. We have chosen for subsequent processing the AGC profile from Figure 5-9.

5.4 PRE-STACK MIGRATION

The shotgather number 60 chosen as example is shown after migration in Figure 5-10. The smiling appearance is typical for pre-stack migration and the circular artifacts are bound to vanish after stacking.

The stacked profile resulting from the migrated shotgathers is presented in Figure 5-11. The aperture in the pre-stack migration was ±45° and the 5500 m/s velocity found in the static offset analysis was used.

5.5 TAU-P FILTERING OF THE STACKED PROFILES

The lack of outstanding reflectors in Figures 5-9 and 5-11 is mainly due to the characteristic seismic response of the crystalline rock mass. This has been observed before with cross-hole and VSP measurements. The conclusion reached then was that the extraction of meaningful information has to be based on phase consistency rather than on amplitude standout. As a means of enhancing the phase consistency Tau-P filtering was used. Figure 5-12 displays the result of Tau-P processing applied to the CMP stack from Figure 5-9. Figure 5-13 presents the same analysis applied to the pre-stack migrated profile from Figure 5-11.

The Tau-P filtering procedure follows the same lines as IP filtering applied to VSP. Firstly, the noise level is estimated in Tau-P space and the events

above this level, most probably representing main reflecting surfaces, are enhanced. The results of this processing step are presented in Figures 5-12 (CMP stacked data) and 5-13 (pre-stack migrated data). The aperture in the Tau-P transform was set to ±25°.

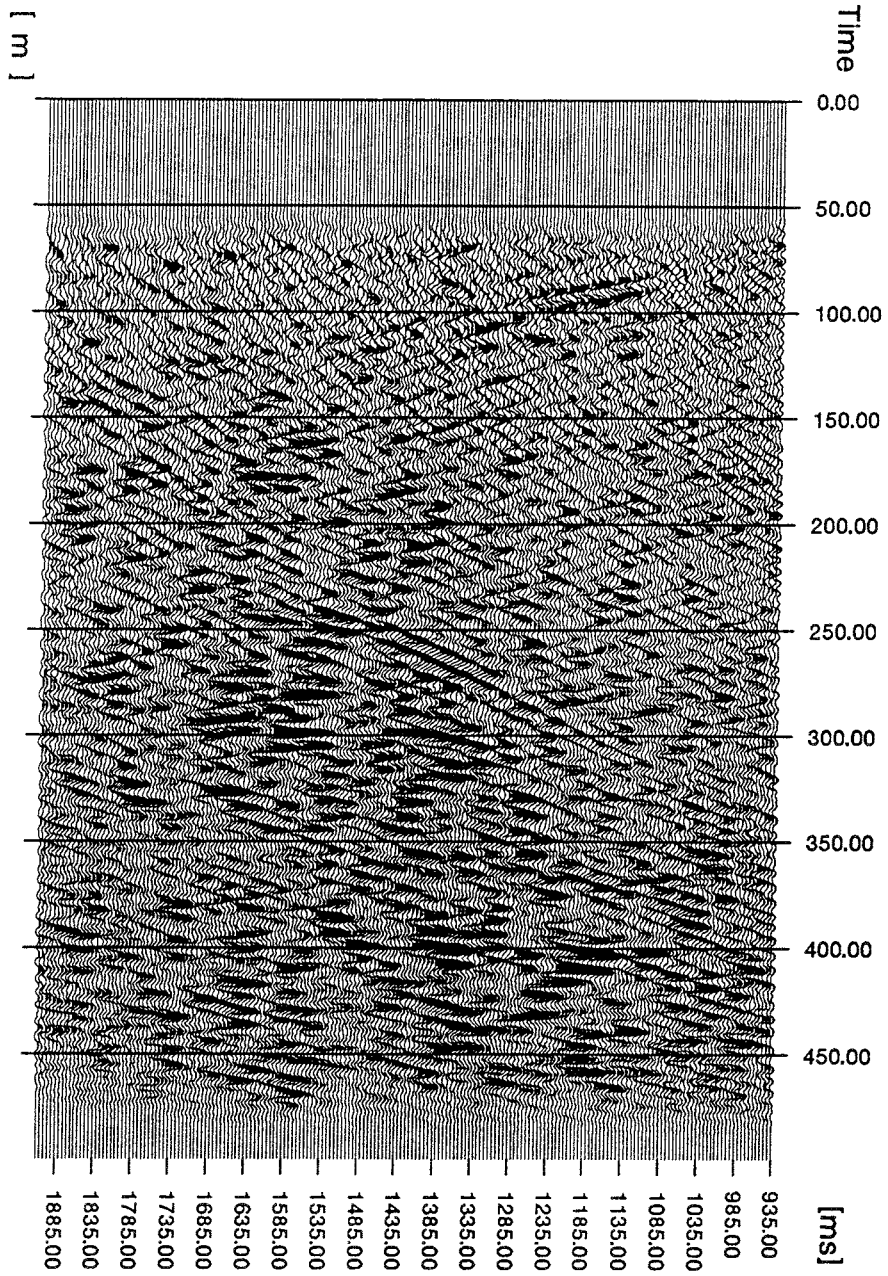

Figure 5-8 NMO-corrected and CMP-stacked data from Image Point processed shotgathers.

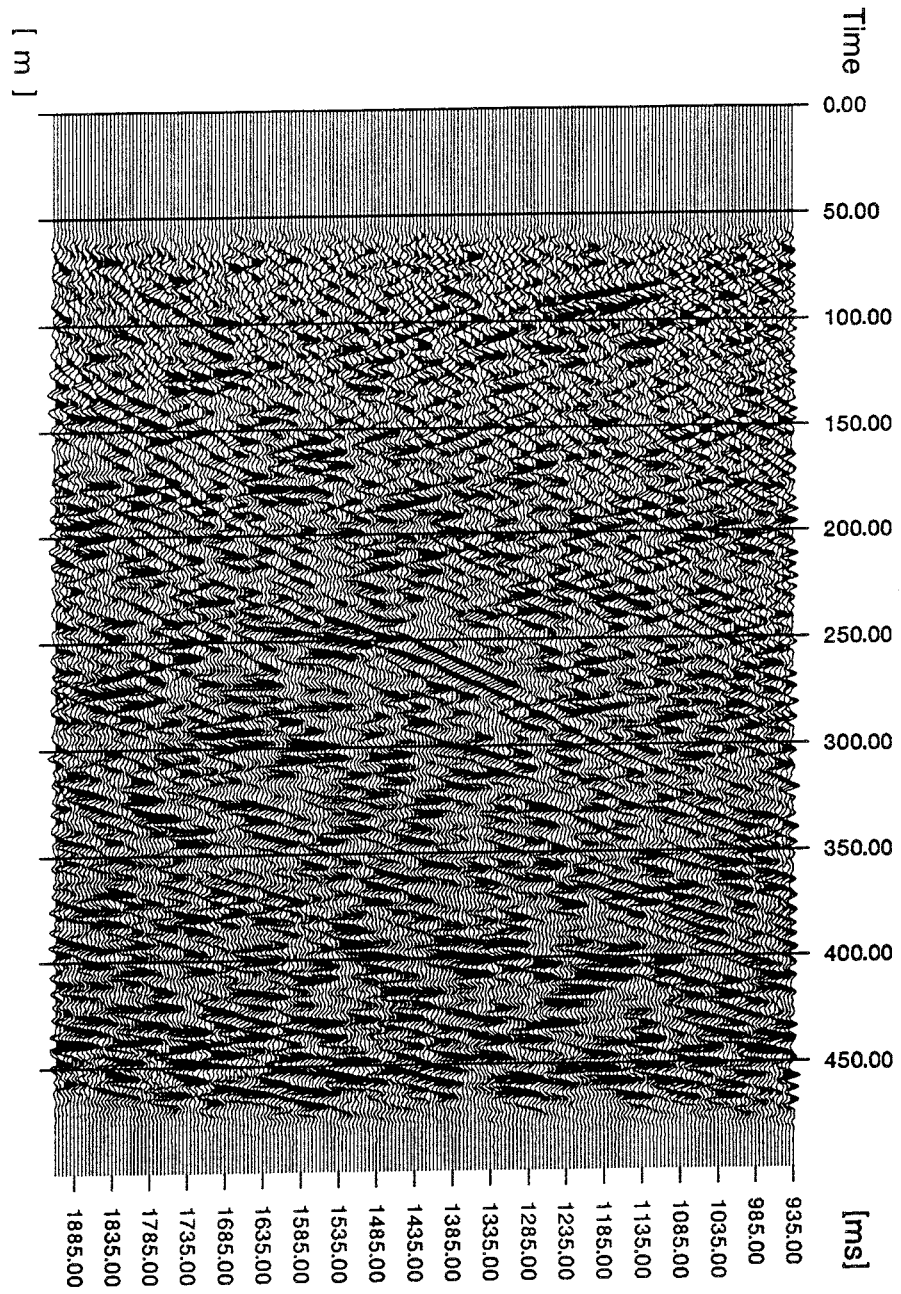

Figure 5-9 NMO-corrected and CMP-stacked data from amplitude equalized (AGC) and Image Point processed shotgathers.

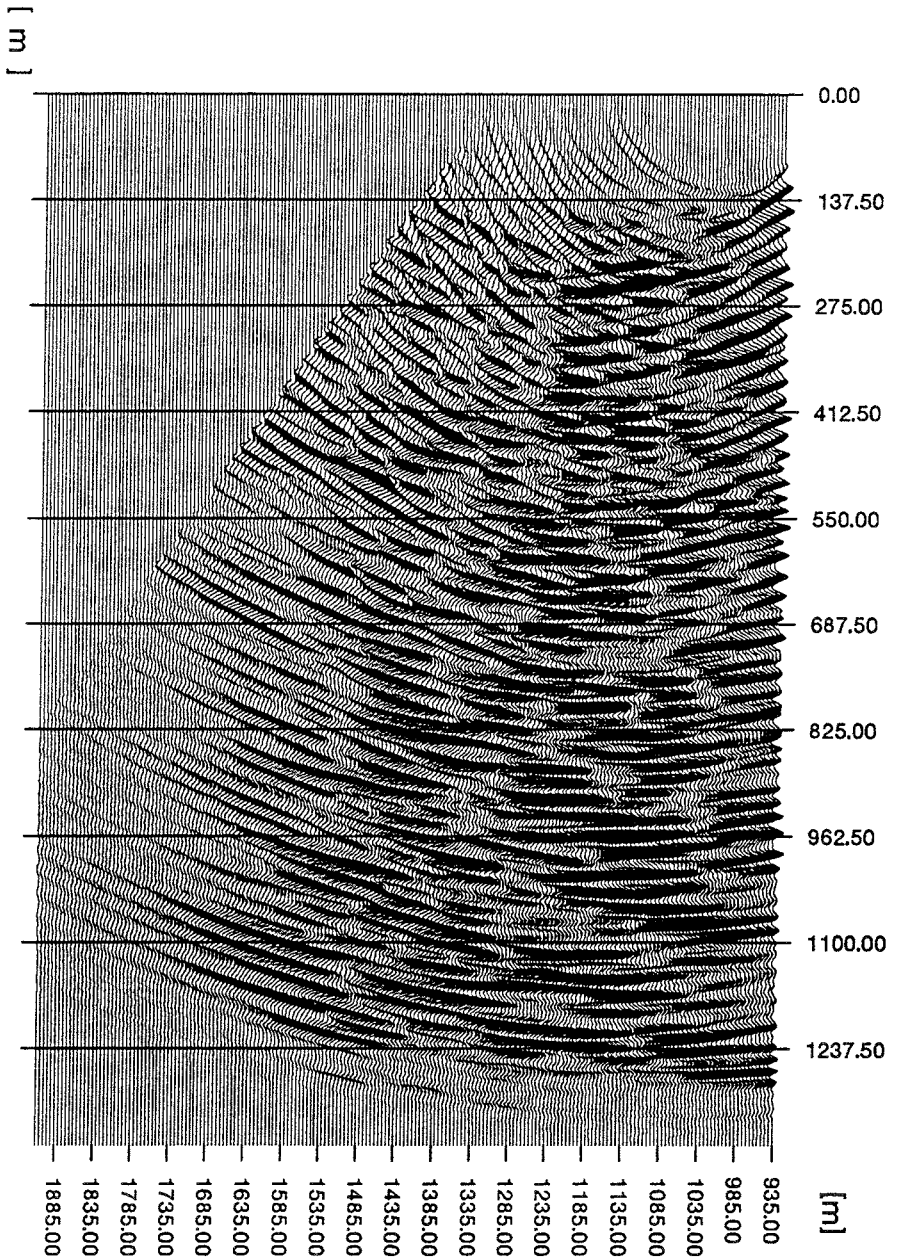

Figure 5-10 Pre-stack migrated shotgather data, record number 60, aperture ±45°, velocity 5500 m/s.

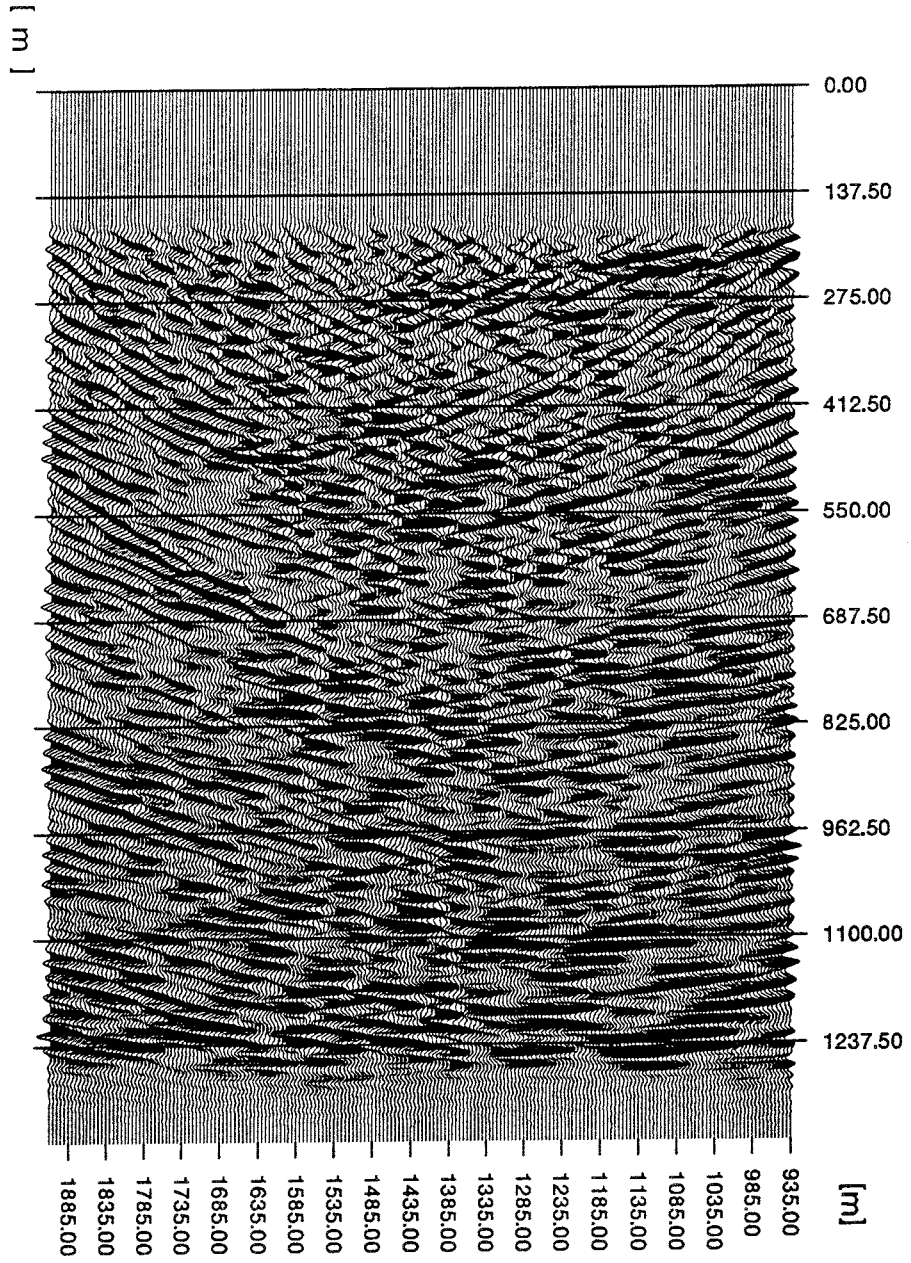

Figure 5-11 Stack of migrated shotgathers.

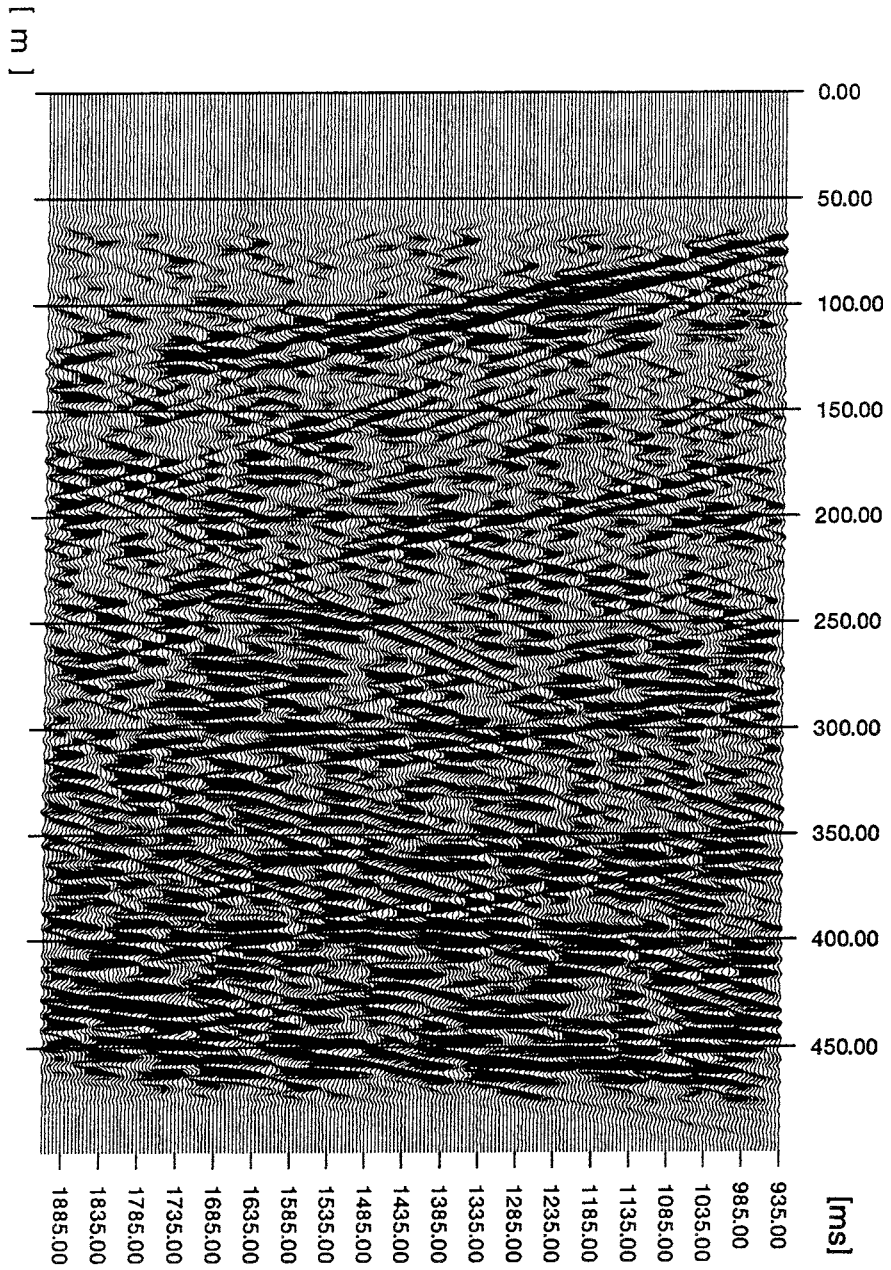

Figure 5-12 Tau-P processed CMP stacked data, apparent dips between -25° and +25°.

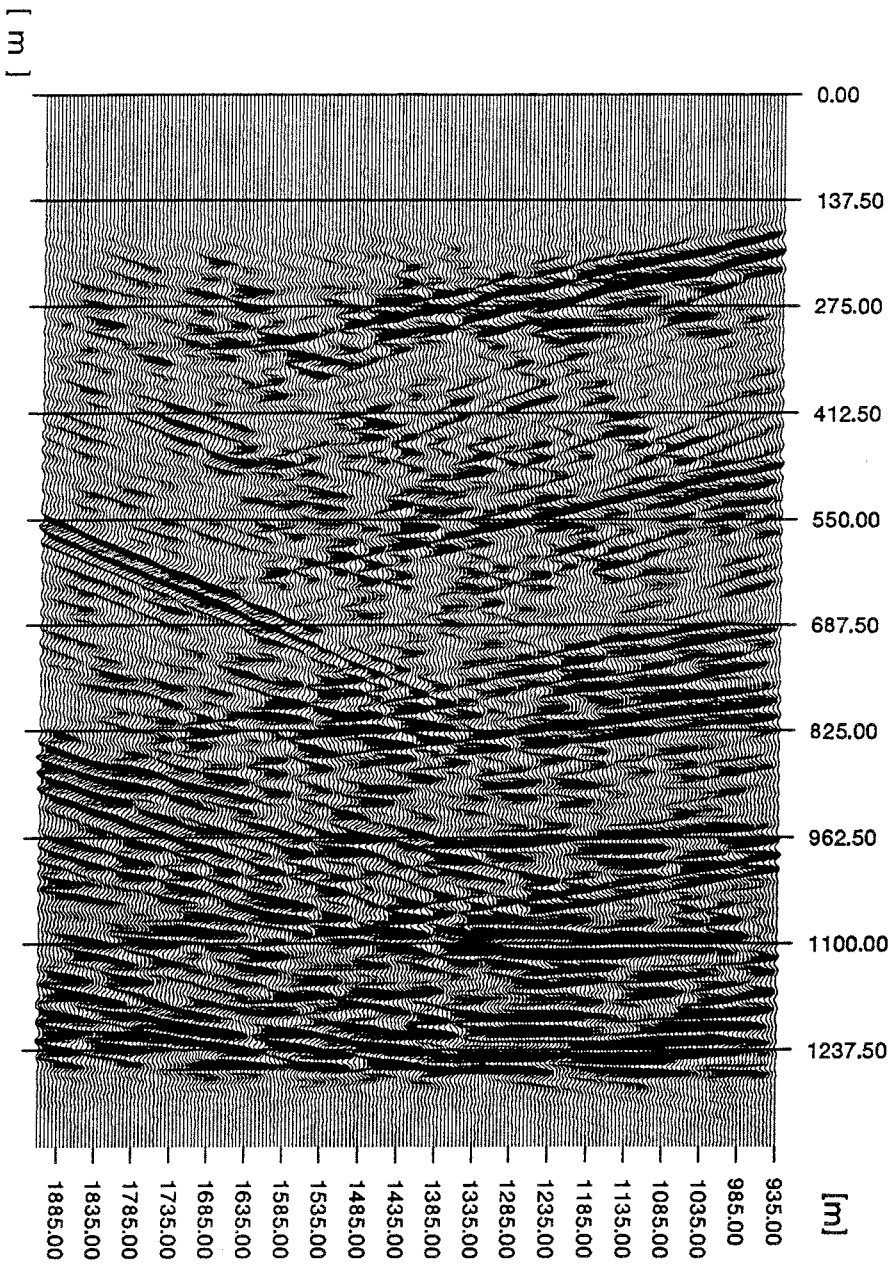

Figure 5-13 Tau-P processed pre-stack migrated data, apparent dips between -25° and +25°.

6 DISCUSSION ON REPROCESSING

6.1 COMPARISON OF PROCESSING RESULTS

Figures 4-6 and 5-3 represent early stages of the processing chain which are directly comparable for the two processing approaches. The same reflector geometries are seen here although the Vibrometric section has a static shift of about -12 ms compared to the Uppsala section. This static shift was introduced to correct for the low velocity overburden. The Uppsala processing did not correct for the overburden at this stage, but rather in the NMO stage of the processing using lower stacking velocities.

At the more advanced stage of processing represented by Figures of 4-3 and 5-9 the Vibrometric section shows a bias towards easterly dipping events resulting in that some steep westerly dipping events are not present on the section which are present on the Uppsala processing. This is due to the image point filter used which was biased towards easterly dips. For a proper comparison of the two sections, the data need to be resorted to receiver gathers and image point filtered again. This has not been done by Vibrometric since the main objective of the study was to image the sub-horizontal reflector Zone 2.

Figures 4-4 and 5-11 are reproduced as Figures 6-1 and 6-2 for the convenience of the reader. The figures are plotted to the same scale to facilitate comparison of the results. These figures show the migrated results where the reflectors are located at their "correct" distance from the survey line. It should be remembered that the reflectors do not need to be located below the survey line due to that reflectors are observed in 3-D space. Zone 2 appears as a distinct reflector in both figures at a depth around 200 m with a shallow dip towards west.

In the depth migrated sections (Figures 4-4 and 5-11) the depth to Zone 2 is similar (about 200 m) although different migration velocities were used. Uppsala used a lower migration velocity based on the lower observed stacking velocities. This lower migration velocity roughly canceled out the -12 ms shift introduced by Vibrometric after depth conversion. See section 6.5 for a analysis of the trade-off between static shift and stacking velocity.

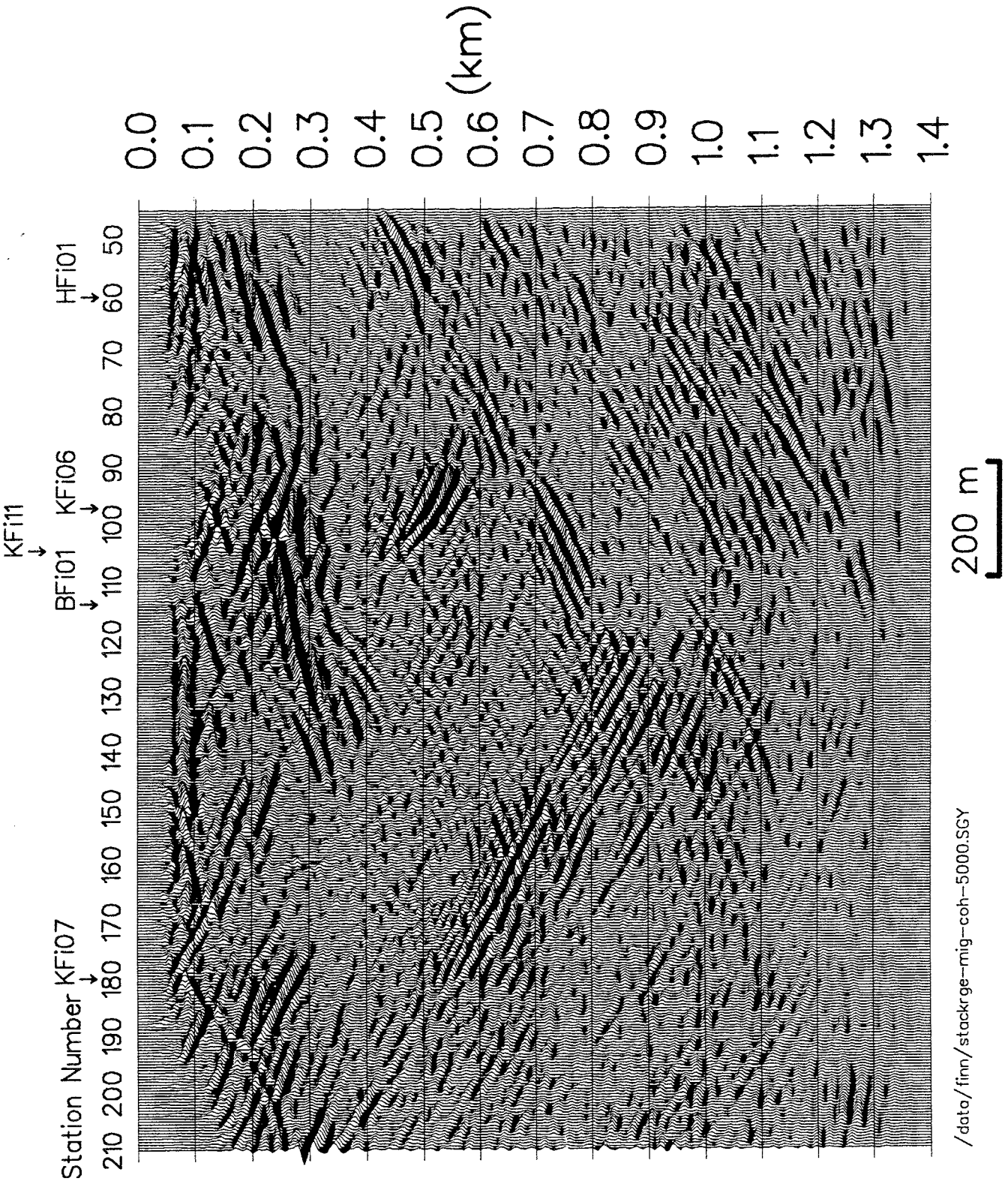

Figure 6-1 Migrated stack obtained after processing by Uppsala University (same as Figure 4-4).

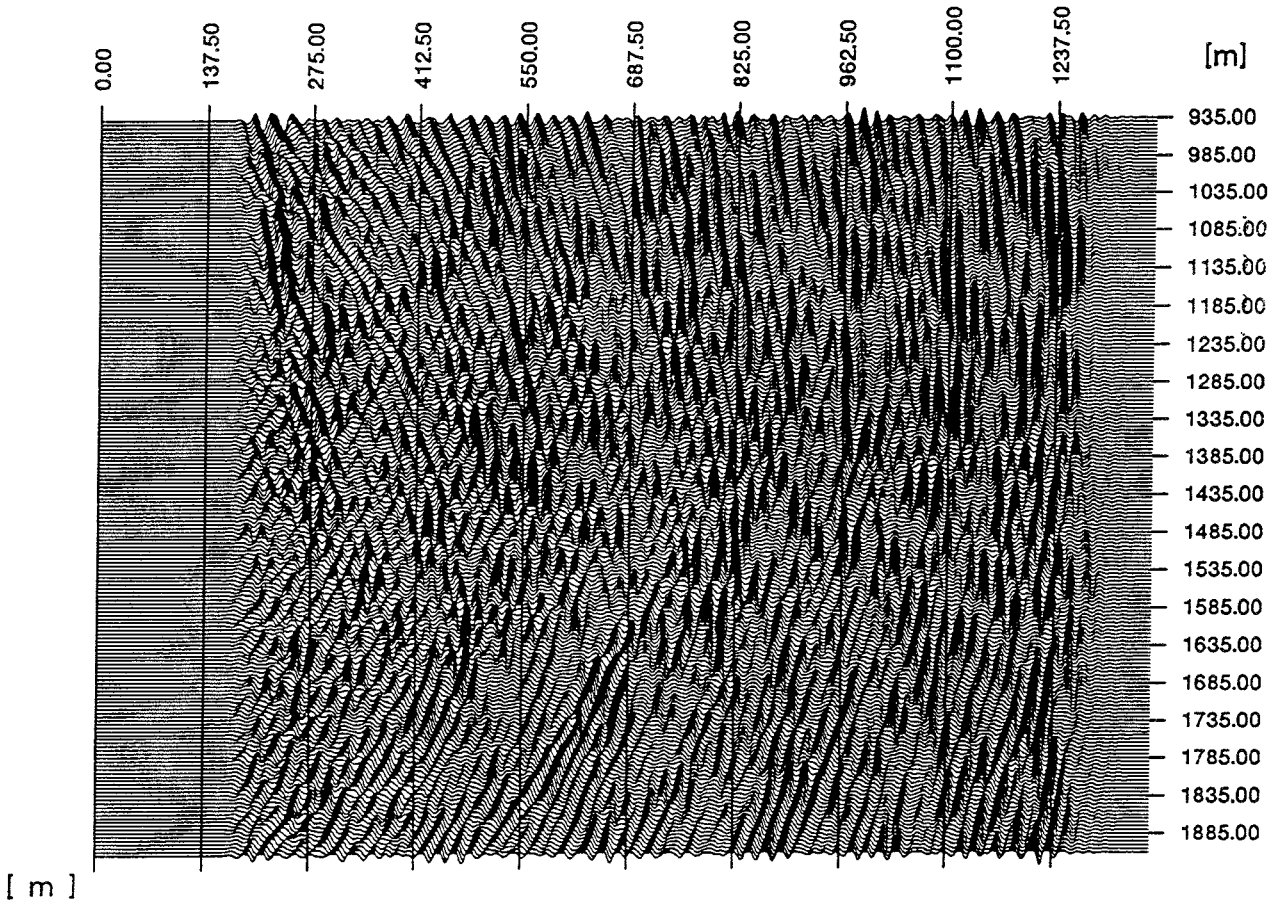

Figure 6-2 Final migrated stack obtained after processing by Vibrometric (same as Figure 5-11).

6.2 SIMULATION OF OTHER FIELD PARAMETERS

The acquisition parameters (120 dB dynamic range and 60 channels) used for the field experiment were unusual for 1987. At that time, 8-bit 24 channel systems were commonly used for "engineering" reflection surveys. As pointed out by Spencer et al (1993), there is a need improve upon even the most up to date field acquisition techniques for shallow surveys where it may be necessary to employ 240 channels or more. It is therefore of interest to simulate the results which would have been obtained using a 30 channel system and/or decreasing the number of shots. The following simulations were run where similar processing parameters to those listed in Table 3-1 were used except that no muting was applied. Simulations were done where:

- only the first 30 channels are included (Figure 6-3)
- only channels 31-60 are included (Figure 6-4)
- only every 5th shot is included (Figure 6-5)

It is interesting to note that zone 2 is hardly observed when only the first 30 channels are included in the stack (Figure 6-3), but shows up reasonably well when only channels 31-60 are stacked. This is somewhat of a paradox since one expects the near offset traces to provide the better image of such a shallow reflector. The reason for this observation may be related to the physical properties of the zone as discussed in next section or to effects of near offset noise. It would appear that only the upper 20-80 ms are sacrificed by having the near offset at 420 m (Figure 6-4). In reality, this is not the case since information has been used from channels 1-30 to calculate the statics and carry out the velocity analyses. However, it is clear that far offset data relative to the depth of the reflector must be recorded in this type of survey. Note that surveys carried out on Äspö to date used only 24 channel instruments.

If one tries to reduce the number of shots and save money on drilling costs then the image obtained is also significantly poorer (Figure 6-5). Zone 2 can approximately be traced as in Figure 4-3, but the image is much poorer and the statics and velocity resolution applied to the data would not be possible with only shots every 50 m. Instead, one should probably consider shooting not only at every geophone point, but also at halfway between geophone points to increase lateral resolution and fold. Note that most of the deeper steeply dipping events have not been imaged at all probably due to a reduction in fold.

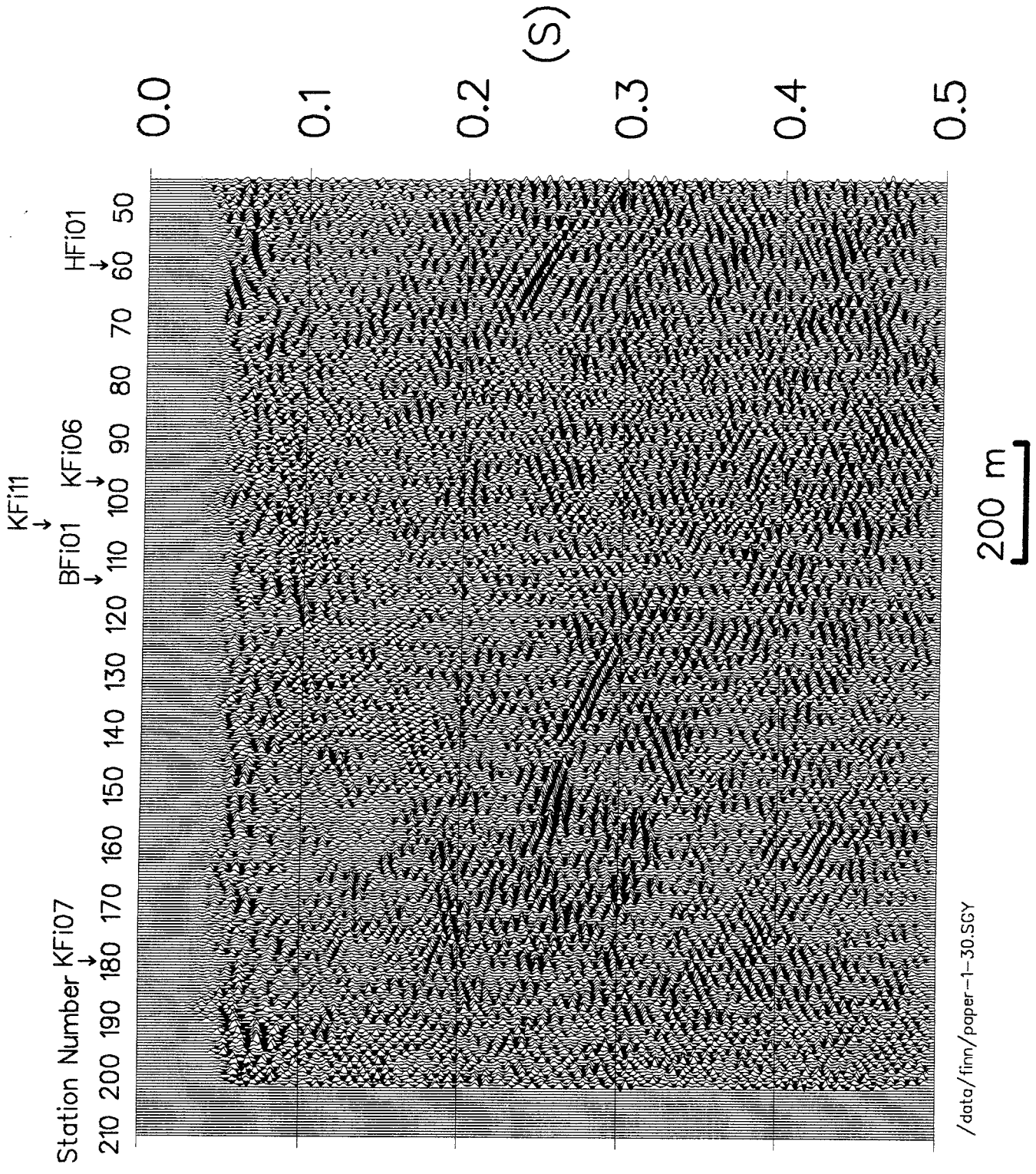

Figure 6-3 Similar processing as in Figure 4-3, but including only the first 30 channels. Station numbers correspond to those shown in Figure 2-2.

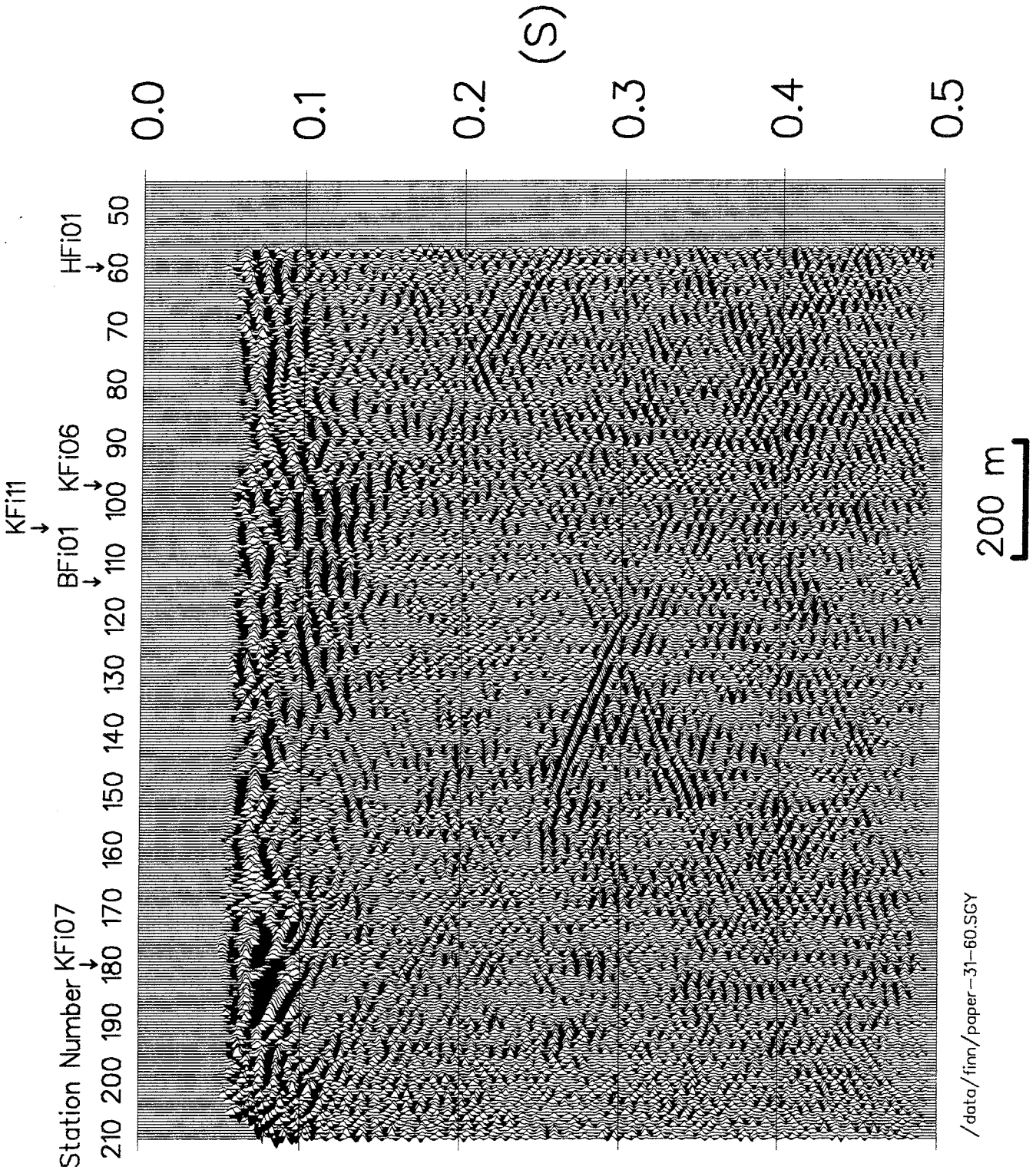

Figure 6-4 Similar processing as in Figure 4-3, but including only channels 31-60. Station numbers correspond to those shown in Figure 2-2.

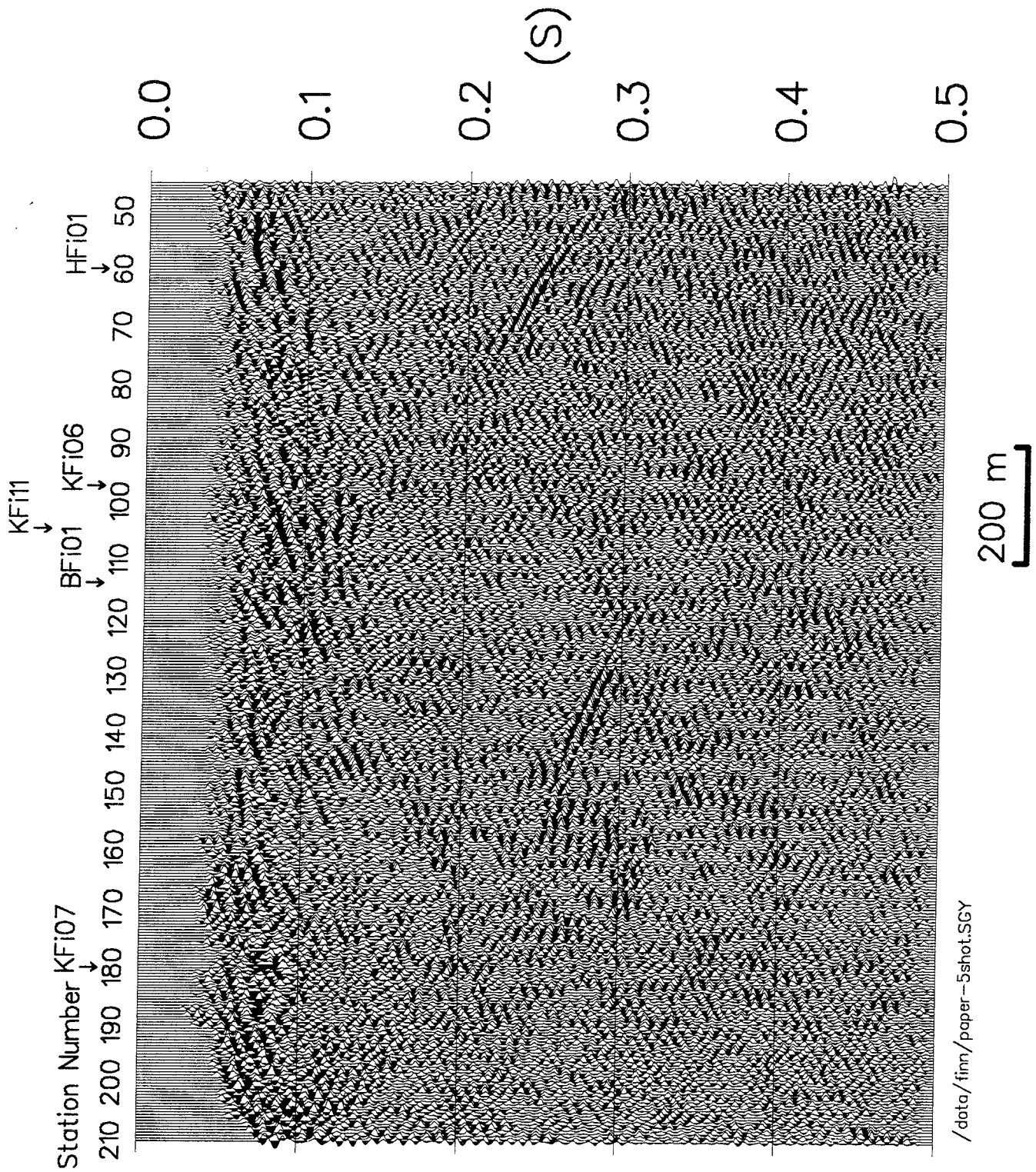

Figure 6-5 Similar processing as in Figure 4-3, but including only every fifth shotpoint. Station numbers correspond to those shown in Figure 2-2.

6.3 REFLECTION PROPERTIES OF FRACTURE ZONES

Given the rather surprising result that stacking of channels 31-60 give a better image of zone 2 than stacking of channels 1-30 it is of interest to investigate the reflective properties of fracture zones. In the oil and gas industry, significant research has been done on studying the amplitude of a reflection off an interface as a function of angle of incidence. It has been shown that in many cases the presence of gas in the rock below the interface will result in a substantial increase in the amplitude of the reflection with increasing angle of incidence. However, there are also cases where phase changes may occur which will result in a deterioration in the final section due to destructive interference when stacking. Figure 6-6 shows the expected traveltime curve for a fracture zone located at a depth of 150 m. The traveltime curves for the P-wave reflections agree fairly well with that marked as the reflection from zone 2 in Figure 4-1.

If the fracture zone has a Poisson's ratio which is close to that of the intact rock then the reflection coefficient will be negative at vertical incidence and decrease in magnitude gradually as angle of incidence increases up to about 45° whereafter it again becomes more negative (Figure 6-7). For such behavior it is desirable to measure as close to vertical incidence as possible. However, measurements too close will result in interference from the direct S-wave and ground roll (Figure 6-6). Note that the P and S wave velocities in Figure 6-7a do not conform to those in Figure 6-6, however, the important parameter is the contrast in Poisson's ratio between the two layers.

If a fracture zone contains larger quantities of water it is reasonable to expect its Poisson's ratio to be closer to that of water (0.5). In a highly permeable zone a value of 0.4 for a fracture zone may be reasonable, although very little data on this subject exist. Using this value, we find a significantly different behavior for the reflection coefficient as a function of angle of incidence (Figure 6-8). The initially negative reflection now rapidly becomes more positive and a phase change will occur at an angle of incidence of about 28°. Note also the higher amplitude of the converted S-wave compared to when Poisson's ratio is 0.25. Stacking of CDP data over the interval corresponding to channels 1-24 would result in destructive interference due to the phase change. However, stacking at farther offsets will result in constructive interference. It is not obvious from examining the shot sections that a phase change occurs, but the above behavior may play an important role in our ability to image permeable fracture zones. Although the above explanation is possible, a simpler one is the presence of shot generated noise. The shot generated noise is less on the far offset traces than on the near offset traces. More experimental and seismic data are needed to evaluate these factors.

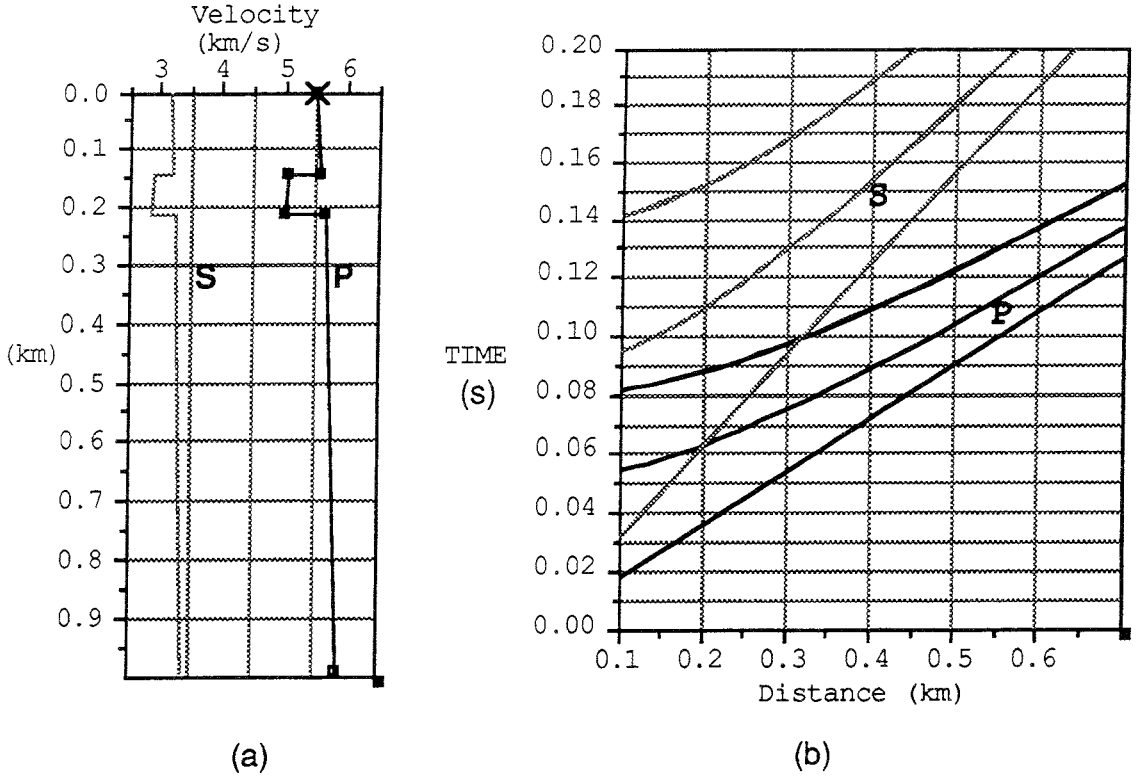

Figure 6-6 a) Velocity model for Zone 2 and b) travel time curves for P and S waves including direct waves and reflections off the top and bottom of the fracture zone.

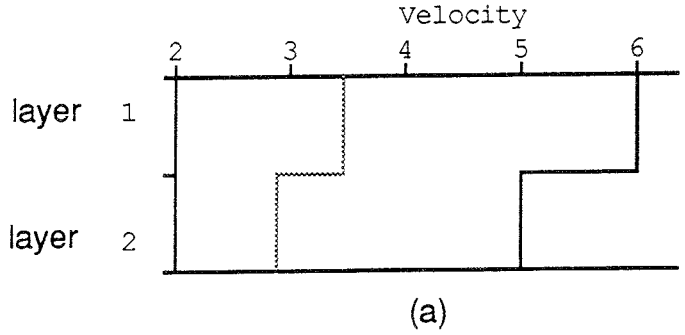

(a)

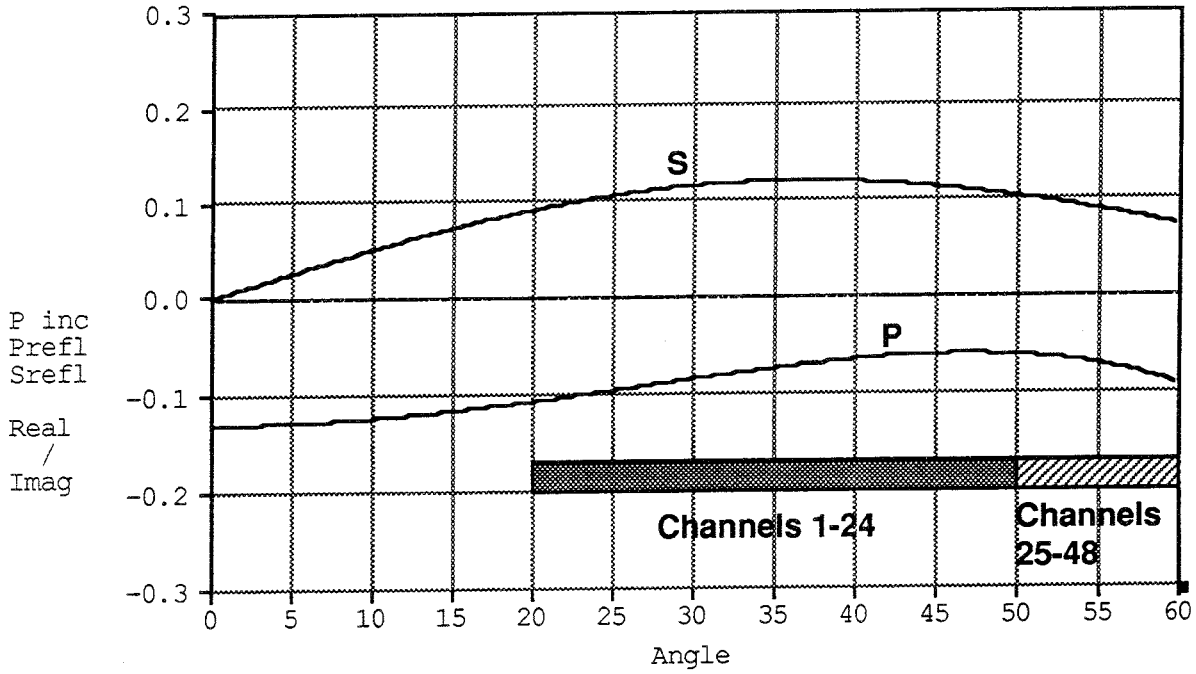

(b)

Figure 6-7 (a) P and S wave velocities at intact/fractured interface where Poisson's ration in the fracture zone 0.25, the same as in the intact rock. Density were set 2.65 g/cm^3 and 2.60 g/cm^3 in layer 1 and layer 2, respectively. (b) P and S wave reflection coefficients as a function of angle of incidence for the model in (a). Corresponding channel intervals for angles of incidence are based on the geometry shown in Figure 6-6.

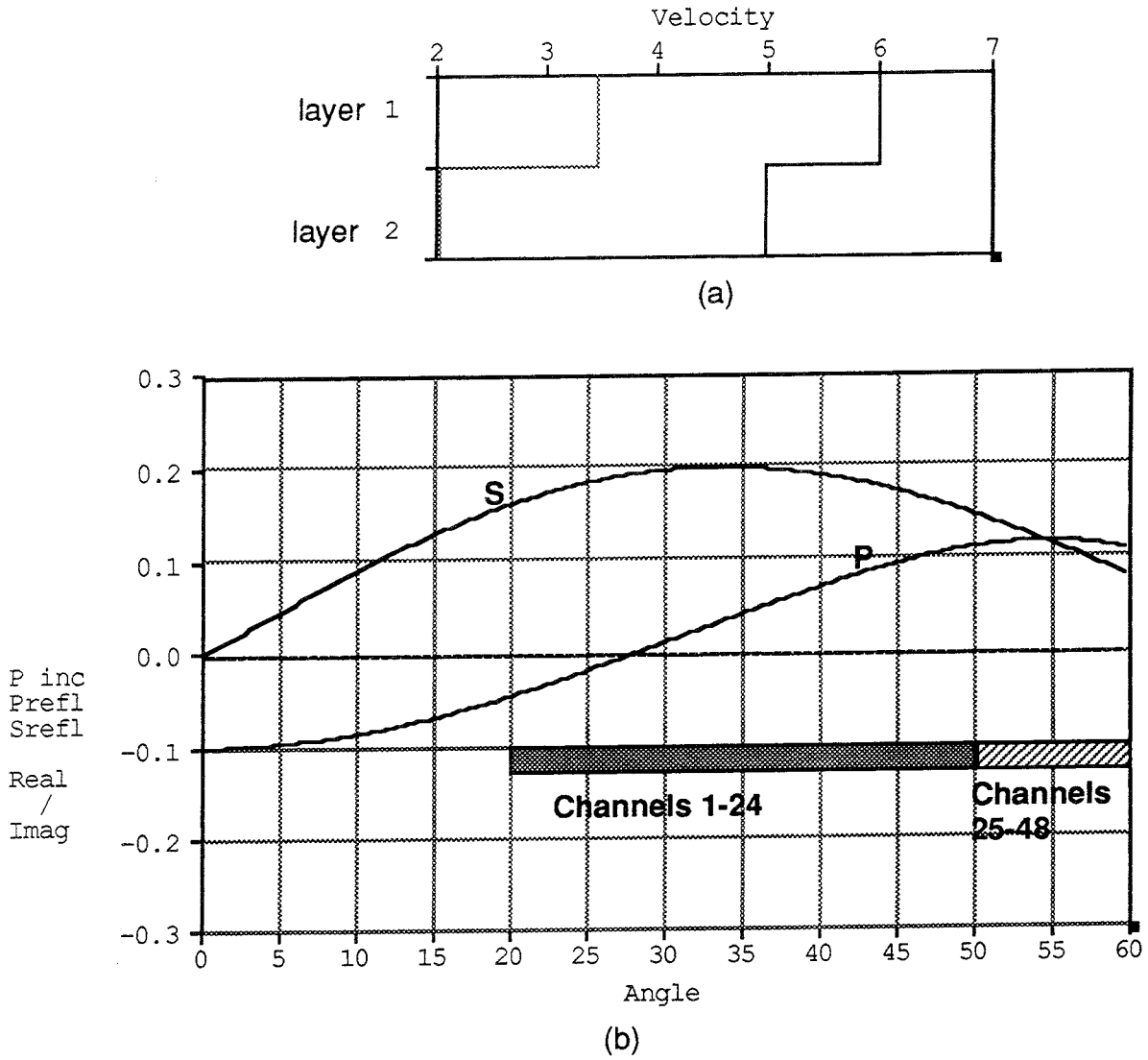

Figure 6-8 (a) P and S wave velocities at intact/fractured interface where Poisson's ratio in the fracture zone 0.4, considerably higher than in the intact rock. (Density were set 2.65 g/cc and 2.60 g/cc in layer 1 and layer 2, respectively. (b) P and S wave reflection coefficients as a function of angle of incidence for the model in (a). Corresponding channel intervals for angles of incidence are based on the geometry shown in Figure 6-6.

6.4 ANISOTROPY CONSIDERATIONS

The gneissic character of granodiorite implies that the rock is probably anisotropic. The degree of this anisotropy may be high as has been found for other similar rocks. If high, then the anisotropy will have to be taken into account when migrating the seismic image to its proper spatial position. The high fracture frequency and stress regime may also influence the anisotropic behavior of the rock and seismic wave propagation through it. Based on 2-D acquisition data it is not possible to evaluate the influence of anisotropy on the results.

6.5 BOREHOLE SEISMIC DATA FROM FINNSJÖN

Sonic logging has been performed in borehole BFi02 (Ekman et al., 1988). This log determines the P-wave velocity along the borehole with a resolution of approximately 0.3 m. A filtered version of this log is shown in Figure 6-9. Filtering was done by forming the average of the P-wave travel time for 1 m intervals along the borehole. The average velocity in the uppermost 40 m of the rock is approximately 5.9 km/s. This interval includes several significant low velocity anomalies. For the interval from 40 m to the top of fracture Zone 2 at 204 m the average velocity is approximately 6.2 km/s. There is an approximately 10 m wide low velocity anomaly at the upper boundary of zone 2 where velocities go down to 5.7 km/s. Then there is a 40 m wide interval where velocities generally are above 6.2 km/s. The most significant low velocity anomaly is located in the interval 253-265 m where velocities as low as 4.6 km/s have been observed. The average velocity in this interval is approximately 5.4 km/s. Below this interval velocities are above 6.0 km/s.

Seismic velocities of the rock have also been estimated from tube wave surveys made in boreholes BFi01 and KFi06 (Stenberg, 1987). A tube wave survey is a type of VSP survey with the objective to identify permeable zones intersecting the borehole. The survey in borehole BFi01 yielded an average P-wave velocity of 5.99 km/s and an average S-wave velocity of 3.7 km/s. The corresponding results from borehole KFi06 were 5.86 km/s and 3.7 km/s for the P- and S-wave velocities, respectively.

The P-wave velocities obtained from the borehole measurements are generally higher than the stacking velocities used in processing of the seismic data. The contrast between zone 2 and the surrounding rock is essentially the same as what was assumed in the analysis of reflection properties presented in Section 6.3. The borehole data indicate that Zone 2 consists of at least two about 10 m wide low velocity zones, one at the top

and one at the bottom of the zone. This observation is corroborated by geological and hydrogeological data.

The difference between stacking velocity, as well as refraction velocities, from the sonic and VSP velocities can have several explanations. One, the difference may be due to anisotropy, the VSP and sonic log measure vertical velocities while the refracted waves, and to a large extent the reflected waves, measure horizontal velocities. A second factor, in the case of the reflected waves, is the near surface low velocity layer. This layer introduces essentially a static shift in the data. If not accounted for, this static shift will reduce the observed stacking velocities (Figure 6-10). Assuming the reflection time may be modeled as

$$T=dt+(T_0+x^2/v^2)^{0.5}$$

where dt is the static shift. Then the observed NMO velocity will be lower if dt is positive and greater if dt is negative. For example a delay in dt of 12 ms (positive static) over an otherwise constant velocity medium of 5500 m/s will result in an observed stacking velocity of about 5250 m/s. If the shift is 20 ms then the observed stacking velocity will be about 5150 m/s. Uncertainties about this upper low velocity layer will affect the observed stacking velocities and thus the migration velocities, as well as comparisons with vertically measured borehole velocities.

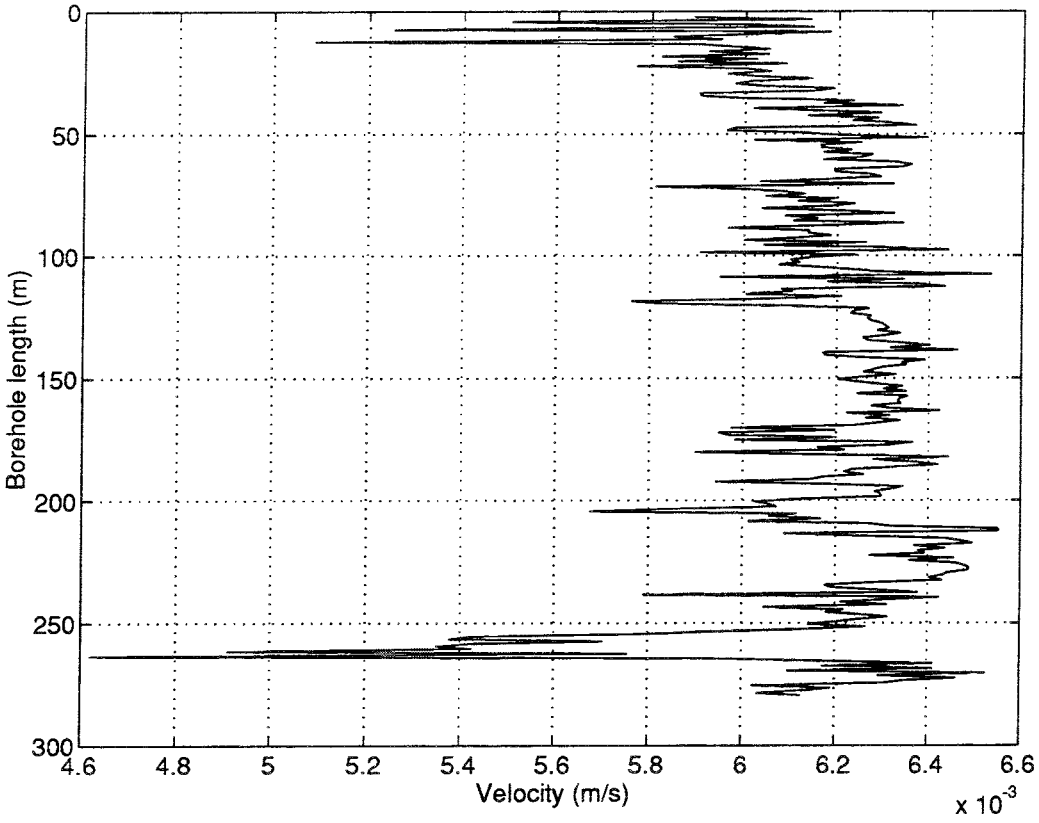

Figure 6-9 Sonic velocity log for borehole BFi02. The upper boundary of Zone 2 is interpreted to be at 204 m.

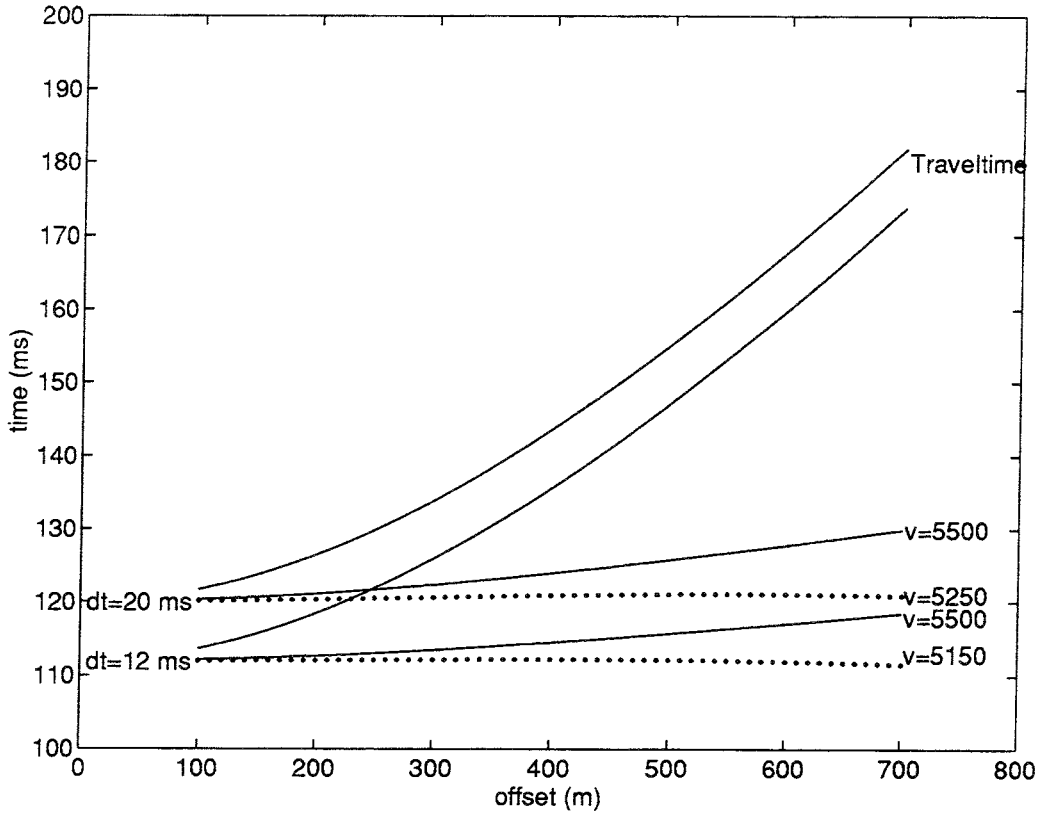

Figure 6-10 Reflection travel times for a reflector located at 100 ms below the low velocity layer in a constant velocity media of 5500 m/s. The low velocity media adds a static shift to the travel times resulting in that lower velocities need to be used when NMO correcting the data.

7 COMPARISON WITH GEOLOGIC INFORMATION

7.1 FRACTURE ZONE 2

If the correct migration velocity has been used then Figures 6-1 and 6-2 form a basis for interpreting the seismic data. Information concerning the occurrence of known fracture zones from boreholes lying near the profile have plotted on top of the migrated seismic section (Figure 7-1). The spatial location of zone 2 east of station 150 agrees well with borehole data, however, it is not clear if the zone extends west of station 150. Instead, what has been labelled zone 2 in borehole KFi07 appears to correlate with a moderately easterly dipping zone, as does the zone 9 above and zone 6 below, respectively. Zone 5 in borehole KFi06 appears to correlate with the high amplitude steeply easterly dipping reflector. Note, that some of the reflections observed on the section may be coming from out of the plane of the profile and that 3-D data is necessary to determine their true strike and dip. In general, there is good correlation between the observation of fracture zones in the boreholes and the location of seismic reflectors on the migrated section.

Although there is good correlation between zone 2 as defined from the borehole data with the seismic, there are some important differences. 1) The zone does not appear to be planar between boreholes BFi01 and HFi01 as interpreted in other reports (Ahlbom et al., 1992). However, the data quality is rather poor between stations 80 and 100 and its appearance may be the result of it being poorly imaged in this interval rather than it truly being non-planar. In addition, there appears to be another reflector of opposite dip cutting across zone 2 over this interval which may be interfering with the reflection from zone 2. Special processing may be required to separate out such interference effects. 2) Zone 2 does not appear to extend west of station 160. This may either be due to zone 2 changing character, eg. becoming less reflective due to decreasing porosity, or to it being cut off by a fault. Vertical faulting has been interpreted in the vicinity of station 150 (Ahlbom et al., 1992), but not with displacements on the order of magnitude suggested by the seismic data. Further processing with different filtering and velocity parameters gave an indication of a continuation of the zone but this was by no means conclusive.

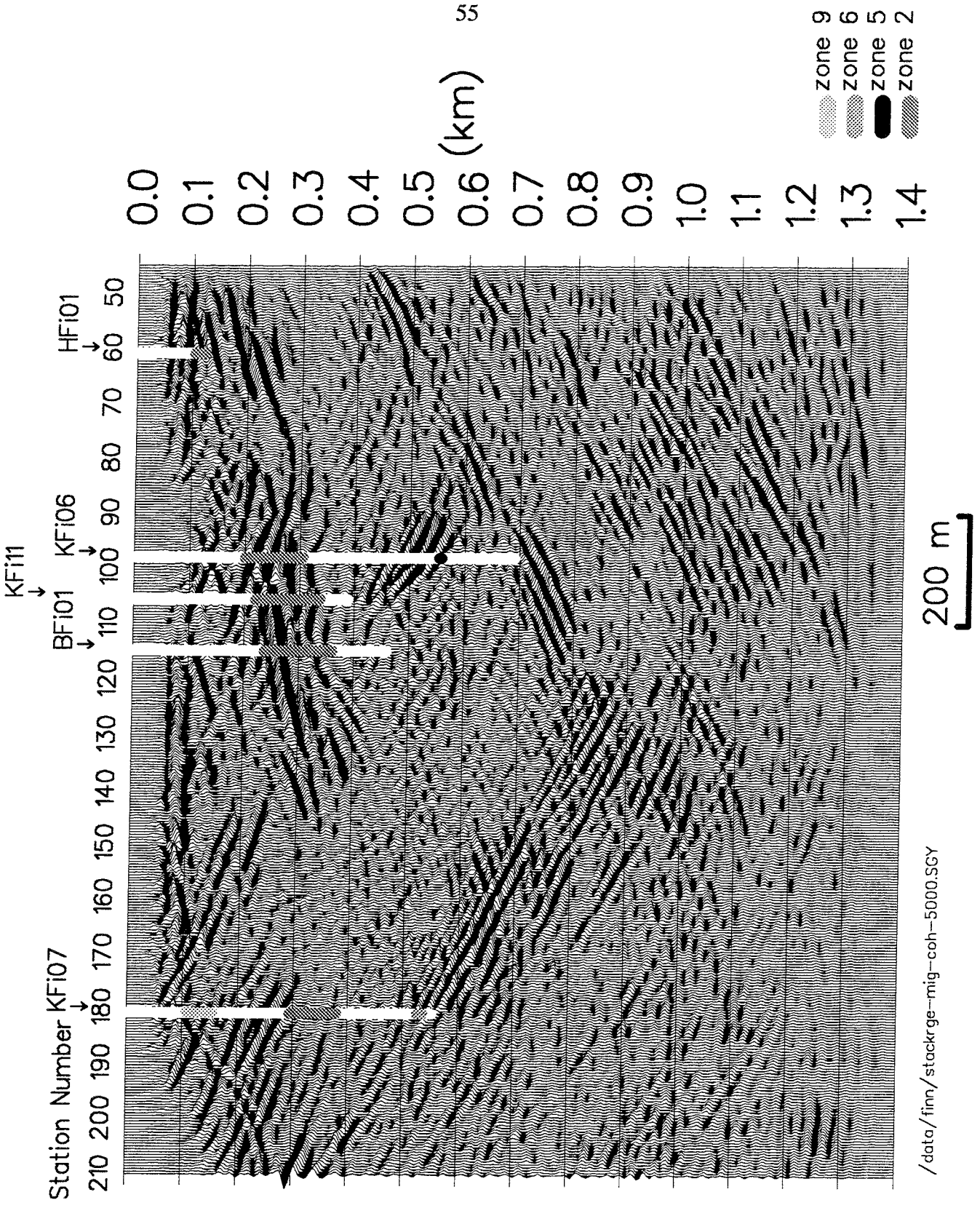

Figure 7-1 Final stack shown in Figure 4-3 after migration (point 16 in Table 4-1). Information about known fracture zones from nearby boreholes have been mapped onto the section.

7.2 DEEPER ZONES

In addition to the fracture zones observed in the boreholes, there are a number of deeper reflectors which have not been drilled through to any greater extent. On the migrated section (Figure 7-1), only two of these are present since the others observed on the time section (Figures 4-2 and 4-3) have migrated off the section. The profile needs to be extended considerably in both directions in order that all of the dipping zones observed on the time section not migrate off the edges of the profile. In addition, the deeper part of the western half of the profile is biased towards reflections with an easterly dip, since westerly dipping reflectors would not have been imaged on the time section, and the reverse is true for the eastern half. With this in mind we may expect the westerly dipping reflector starting at about 400 m at station 45 and going to about 900 m at station 150 to extend past this point if the profile is extended to the west. The reverse is true for the westerly dipping reflector starting at about 300 m at station 210 and extending to about 900 m at station 130. In fact this reflector projects to the surface to the eastern shore of Lake Finnsjön where the steeply dipping zone 14 has been identified (Figure 2-2) which may be part of a larger northerly trending lineament (Ahlbom et al., 1992).

Inspection of the time section (Figures 4-2 and 4-3) indicate there to be a series of relatively steeply dipping zones parallel to and below the ones discussed above. To image these properly and trace them properly would require considerable extension of the profile in both the east and west direction with larger shots being fired for the deeper sections.

7.3 MIGRATION VELOCITY

The migration velocity used by Uppsala University was 5000 m/s which results in almost perfect agreement with the location of zone 2 in the boreholes with its position on the seismic section. A higher velocity, such as 5500 m/s, which is close to the velocity of the direct P-wave, would result in its position on the seismic section being somewhat deeper than in Figure 7-1 and the agreement between fracture zones in the boreholes and events on the seismic section would not be nearly as good. However, 5000 m/s is probably a better choice for a migration velocity. Stacking velocities to zone 2 are generally around 5300 m/s (Appendix B) and it is common to use migration velocities lower than the stacking velocities in seismic data processing. The good agreement in Figure 7-1 also justifies a migration velocity of 5000 m/s. Since no bulk static shifts were applied on the Uppsala processing the near surface low velocity layer reduces the obtained stacking velocity and migration velocities.

8 GEOPHONE AND SHOT COUPLING ANALYSIS

8.1 INTRODUCTION

After presentation of results (Sections 4 and 5) from reprocessing of data from the Finnsjön seismic reflection experiment in April 1993, it was decided that an analysis should be carried out to determine the effect of local geological factors on the quality of the shot gathers recorded. One of the goals of the study was to determine if shots fired in loose sediments or glacial till are of poorer quality than shots fired in bedrock. This is highly relevant for production seismic reflection acquisition since acquisition costs will increase significantly if the source needs to be placed in bedrock in order to obtain high quality data.

Out of the 139 shots analyzed, 124 of these were fired in bedrock, the remaining 15 were fired in the overlying peat or till. In addition, 62 of the 139 shots had no cover at all. Only one shothole did not penetrate into the bedrock. The thin cover in this area may make the current data set atypical for Swedish conditions in general, but perhaps not for a nuclear waste disposal site where a thin overburden may be an advantage for the siting.

In addition to analyzing the shot strength as a function of geological factors, some minor analyses of frequency content as a function of geological factors have also been carried out. It was not possible to carry out a complete analysis, as with the shot strength, since this would have required a significant programming effort.

The extraction of the shot strength in a surface consistent manner allowed for the average amplitude decay with distance of the first arrivals to be extracted from the data. This decay function has been used to estimate Q, or the damping factor, for the area.

8.2 DATA PROCESSING

8.2.1 Theory

There are several factors which affect the strength of the signal recorded on a seismic trace and the problem of extracting the shot strength from the data is not trivial (see Juhlin (1990b) for a review of some of the factors).

Fortunately, oil companies have long been interested in extracting true amplitude information from seismic data and routines exist to analyze reflected waves for their changes in amplitude with offset. These same routines may be used to extract both the shot strength and the geophone coupling factor from seismic data where the fold is high. The routines are based upon the assumption that the amplitude of a recorded event may be decomposed into four components

$$a=s*g*o*c \qquad \textbf{(8-1)}$$

where a is the recorded seismic response, s is the shot component, g is the geophone component, o is the offset component, c is the CDP component or geological component and (*) denotes convolution. Taner and Koehler (1981) present a method to solve equation (8-1) in a surface consistent manner. Surface consistent implies that the solution is such that s and g are constant at each shot and receiver location for the entire data set, that is the same shot and receiver corrections will be applied at each station regardless of any other factors.

Although equation (8-1) was developed for applications on reflected waves for amplitude versus offset studies and static correction problems, it can also be applied to direct waves. However, in this case c takes on a different meaning. For reflected waves c is roughly proportional to the normal incidence reflection coefficient. For refracted waves it will be related to the transmission properties of the media.

When solving for the shot and geophone responses, the output from the program used gives a scaling factor for each shot and geophone location. A small value for the scaling factor indicates that, relative to all the other stations, the amplitude component of that shot or geophone station is greater than the average, while a large value indicates that the component is less than average. A value of around one indicates the shot or geophone position is around average.

8.2.2 Parameters

The seismic data were corrected for shot and receiver static corrections and then bandpass filtered into two subsets, a P-wave set and an S-wave set. The P-wave set were filtered with a 120-360 Hz bandpass filter and the S-wave set with a 60-180 Hz filter. The amplitudes were analyzed in a first arrival window of 100 ms for the P-wave set and for a 300 ms window for the S-wave set and were used to determine the shot and geophone scaling factors. The locations of the windows were based upon a P-wave first arrival velocity of 5500 m/s and an S-wave velocity of 3000 m/s. In those cases

where a shot had been fired twice in the same shothole, only the data from the first shot were included in the analyses.

Figure 8-1 shows one of the stronger and one of the weaker shots along the profile prior to scaling for shot corrections only. There is about a 10 times difference in scaling factor for the two shots. The scaled shots show the same general amplitude level indicating that the program is working as expected. Note the significant difference in amplitude levels at various offsets due to no geophone corrections having been applied.

8.3 RESULTS AND DISCUSSION

8.3.1 Charge profile

Inspection of Figure 8-2 shows that most of the shots were fired in bedrock near the bottom of the shotholes, however there are a number of shots that were fired quite shallow in the shotholes. Eight shots were fired at depths of 1 meter or less, but all within bedrock or at the bedrock-till interface. These shots were fired at stations 71, 72, 94, 100, 101, 116, 128 and 162. A factor which is believed to be important in the analyses, but is not being considered here is if the shots were fired above or below the ground water level. The observers logs show that most of the shots on the eastern part of the profile were tamped with water while most of the shots on the western side were tamped with sand. It is assumed that shots tamped with water were fired below the ground water table. In future studies the ground water depth needs to be recorded accurately.

8.3.2 Shot response

The P and S-wave shot responses were calculated over different windows, frequency ranges and wave types, however, the resulting scaling factors show similar behavior (Figure 8-3) although there are important differences. It is generally assumed that shots fired in bedrock produce higher quality data than shots fired in the till or loose sediments overlying the bedrock. A plot of P-wave scaling factor versus depth into bedrock (Figure 8-4) appears to confirm this. However, a plot of P-wave scaling factor versus simply depth shows a more consistent trend (Figure 8-5). It appears that in this data set the most important factor for generating strong P-wave energy is the depth the shot was fired at, regardless of the type of material it was fired in. A similar plot for S-wave scaling factor versus shot depth shows no such trend (Figure 8-6) and it appears that the S-wave shot strength must be related to some other factor.

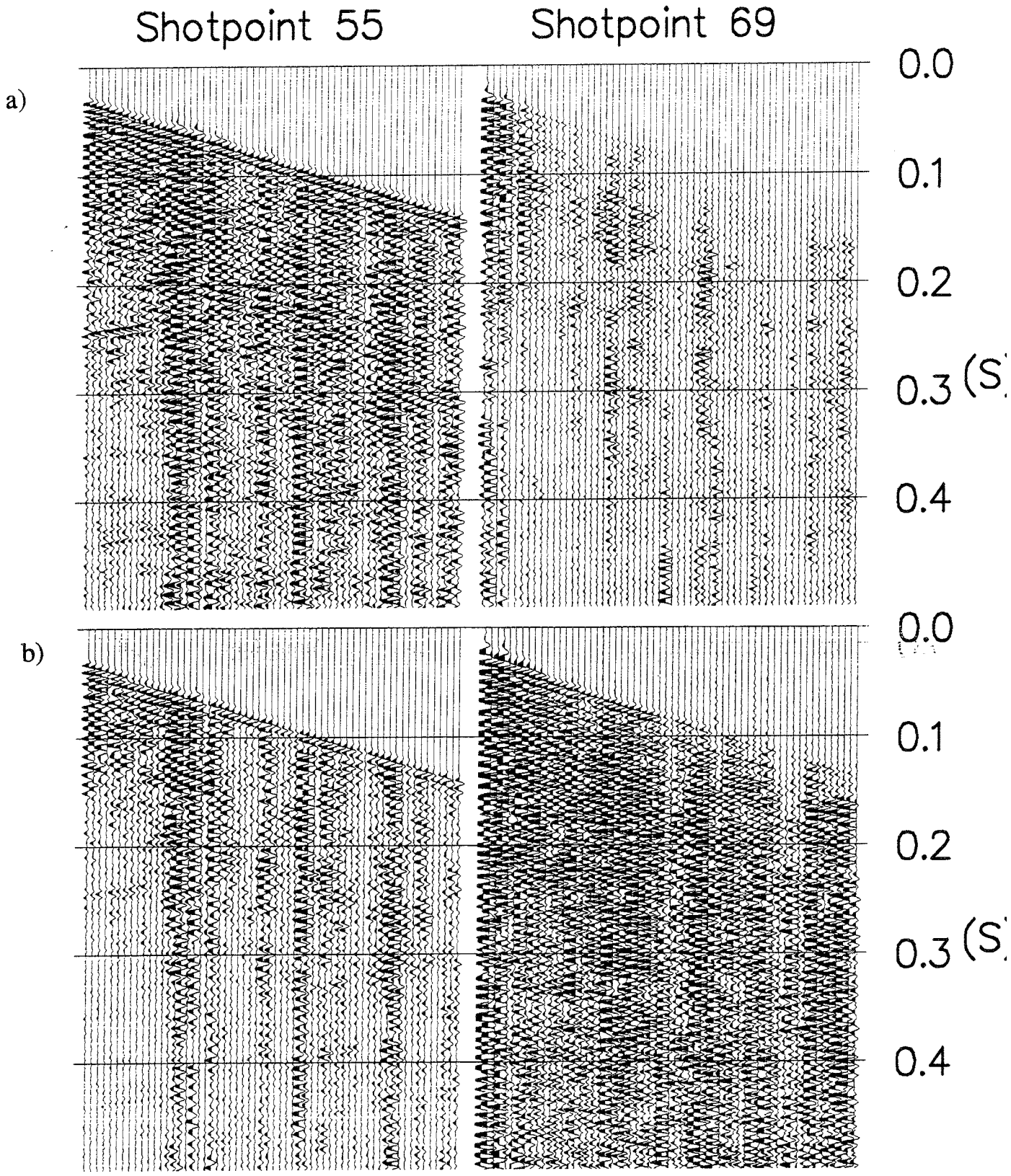

Figure 8-1 a) Bandpass (120-360 Hz) spherical divergence corrected shot gathers before shot scaling has been applied, b) same gathers after application of shot scaling.

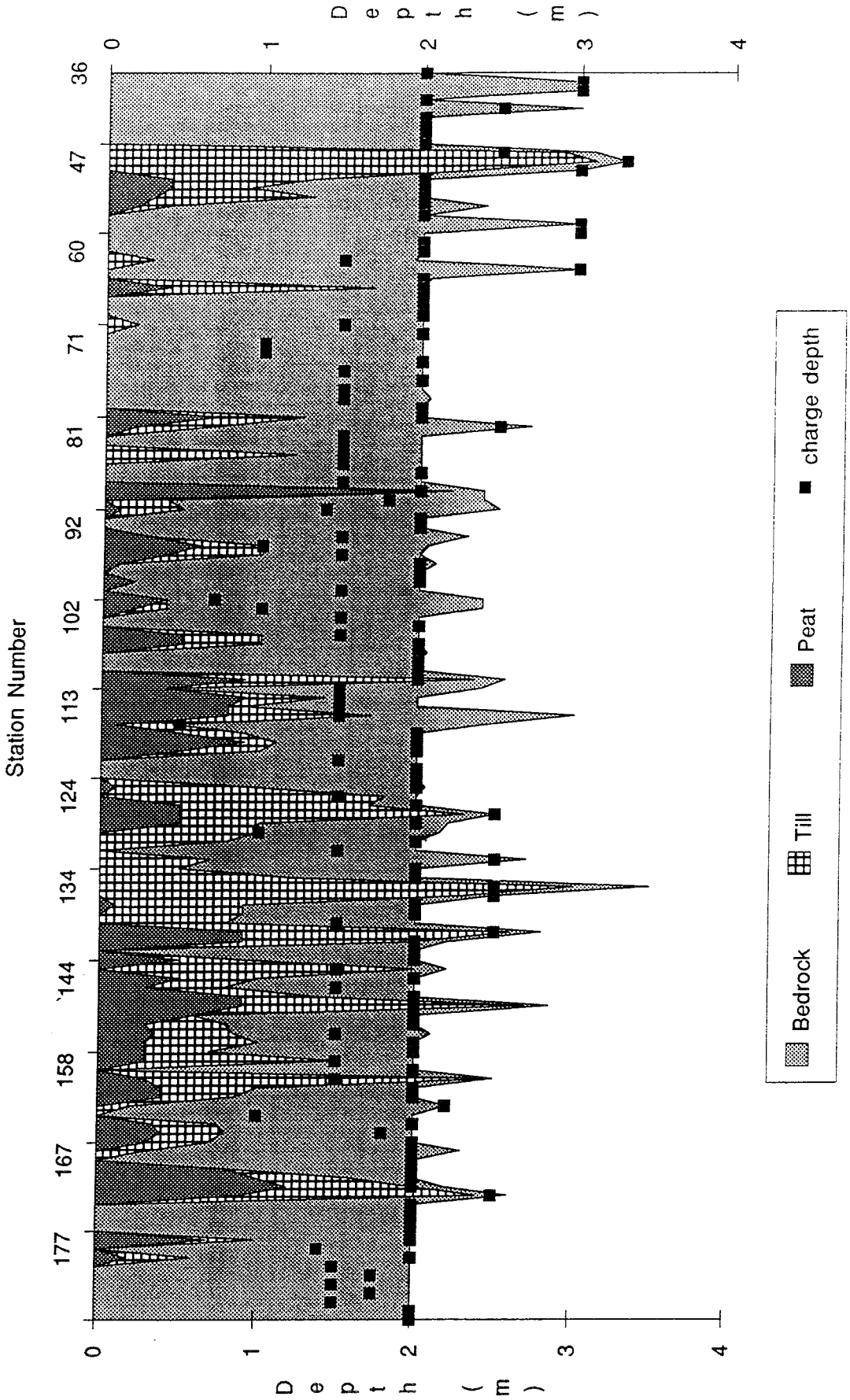

Figure 8-2 Profile of the shots included in the analyses. The station numbers do not exactly correspond to those given in Sections 3 through 7 since shots were not fired at all stations.

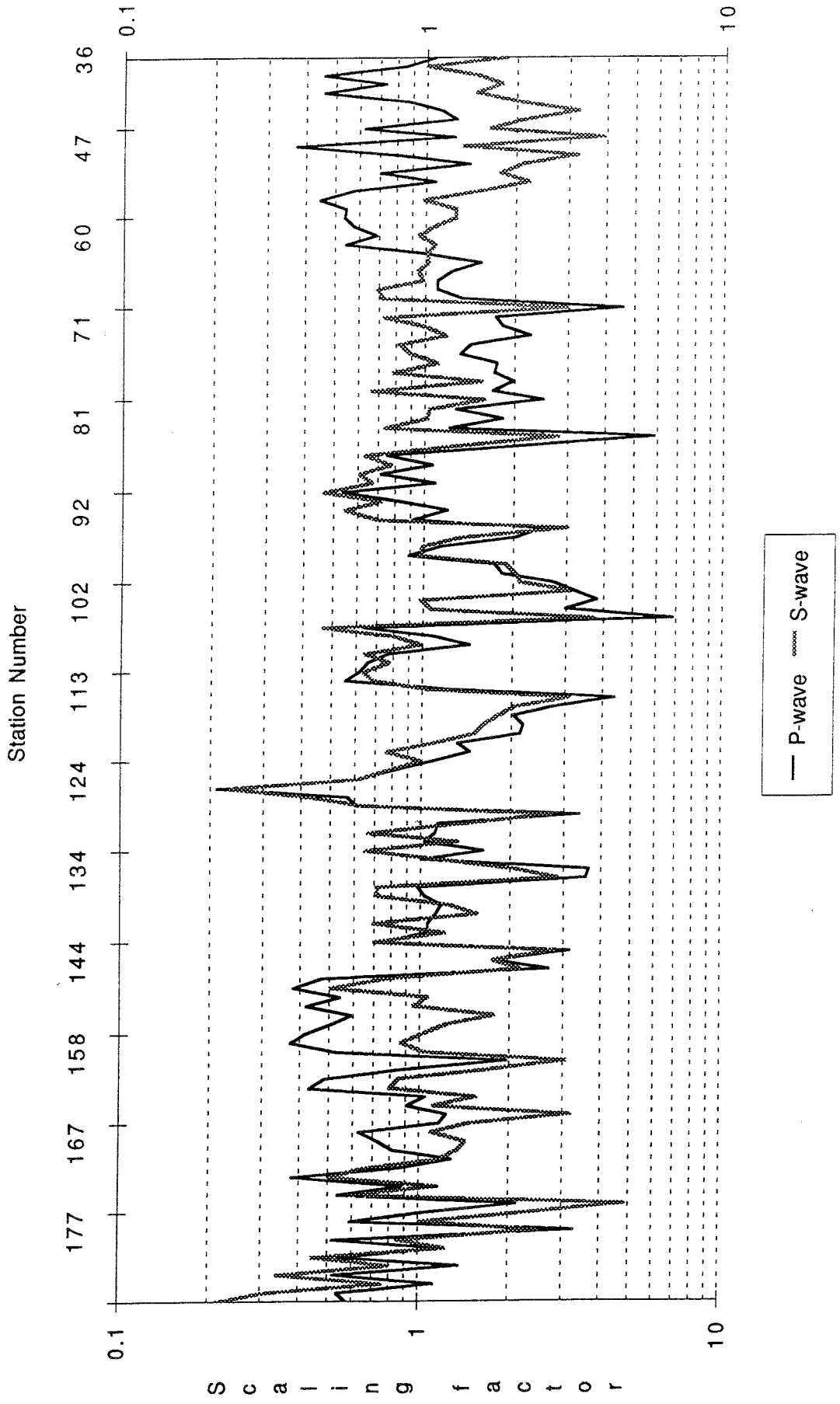

Figure 8-3 P and S-wave scaling factors along the profile. A high scaling factor implies a relatively weak shot and a low scaling factor implies a relatively strong shot.

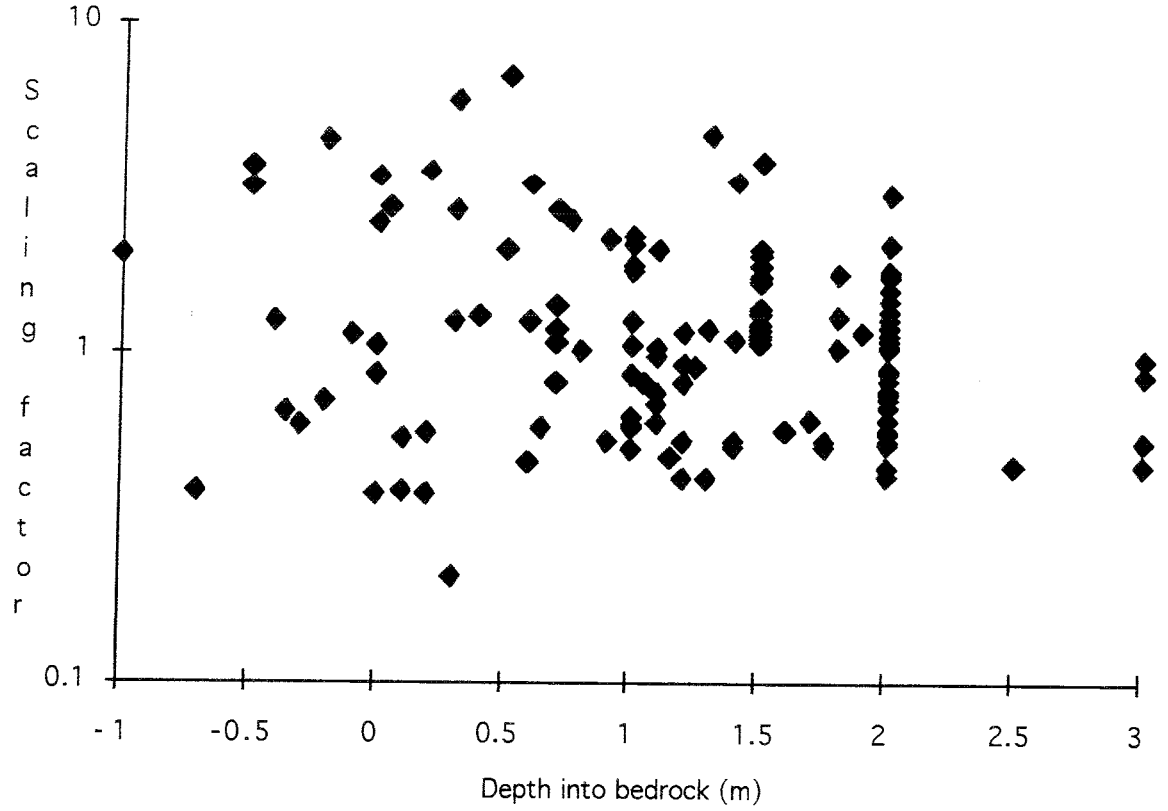

Figure 8-4 P-wave scaling factor versus depth into bedrock. A negative depth implies that the shot was fired in the overlying peat or till.

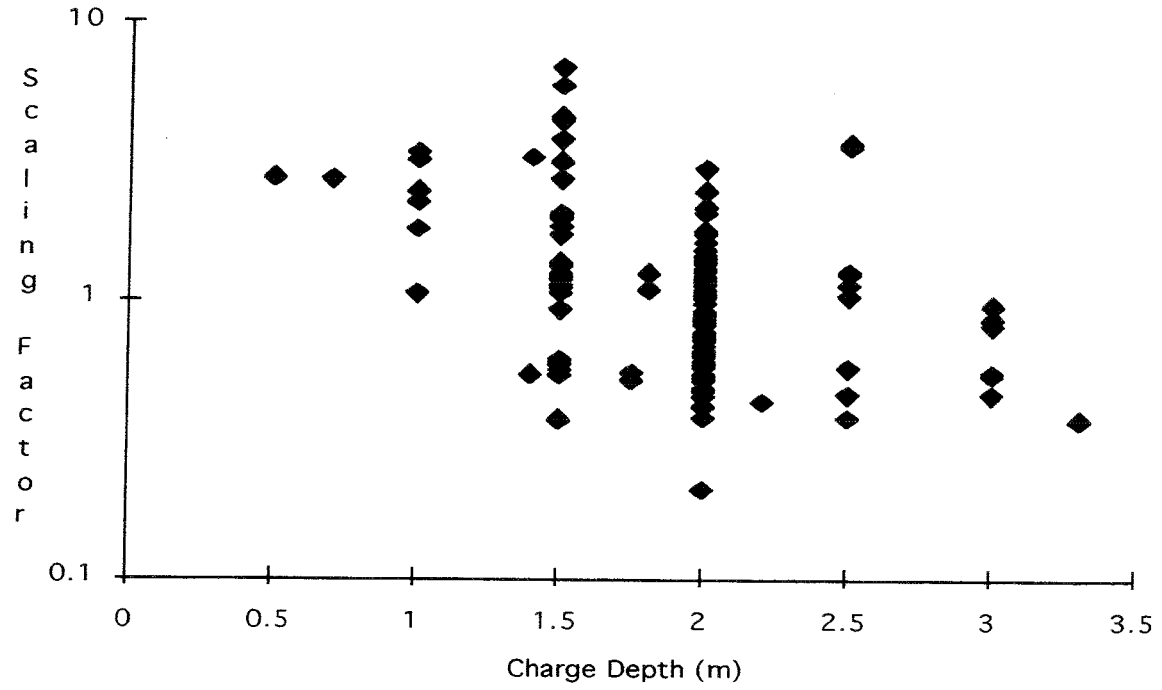

Figure 8-5 P-wave scaling factor versus depth.

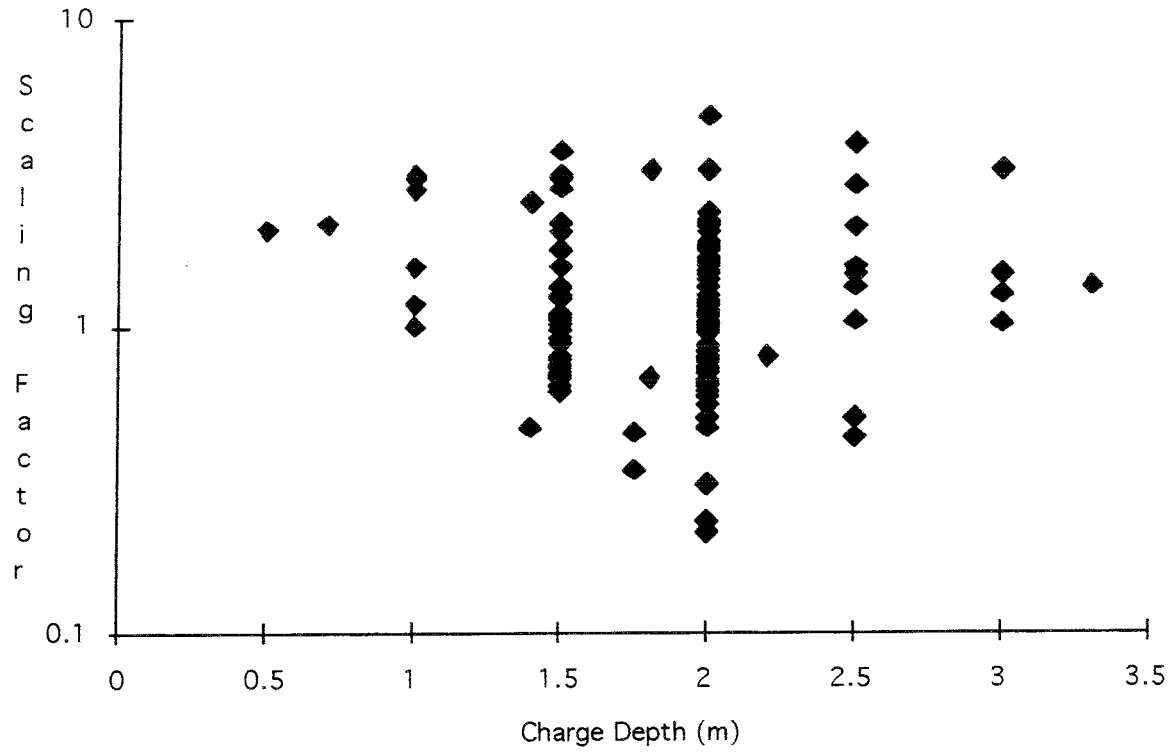

Figure 8-6 S-wave scaling factor versus depth.

8.3.3 Geophone response

Since the near surface geology appears to have little impact on the shot strength in this data set it is of interest to study the influence of the geophone response on near surface geology. A plot of the geophone scaling factors for P and S-waves shows what appears to be higher scaling factors (weaker signals) where there is bedrock outcropping. This correlation is especially marked at the eastern end of the profile. Cross-plots (Figures 8-8 and 8-9) confirm a weak trend toward higher scaling factors where the cover is absent or thin. The need to scale up the amplitude of data recorded on or near bedrock compared to the data recorded on till or peat may appear inconsistent at first. However, if transmission laws are considered this is then to be expected. A wave propagating in a high impedance media will increase in amplitude as it enters a low impedance media. The velocities in the till and peat are probably considerably lower than in the bedrock which is then consistent with the amplitude observations at the geophone stations. It may be more useful to compare the frequency content of the geophone station with surface geology rather than the amplitude scaling factor. The frequency content of data recorded on the bedrock should be higher than that recorded on the till and peat.

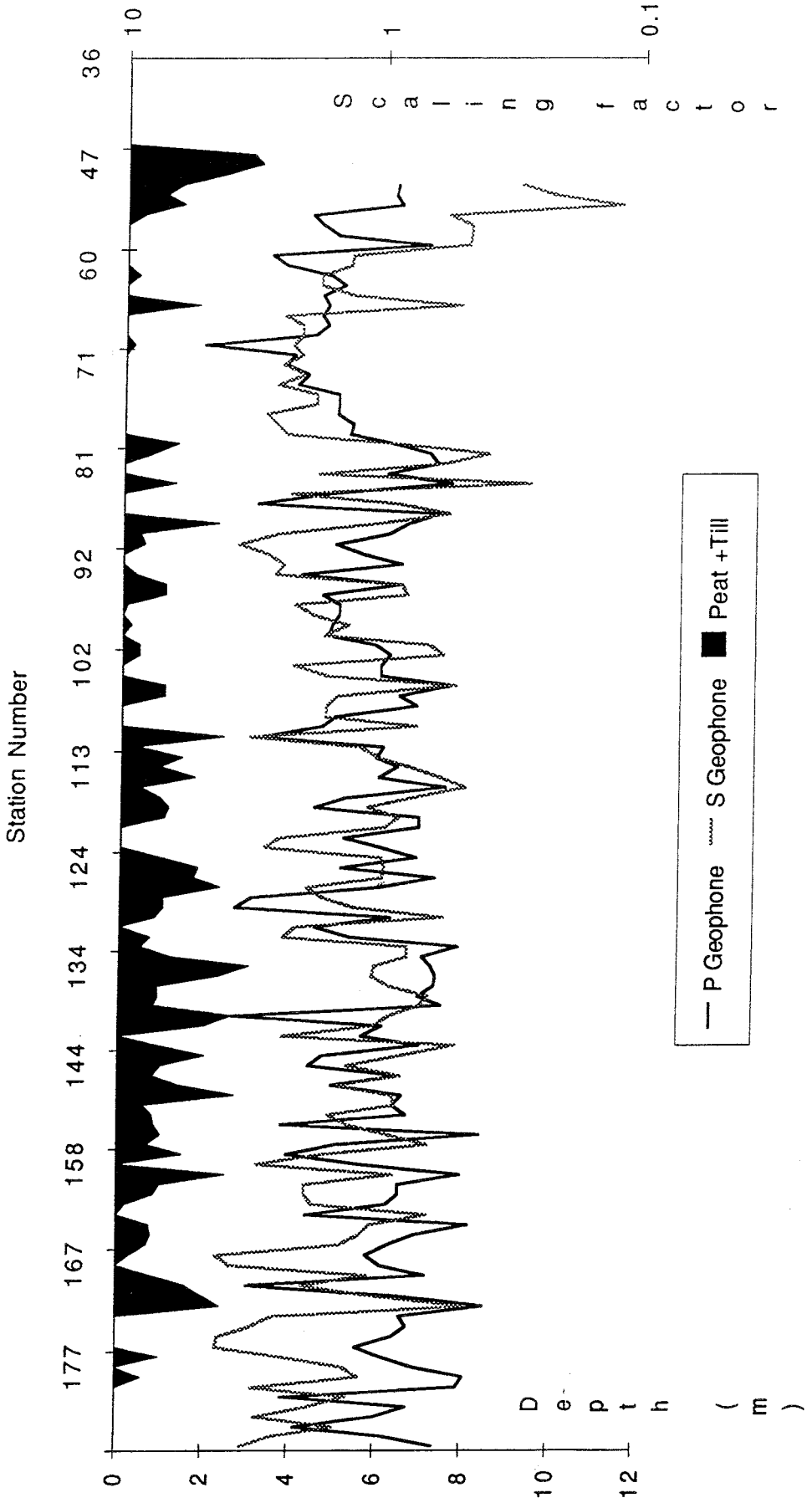

Figure 8-7 Geophone response scaling factors along the profile and depth of overburden. A high scaling factor implies that the signals recorded are weaker than the average signal level.

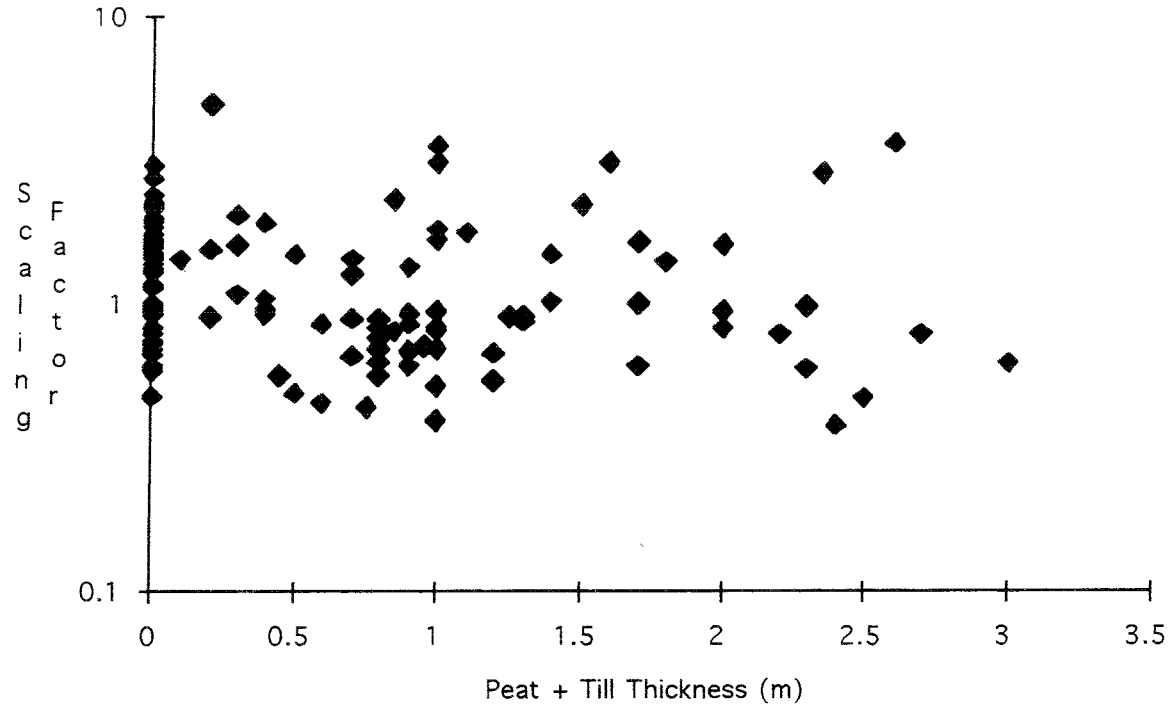

Figure 8-8 Geophone response scaling factor for P-wave energy versus cover thickness.

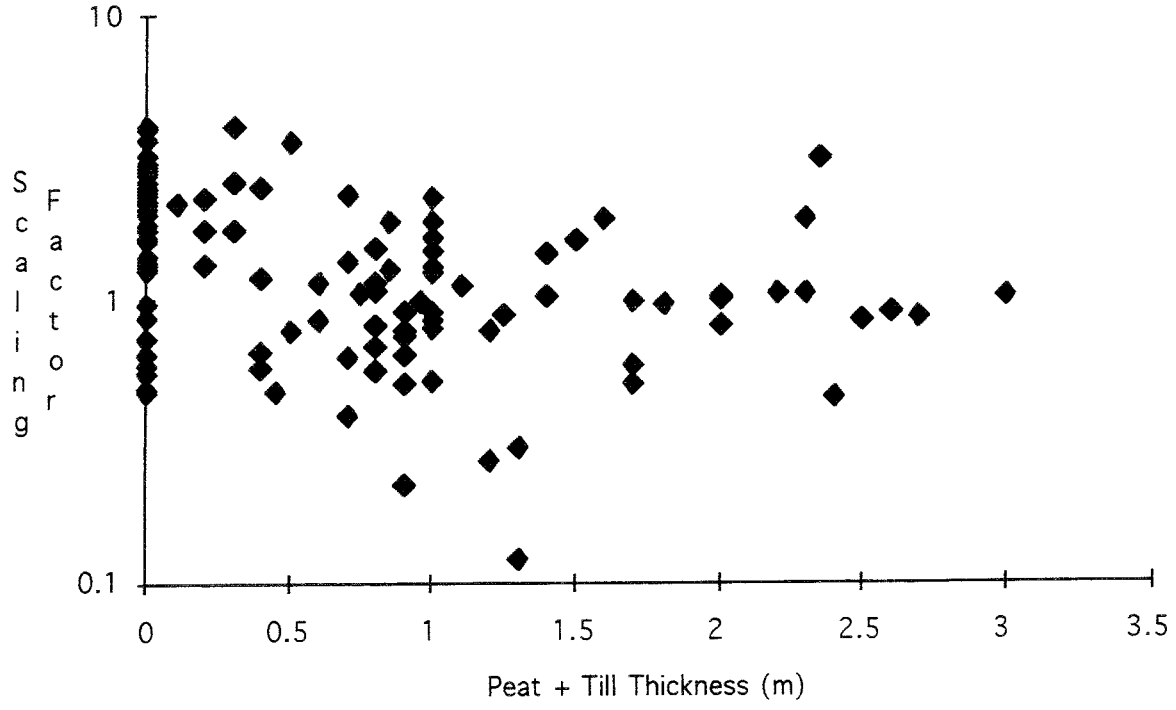

Figure 8-9 Geophone response scaling factor for S-wave energy versus cover thickness.

8.3.4 Frequency response

Even though it is not possible to study the frequency content of the first arrivals in a surface consistent manner, it is still of interest to look at the data qualitatively from a frequency perspective. Four bins were selected which were considered representative of the various shot conditions:

a. shots fired in bedrock below the water table

b. shots fired into bedrock above the water table and tamped with sand

c. shots fired at shallow depth (less than or equal to 1 meter)

d. shots fired above bedrock

Eight shots from each group were picked at random and used in the analyses. Plots of the 32 shots are shown in Figures 8-10 and 8-11. Processing steps were:

1. Spherical divergence correction

2. Exponential gain (27 dB/s)

3. Bandpass filter 10-240 Hz

The last 10 traces from each shot were analyzed for their frequency content in two windows, the P-wave window (0-170 ms) shown in Figure 8-12 and the R-wave window (330-450 ms) shown in Figure 8-13. The resulting spectra show clearly that the shots fired in bedrock below the water table give the highest frequency signals which is consistent with what is observed in the shot gathers (Figure 8-10a). Shots fired above bedrock appear to give the poorest quality data. In addition, shots fired above bedrock show very low frequency content in the R-wave window (Figure 8-13). These results indicate that shots fired in bedrock and below the water table produce the highest frequency P-wave signals and the lowest amplitude R-waves while shots fired above bedrock produce less P-wave signal and significantly more R-wave energy. Shots fired in bedrock, but tamped with sand, show little difference in their frequency content compared with the shallow shots. The data suggest that in order to produce high frequency signals that the shots should be placed in bedrock below the water table.

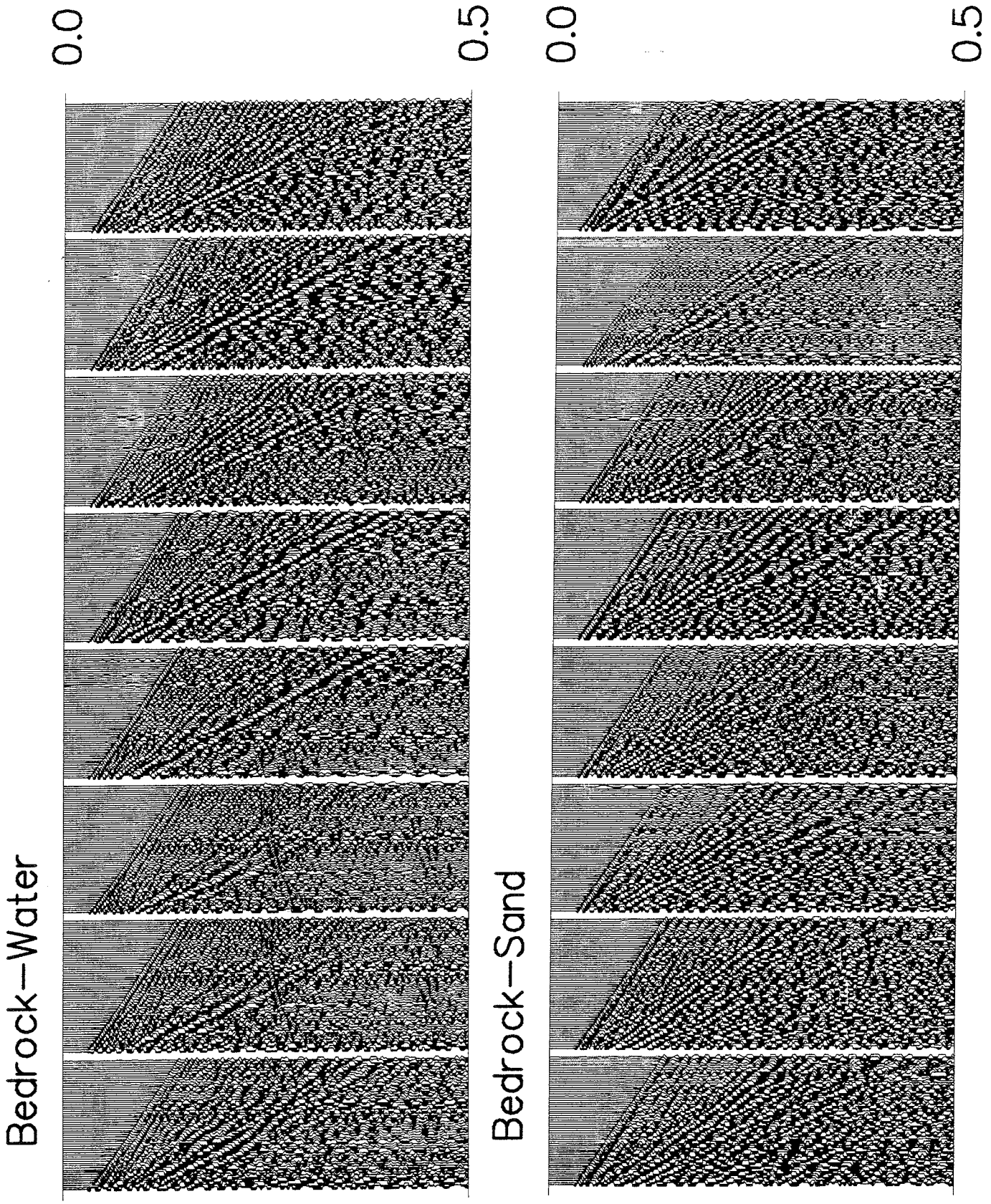

Figure 8-10 Shots used in the frequency analyses. a) shots fired in bedrock below the water table, and b) shots fired into bedrock above the water table and tamped with sand.

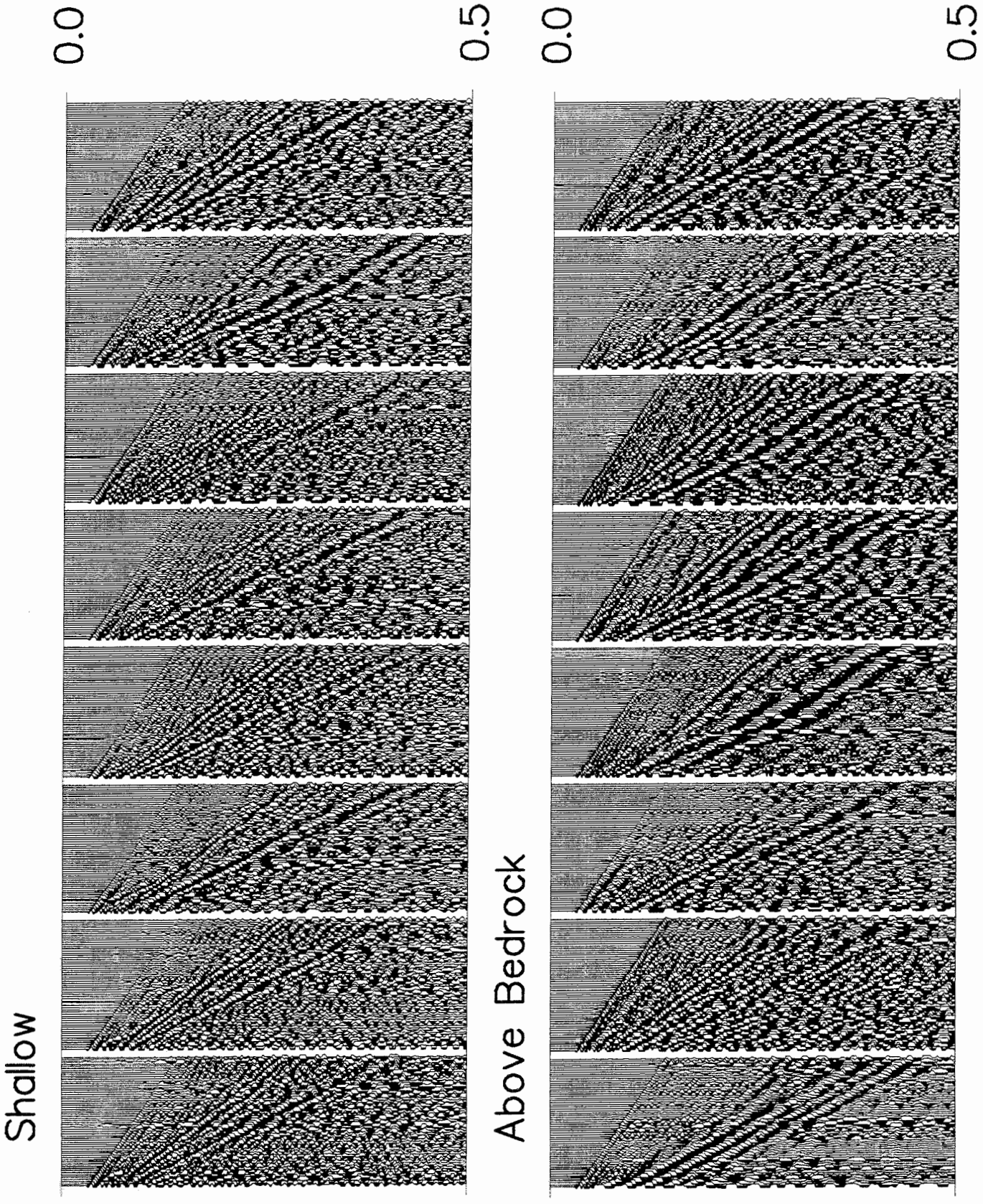

Figure 8-11 Shots used in the frequency analyses. a) shots fired at shallow depth (less than or equal to 1 m), and b) shots fired above bedrock.

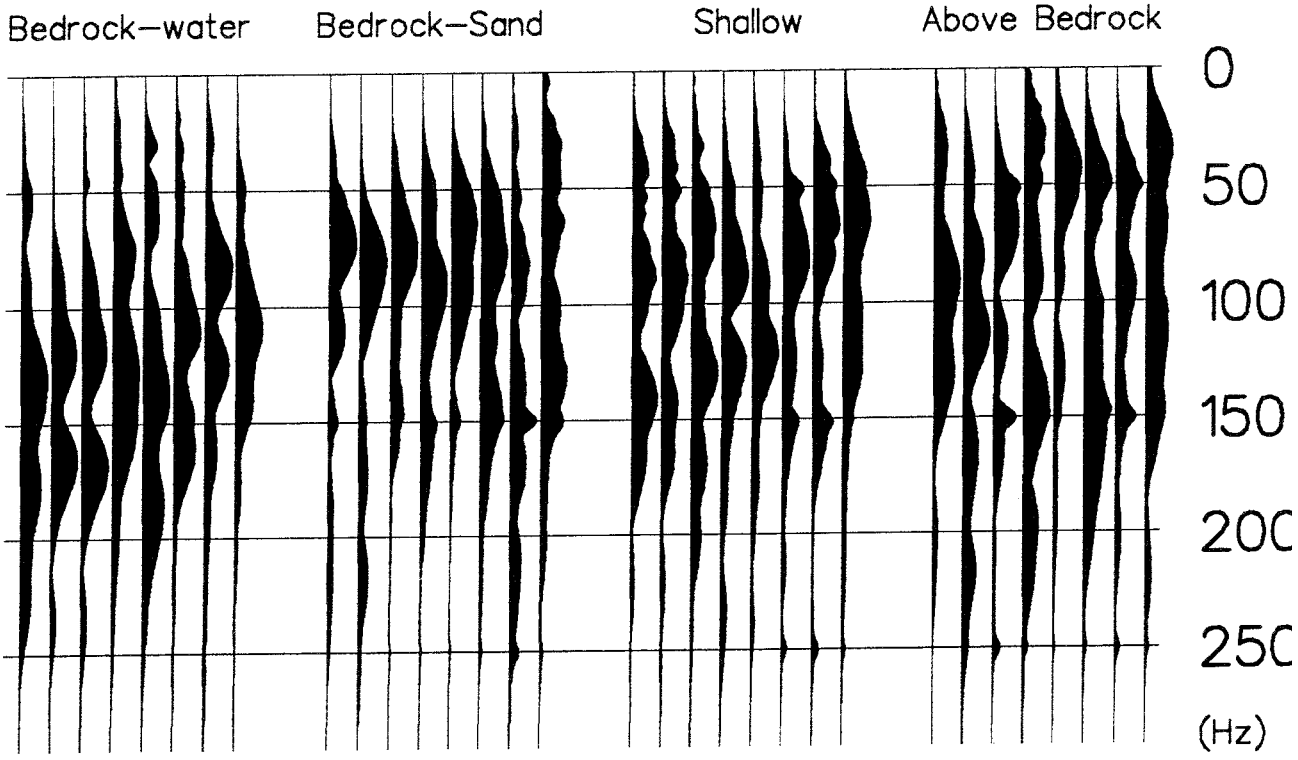

Figure 8-12 Frequency content of shots shown in Figures 8-10 and 8-11 in the P-wave window.

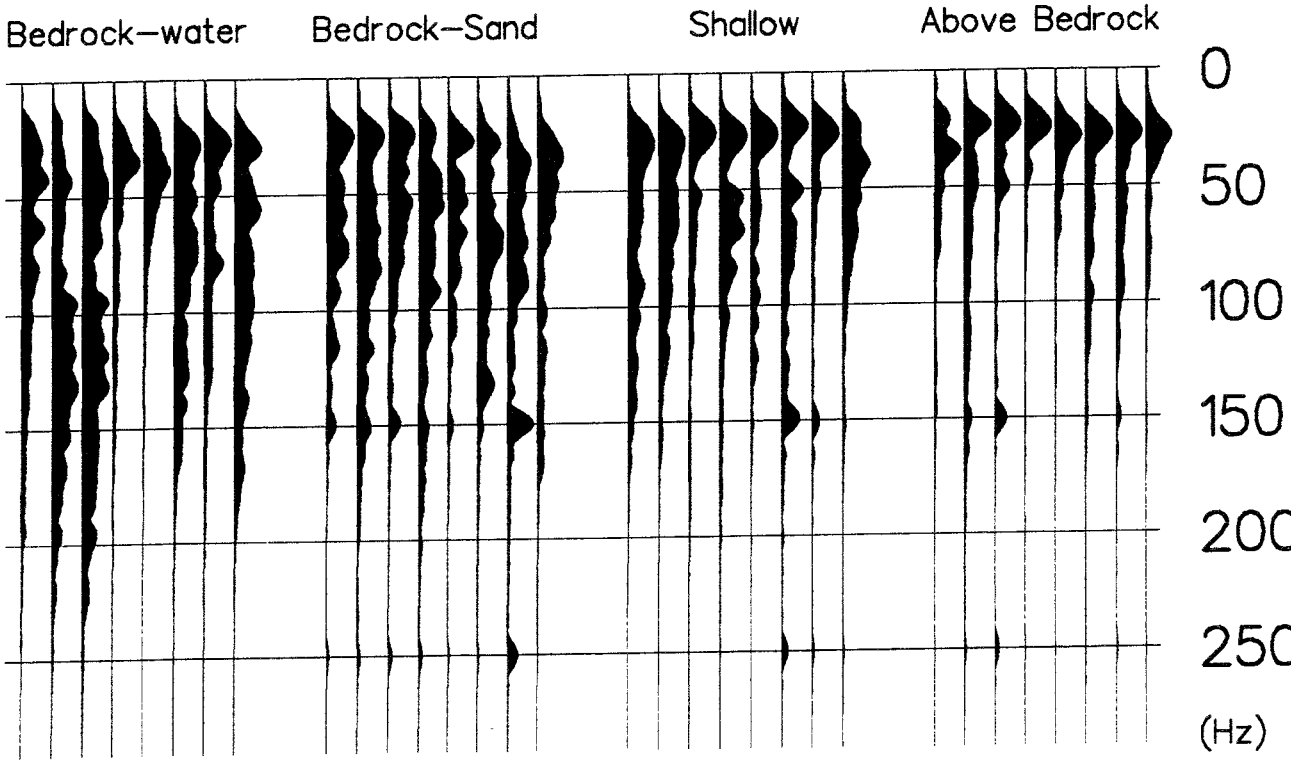

Figure 8-13 Frequency content of shots shown in Figures 8-10 and 8-11 in the R-wave window.

8.3.5 Estimating the attenuation factor, Q

It is possible to determine Q, or the damping factor, from analyses of the amplitudes of the first arrivals. In the shot-geophone strength analysis an offset factor was also solved for, *o*, in equation (8-1). This function gives the average amplitude decay as a function of distance from the shot. This amplitude decay may be compared with the expected one for lossy media using the equation

$$A(x_2)=A(x_1)\exp\left(\frac{-\pi f(x_2-x_1)}{Qv}\right) \qquad \textbf{(8-2)}$$

where x is distance, f is frequency, and v is velocity. Figure 8-14 shows a comparison between calculated and observed amplitude decay curves for three Q values assuming an average frequency content of 150 Hz and a velocity of 5500 m/s. A Q factor of 10 fits the data well. This is quite low, but the P-wave first arrivals are limited in their depth of penetration and a value of 10 is probably valid for the upper 50-100 m. It should be regarded as a lower limit for reflection seismic modeling. For comparison, in the depth range 0-1500 m, Juhlin (1990c) calculated Q to be 30 in the Gravberg-1 deep borehole and Båth (1985) reports a Q of 50 in the Grängesberg area in the upper 1400 m. A value of 10 in the upper 100 m for the Finnsjön area appears to be consistent with these results.

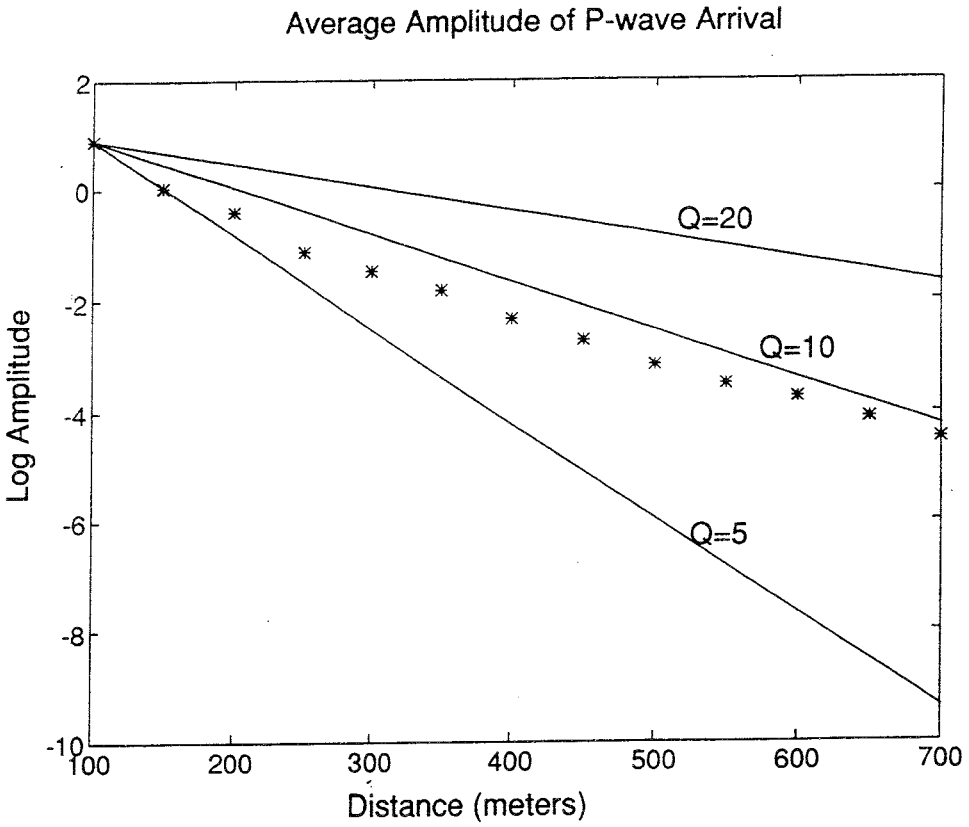

Figure 8-14 Observed amplitude decay curves (*) of first arrivals and theoretical decay curves for selected values of Q.

9 THEORETICAL STUDIES OF FIELD PROCEDURES

9.1 INTRODUCTION

One of the objectives for this part of the study is to find suitable data acquisition procedures for reflection seismic surveys in crystalline rock that provide sufficient data quality at reasonable cost. The results of the reprocessing of the Finnsjön data collected in 1987 show that reflection seismics is a viable technique for mapping fracture zones in crystalline rock and that the data acquisition procedures used at Finnsjön were basically sound. A practical drawback was the comparatively high cost resulting from drilling boreholes along the profile and keeping the boreholes open.

The specific objective for this task was to propose and evaluate optimized data acquisition procedures under different overburden conditions. The optimization has been done with respect to data quality and cost.

The task has been approached by seeking answers to a set of questions:

a) Is it feasible to use a surface source and place the geophones on the ground surface and thus eliminate drilling?

b) If conducting the survey on ground surface diminishes the data quality beyond acceptable limits, how deep should the source and, respectively, the geophones be placed? Can they be in the overburden, or should the installation boreholes be always drilled to the bedrock?

c) If downhole geophones are used, is it more economical to keep the holes open just long enough to place the geophones and retrieve only part of the geophones after measuring?

d) What signal sources can be used while drilling the boreholes, so that geophones can be installed in the same holes?

9.2 MODELLING

9.2.1 Model layout

A modelling study was performed to answer questions a) and b) defined in the previous Section.

The layout used for the models has been taken from the 1987 test performed at Finnsjön. A 60 station geophone spread, with 10 m spacing, was used, the distances from the source to the first and last geophone being 100 m and 690 m.

The model computations were done by an algorithm developed by Kind and Odom (1983). This algorithm accepts as input a layered structure, where the P- and S-wave velocities, the P- and S-wave attenuation (Q factors) and the density are given for each layer. The algorithm computes the production of surface waves and P-S conversions, keeping track of the attenuation, geometrical spreading and polarization.

The depth and thickness of the layers, as well as the depth and radiation pattern of the source can be chosen without restrictions but, with this version of the program, the receivers can only be placed on the ground surface. Tests regarding the influence of the geophone depth on the data quality were performed on a limited basis together with drilling tests, in the second part of this work.

The source signature was modelled by applying a causal Butterworth filter to a spike. The filter is flat between 120 Hz and 180 Hz, with the low cut slope of 80-120 Hz and a high cut slope of 180-240 Hz.

The P and S velocities used are typical for the Finnsjön test. The Q values are inferred from the analysis presented in Section 8. The densities were set to typical values for the respective formations.

The source was placed at five depths: 0 m (surface), 1 m, 2 m, 4 m, and 6 m and the model calculations were performed for each source depth. The geophone array was placed on the ground surface.

Four models, each consisting of 7 horizontal layers, were built. These models differ by the thickness of the overburden. Table 9-1 lists the model parameters. The thickness of the overburden, marked by "D" in Table 1 has been: 1 m, 3 m, 5 m, and 10 m.

Table 9-1 Parameters for model.

Layer	Description	Depth (m)	VP (m/s)	VS (m/s)	Dens. (kg/m^3)	QP	QS
1	Overburden	0-D	2000	800	2000	5	5
2	Weathered	D-50	5100	3100	2600	10	10
3	Rock	50-320	5500	3100	2600	10	10
4	Zone 1	320-330	4500	2500	2400	10	10
5	Rock	330-500	5500	3100	2600	10	10
6	Zone 2	500-505	4500	2500	2400	10	10
7	Rock	505-	5500	3100	2600	10	10

9.2.2 Discussion of modelling results

The first conclusion of the modelling study is that sources placed on or near the ground surface produce a very weak signal, barely detectable for thicker overburden areas. Figure 9-1.a presents a synthetic profile for 5 m thick overburden with the shot at 3 m, i.e. in the overburden. Figures 9-1.b through 9-1.e display profiles for 1 m, 3 m, 5 m, and 10 m, respectively, with the shot at ground surface. It can be seen that the records are practically blank, except for the 1 m case (Figure 9-1.b) and even there most of the energy is received as surface waves. The same normalization factor has been used for all five plots.

Figures 9-2.a through 9-2.e present the same profiles as Figure 9-1 with random noise added. The noise level is 2.5% of the maximum amplitude of all the synthetic profiles. This level corresponds roughly to the signal-to-noise ratio of the best traces recorded at Finnsjön. The plots are trace-normalized. Figure 9-2 also demonstrates the gain in data quality when placing the source under the ground surface.

The second conclusion of the modelling study is that it is not always necessary to place the source in the bedrock. Figures 9-3.a through 9-3.d are obtained for overburdens of 1 m, 3 m, 5 m, and 10 m, with the shot always placed at 3 m. A constant normalization factor has been used. Figures 9-4.a through 9-4.d present the same profiles trace-normalized and with noise added. The best profile (Figures 9-3.c and 9-4.c) corresponds to a bedrock depth of 5 m. Therefore, the shot at 3 m depth is in the overburden. There are two candidates for the poorest shot: 10 m to bedrock (Figures 9-3.d and 9-4.d) and 1 m to bedrock (Figures 9-3.a and 9-4.a). In the first case the poor quality is due to amplitude loss in the overburden. This can be taken care off by placing the shot somewhat deeper. The second case displays comparatively high amplitude surface waves. If the overburden is

homogeneous and the interface to the rock is flat, as in this model, the surface waves can be largely suppressed by processing. For a real survey these assumptions may not be valid and suppressing the surface waves may become laborious and costly.

As it can be seen in Figures 9-5.a through 9-5.e, the low amplitude of the surface waves is an effect of the thickness of the overburden and does not depend on the shot depth. For a center frequency of 150 Hz, which has been used for modelling, this tuning effect appears for a depth of 5 m. If sources of higher frequency are used the depth will decrease, reaching the average rock depth for the second case of our study. This effect should be kept in mind for future field tests.

Because the output of surface waves is not sensitive to the shot depth (unless the shot is deep in the rock, which is unfeasible practically), the only way to reduce the surface waves seems to be by placing the geophones in boreholes.

Some simple data processing (AGC) has been applied for demonstrating the reflections from the low velocity zones included in the model. Figure 9-6 shows a comparison between two gathers, one with pronounced surface waves (Figure 9-6.a) and another with an average amount of surface converted energy (Figure 9-6.b). In Figure 9-6.b Zone 1, which is 10 m thick appears clearly and there is a indication of from Zone 2 (5 m thick) as well. In Figure 9-6.a both zones are masked by the surface waves.

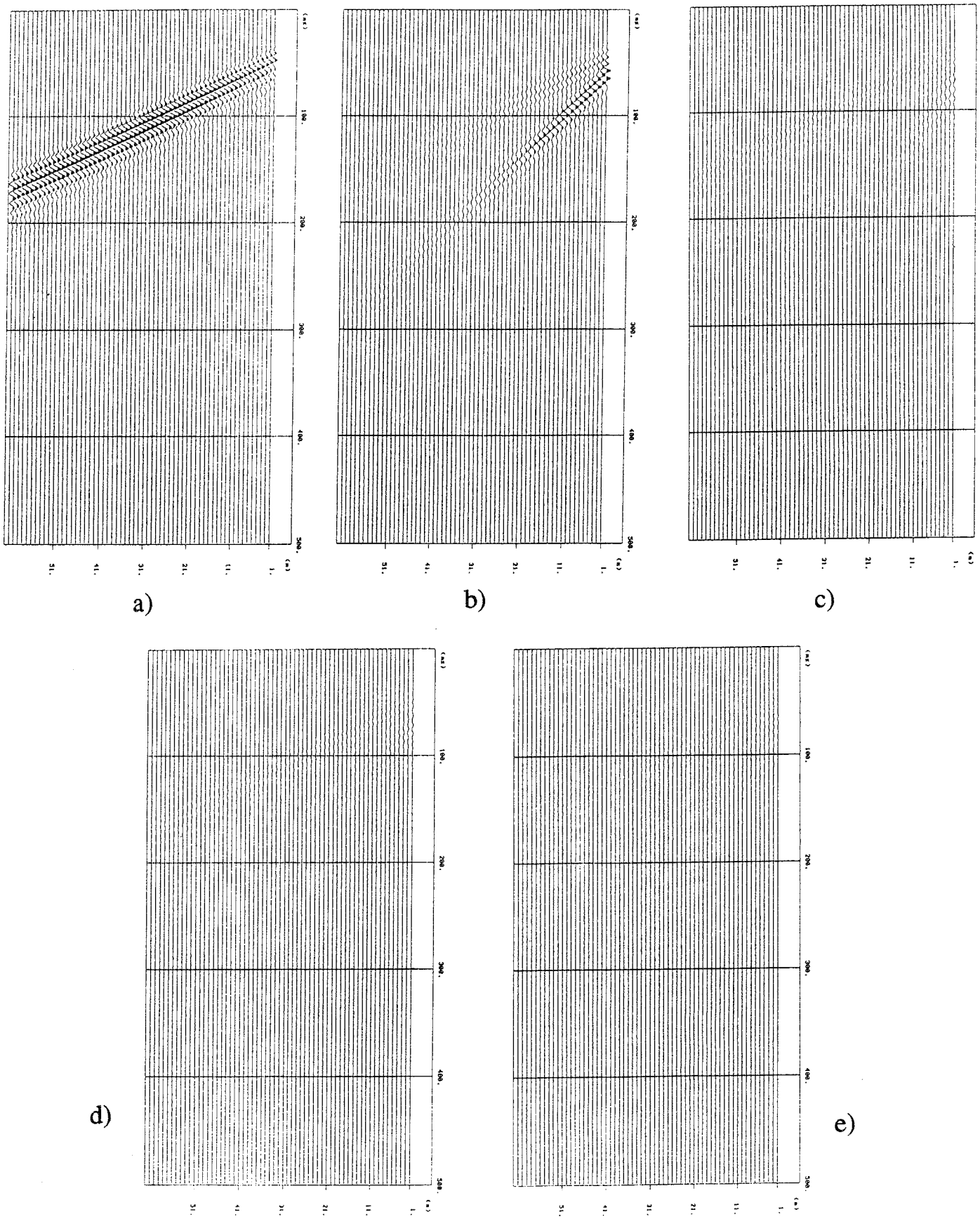

Figure 9-1 Shot gathers for a) 5 m overburden, shot at 3 m depth, b) 1 m overburden, c) 3 m overburden, d) 5 m overburden, for figures b) through e) shots are placed at ground surface.

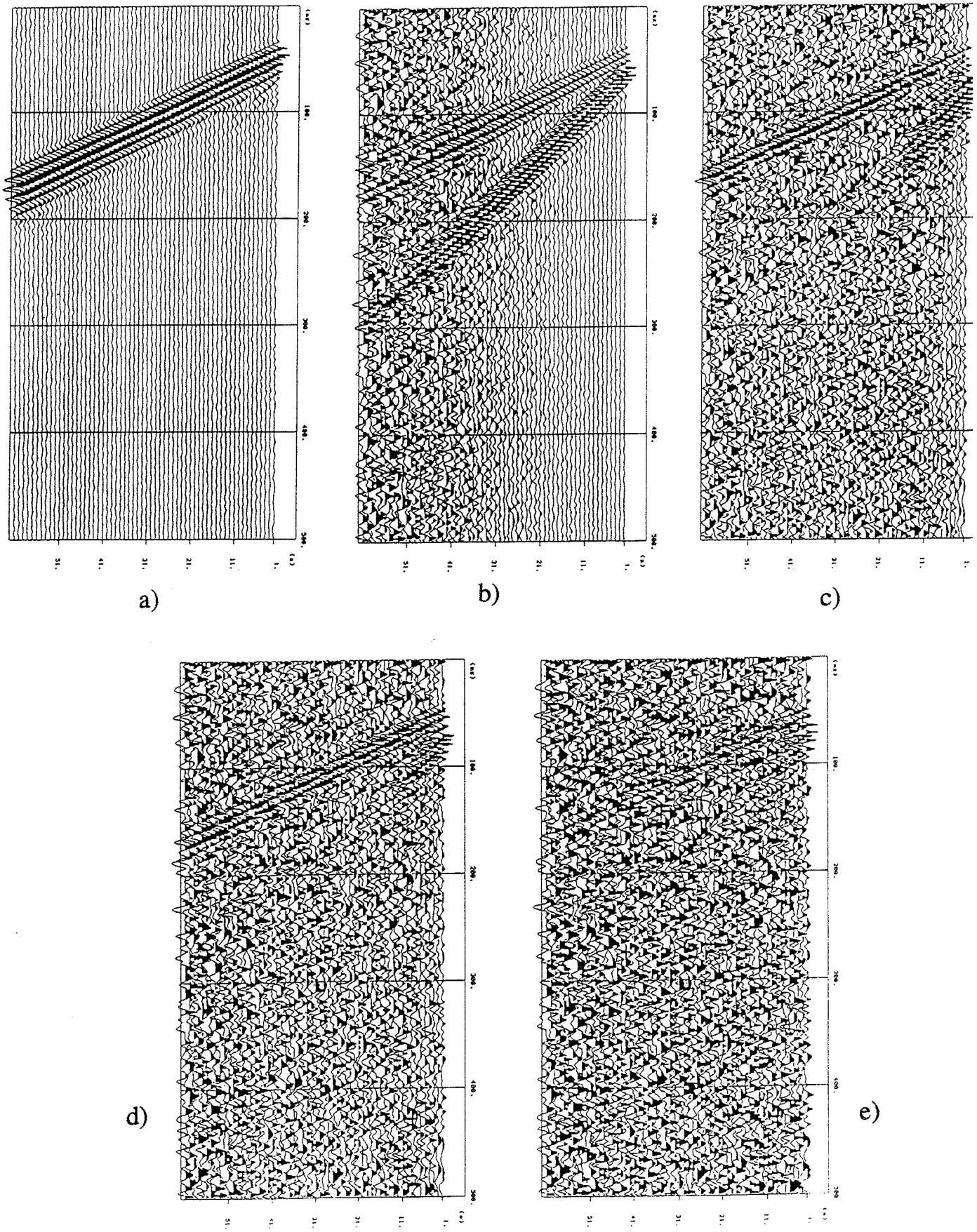

Figure 9-2 Shot gathers with random noise added for a) 5 m overburden, shot at 3 m depth, b) 1 m overburden, c) 3 m overburden, d) 5 m overburden, e) 10 m overburden, for b) through e) shots placed at ground surface.

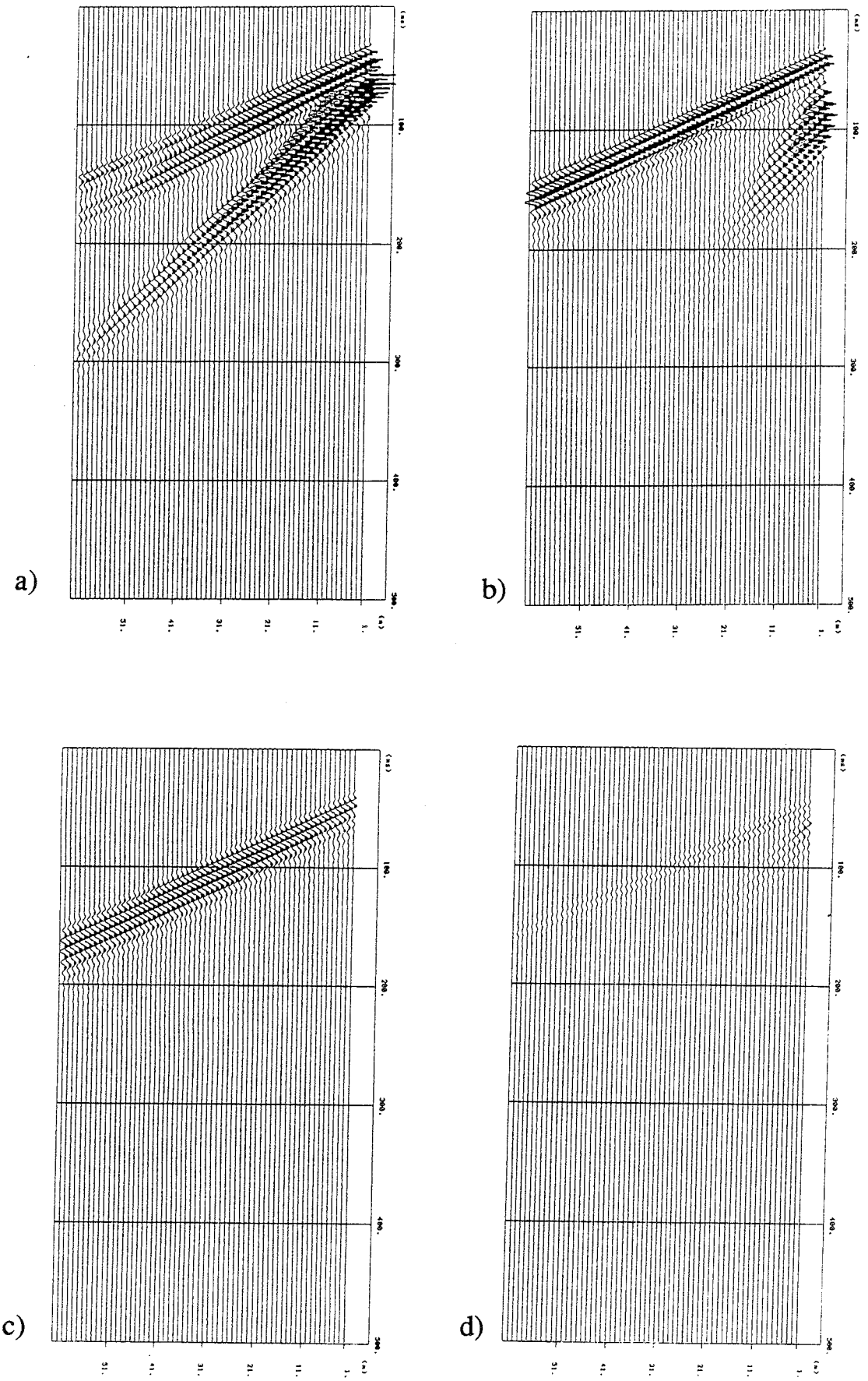

Figure 9-3 Shot gathers for shots at 3 m depth and a) 1 m overburden, b) 3 m overburden, c) 5 m overburden, and d) 10 m overburden. Normalized traces.

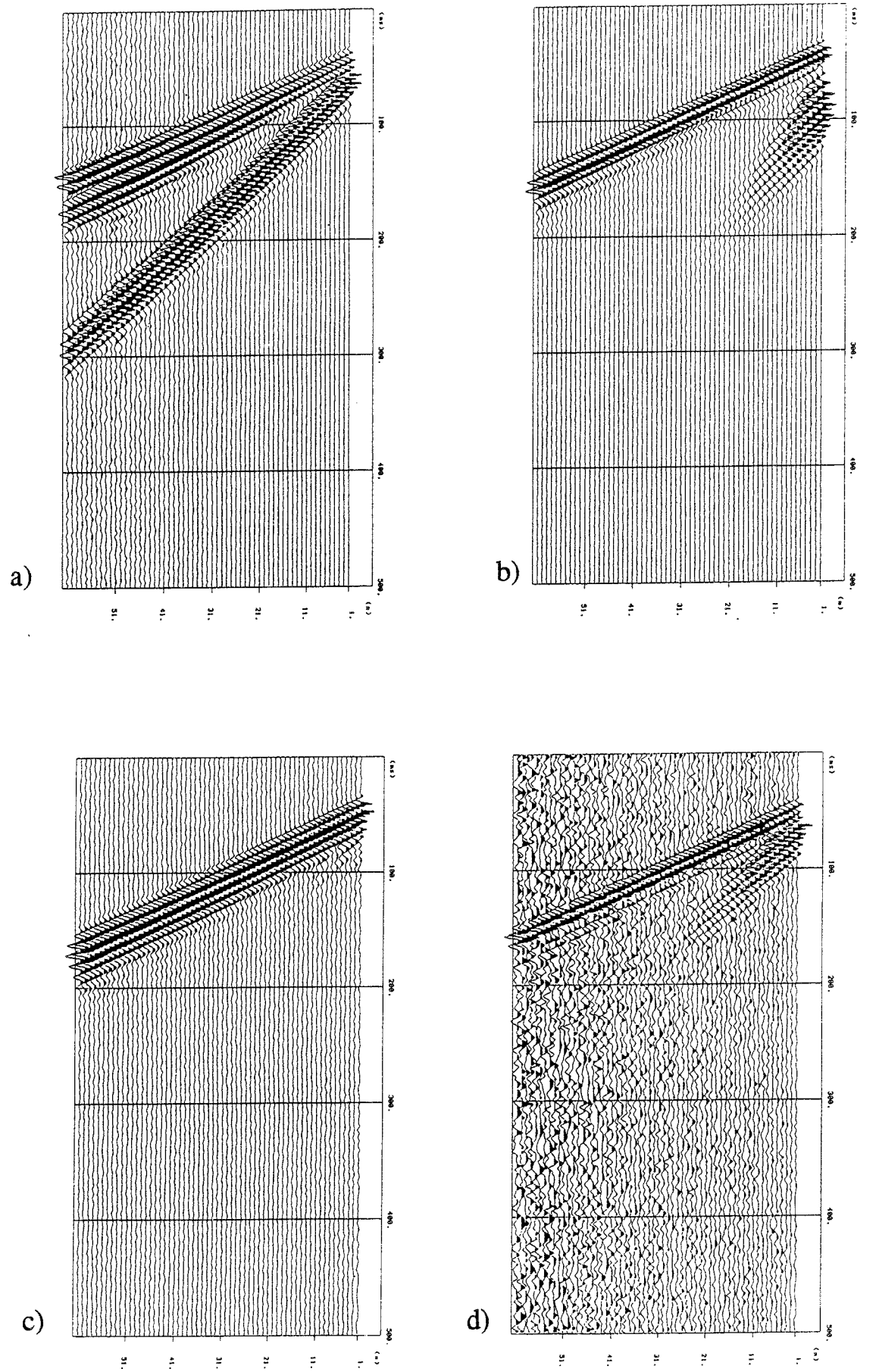

Figure 9-4 Shot gathers with random noise added for shots at 3 m depth and a) 1 m overburden, b) 3 m overburden, c) 5 m overburden, and d) 10 m overburden. Normalized traces.

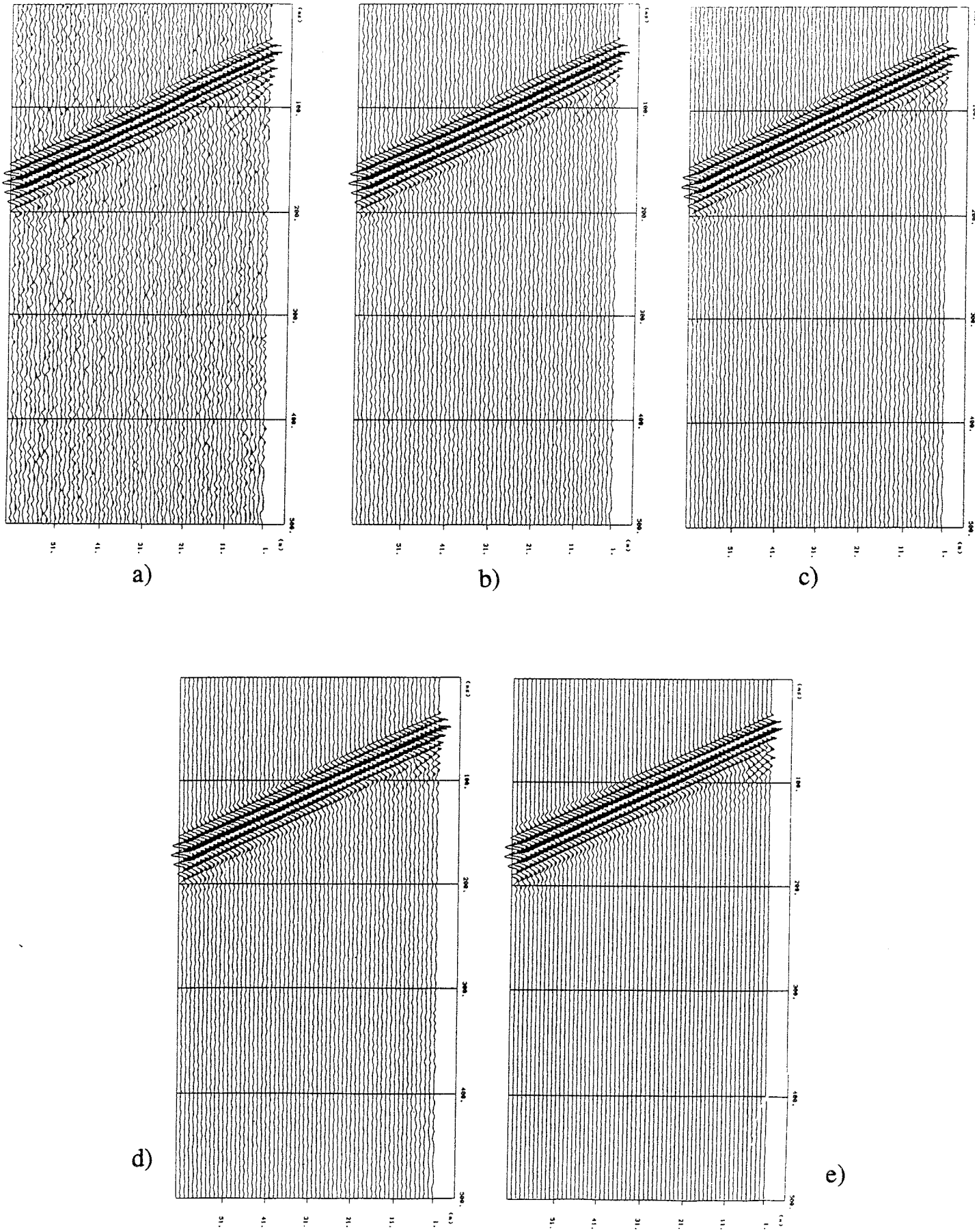

Figure 9-5 Shot gathers for 5 m overburden and shot depths of a) 1 m, b) 2 m, c) 3 m, d) 4 m, and e) 6 m. Normalized traces.

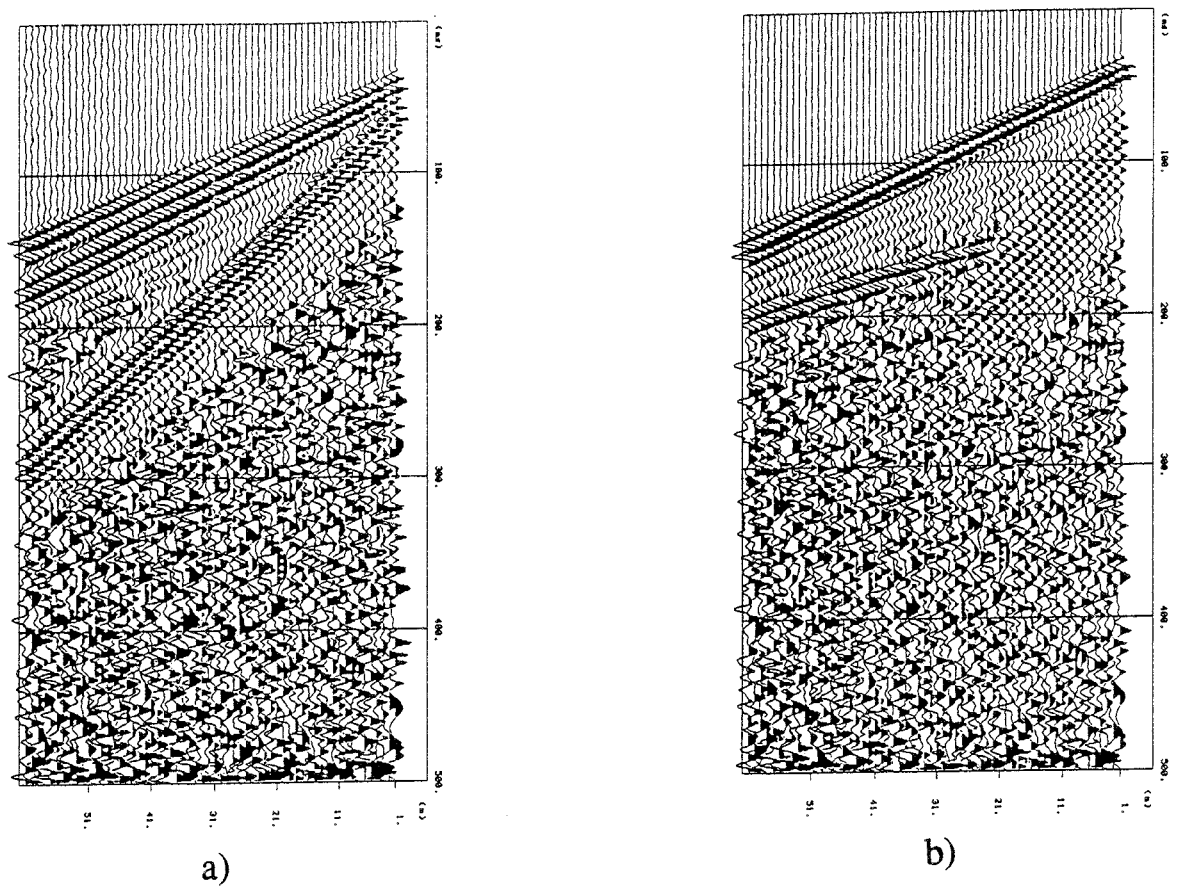

a) b)

Figure 9-6 a) Processed data (AGC) with strong surface waves, b) processed data (AGC) with surface converted energy.

9.2.3 Receiver arrays

The increase of the data quality at the receiver end can be in principle achieved by using geophone groups instead of single geophone stations or by placing the geophones in boreholes rather than on the ground surface.

These conditions can not be fulfilled simultaneously within reasonable cost frames. The choice is then: geophone groups on ground surface, or single geophone stations in boreholes.

A limited test was performed in Finland, at Olkiluoto. A 76 mm borehole was drilled through the 10 m thick moraine 3 m into the rock. A geophone was placed at the bottom of the hole, in contact with the rock. A light drilling rig was used as a source at approximately 40 m distance from the geophone borehole. The source generates a repeatable pulse at 30 - 40 ms intervals. As seen in figure 9-7.a, the signal was received clearly with the geophone at the bottom of the hole. When lifting the geophone in the overburden (3 m depth), the received signal appeared as in Figure 9-7.b. The

center frequency dropped from 500 Hz to 180 Hz which, together with the surface waves tail, extended the duration of the pulse at the receiver end over the interval between adjacent pulses.

If we extrapolate these observations to a real survey, the resolution obtainable with geophones placed in the overburden near the surface is at best 50 ms, which is approximately equivalent to a distance between reflectors of 150 m. If the geophones are placed in the rock, the resolution can reach 10 ms, corresponding to a spatial resolution of 30 m.

In principle, the duration of the transient can be shortened by suppressing the surface waves. In practice, suppressing the surface waves by using longitudinal geophone spreads instead of single geophone stations meets with difficulties due to the variation of the overburden thickness and velocity along the profile. The rapid variation of the overburden conditions will affect negatively also transversal geophone spreads.

In conclusion, a realistic way to increase the data quality at the receiver end is by placing the geophones in boreholes. Doing this in an economical way will require the optimization of the drilling.

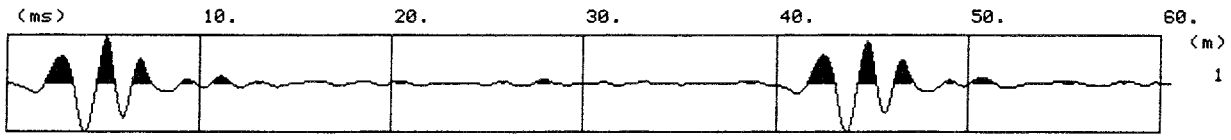

a)

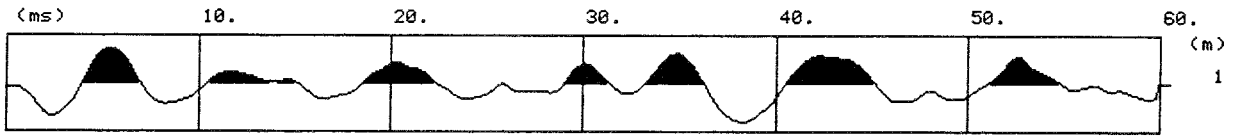

b)

Figure 9-7 a) Signal from a geophone placed at the bottom of a hole and b) signal from a geophone placed at 3 m depth in the overburden.

9.3 SEISMIC SOURCES

The modelling study indicated that the sources must be placed in boreholes, but not necessarily in the bedrock. However, the model does not take into account the non-elastic phenomena in the immediate vicinity of the source, of which the most important is the decrease of frequency when the source is placed in the overburden. The analysis of the Finnsjön data set showed that such a reduction in frequency for shots fired in the overburden takes place in practice (see Section 8.3.4). Of course, this applies to sources which are by themselves capable of producing high frequencies. For explosive sources, the frequency drop when shooting in the overburden can in most cases be overcome by processing. With other sources, e.g. drilling bit and air gun, the data quality decreases dramatically when they are placed above the bedrock level.

9.3.1 Explosive sources

With a correct choice of the explosive and detonator type, the explosive sources can be very accurate and repeatable. With good quality seismic detonators and Nobel Prime charges, a time accuracy better than 0.2 ms has been reached at recent VSP tests at Äspö.

A practical drawback in the case of reflection profiling would be that the shot holes must stay open after completing the drilling and can not be used for placing geophones after shooting. For outcrops or thin overburden (less than 1 m), keeping the holes open will pose no particular problems. For thicker overburden, the holes will have to be cased. If the same holes are to be used for geophones, the shooting must be done behind the array.

9.3.2 Measuring while drilling

If the drilling noise can be used as seismic signal, the collapsing of the boreholes after retrieving the drilling column is not anymore a problem. This will avoid casing the holes, which reduces the costs.

However, tests with using drilling noise as a source signal has so far not been fully successful. There have been problems with data quality and the technique does not seem to provide any cost advantages. Measuring while drilling is much slower and the costs for keeping a complete survey team and equipment at the site for a longer time are much larger than the extra expense related to keeping all the holes open.

9.3.3 Other sources

Other sources may be considered in principle, if they can decrease the need of drilling. Possible sources to use above ground are; shot-guns (preferably fired in a 0.5 m deep hole) and vibrators (e.g. the Mini-Sosie). Surface sources seem to run into problems. Shooting industrial slugs in the ground will also run into problems for thin overburden, outcrops, and generally when the overburden conditions vary rapidly along the profile. Engineered sources for boreholes do not decrease the amount of drilling needed and are more difficult to handle than explosives.

10 3-D DATA ACQUISITION

10.1 3-D ACQUISITION IN GENERAL

In many oil and gas producing areas 3-D seismic acquisition, processing and interpretation is now standard, especially in marine environments where data acquisition costs are relatively low. However, in heavily explored land areas, i.e. Texas, much of the acreage has also been covered by 3-D acquisition. It is reported that the entire country of the Netherlands has been shot using 3-D acquisition.

3-D acquisition may consist of several parallel 2-D lines which are then processed using 2-D techniques and only interpreted in 3-D. This method has drawbacks if the structure is complex since the subsurface sampling is generally significantly less perpendicular to the lines than parallel to the lines. More advanced 3-D methods attempt to sample the subsurface in a radially symmetric manner. This omits some of the bias caused by sampling along lines, but results in complex acquisition geometries

In order to determine the strike and dip of a plane reflector it is sufficient to have two non-parallel lines over it. By increasing the number of lines it is possible to observe if the reflector is non-planar. In general, the more lines, the more 3-D information can be obtained.

10.2 APPLICATIONS IN COAL PRODUCTION

Curtin University of Technology in Perth, Australia have been carrying out acquisition, processing and interpretation of 3-D seismic data over coal fields for a number of years (Lambourne et al., 1989; Urosevic et al., 1992). They have also been involved in land 3-D acquisition on larger scale in the Perth Basin (Stewart and Evans, 1989; Young et al., 1990). The coal seams are located a few hundred meters below the surface and are mined underground along the seam using a specially designed machine. A fault of as little as 3 m will disrupt the mining operation and it is of great importance to be able to know in advance where these faults are located. By collecting low fold 3-D data Curtin University has been able to provide 3-D images of where faults are located. The techniques developed there are continually tested in the field by the mining operations.

A coal seam imbedded in sandstone forms an interface with high reflection coefficient, great lateral continuity and nearly horizontal attitude, an ideal target for reflection seismics. A fracture zone in crystalline rock may only be weakly reflective, have varying lateral continuity and have significant dip. However, experience in Sweden and abroad has shown that important fracture zones are often observable on single shot gathers indicating that the methods used for fault detection in coal mining may be applicable for mapping of fracture zones in crystalline rock. In addition, if the primary zones of interest are sub-horizontal, then the methods may be highly applicable.

10.3 OTHER 3-D OPERATIONS

Virginia Polytechnic Institute has also been carrying out 3-D surveys in the Appalachians. Detailed information about the acquisition parameters and results are not available at this time, but will be in the future. Their surveys have been on a fairly large scale and scientifically oriented. Goals have been to image the boundaries separating crustal units in the mountains.

10.4 BASIC ACQUISITION STRATEGY

If an unbiased image of sub-horizontal to moderately dipping (up to 45°) reflectors in 3-D is the goal of a seismic survey then it is necessary to sample the subsurface in equal sampling intervals both in the E-W and N-S direction (or any rotated coordinate frame). The simplest way to accomplish this at relatively low cost is to make the shot line perpendicular to the geophone line. Figure 10-1 shows two shotpoints and the corresponding CDP subsurface coverage when fired into the geophone line. By firing a shot line perpendicular to the geophone line at the same spacing as the geophones then a rectangular area is covered where horizontal reflectors will be sampled with equal frequency in two orthogonal directions (Figure 10-2). If a second geophone line is introduced (Figure 10-3) then the two rectangular areas will overlap to a certain extent and the fold will be increased to two over this area. If five shot lines are fired and recorded into five geophone lines (Figure 10-4) then it is possible to increase the fold up towards 25 in the central portion of the survey. A fold of ten is considered highly desirable since then it is possible to use multichannel filtering to eliminate unwanted wave trains and to provide stability in static correction programs.

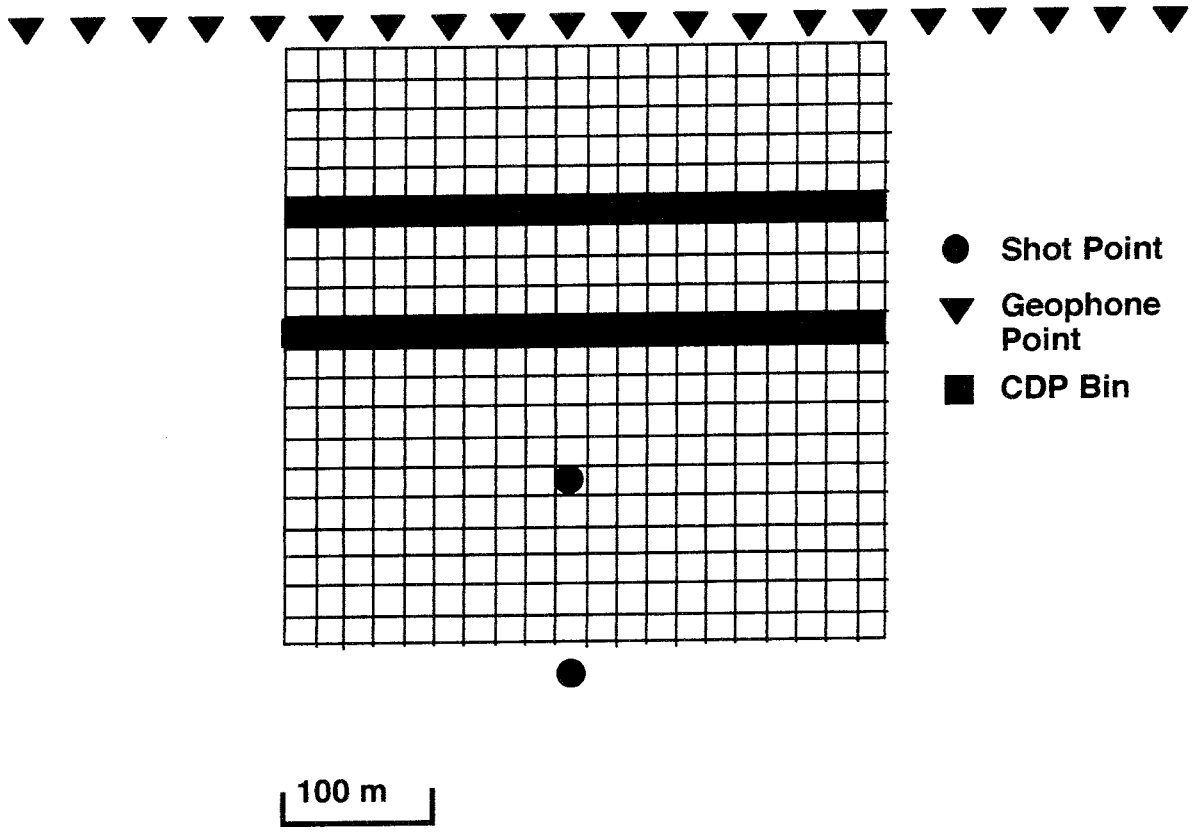

Figure 10-1 Two shot points, geophone line and corresponding common midpoints. The light squares indicate that no traces have been binned to that area while the dark squares indicate that a trace has been binned to that area.

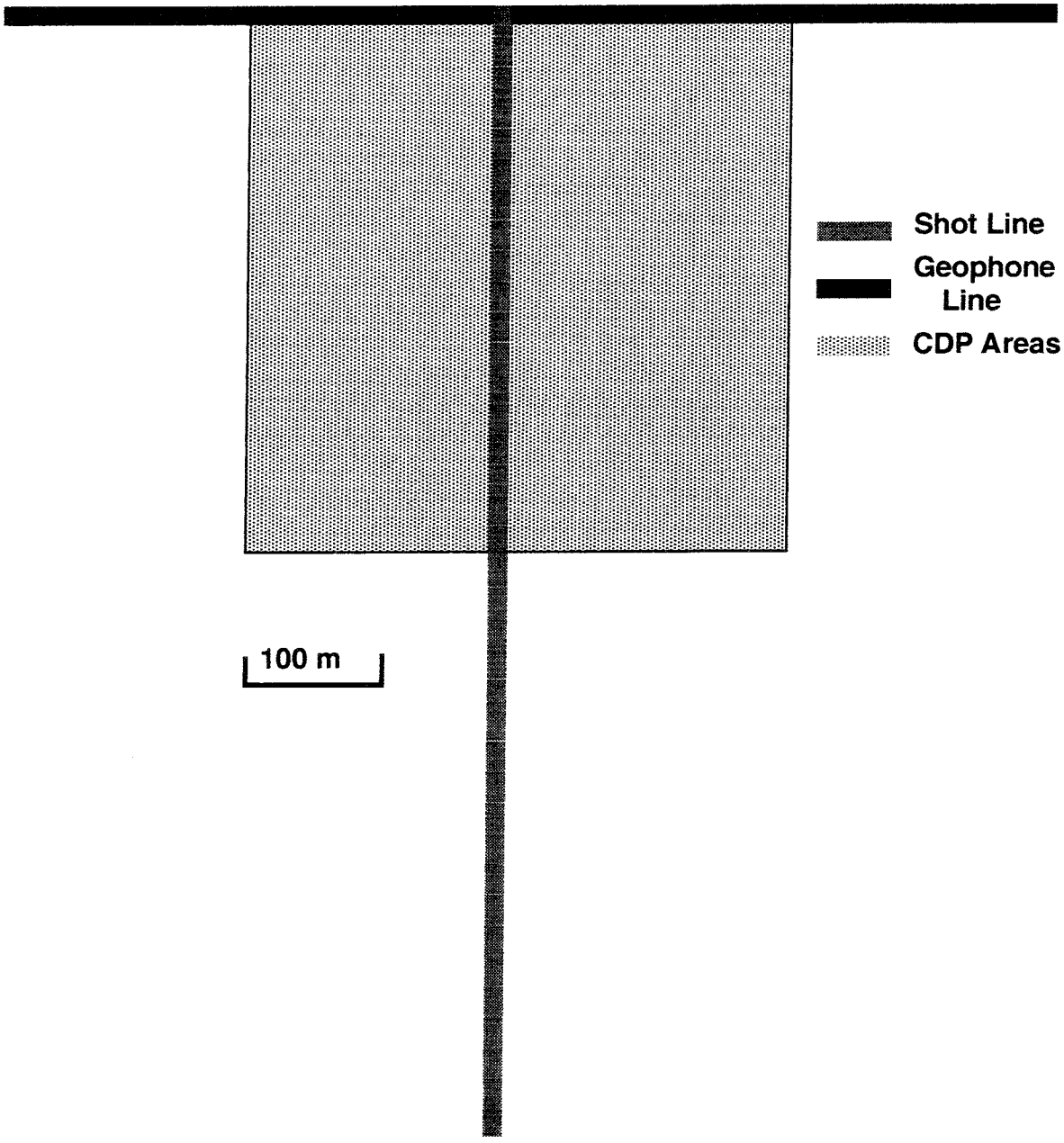

Figure 10-2 Total CDP area that is covered by one shot line and one geophone line. The shaded area comprises a set of darkened squares as shown in Figure 10-1.

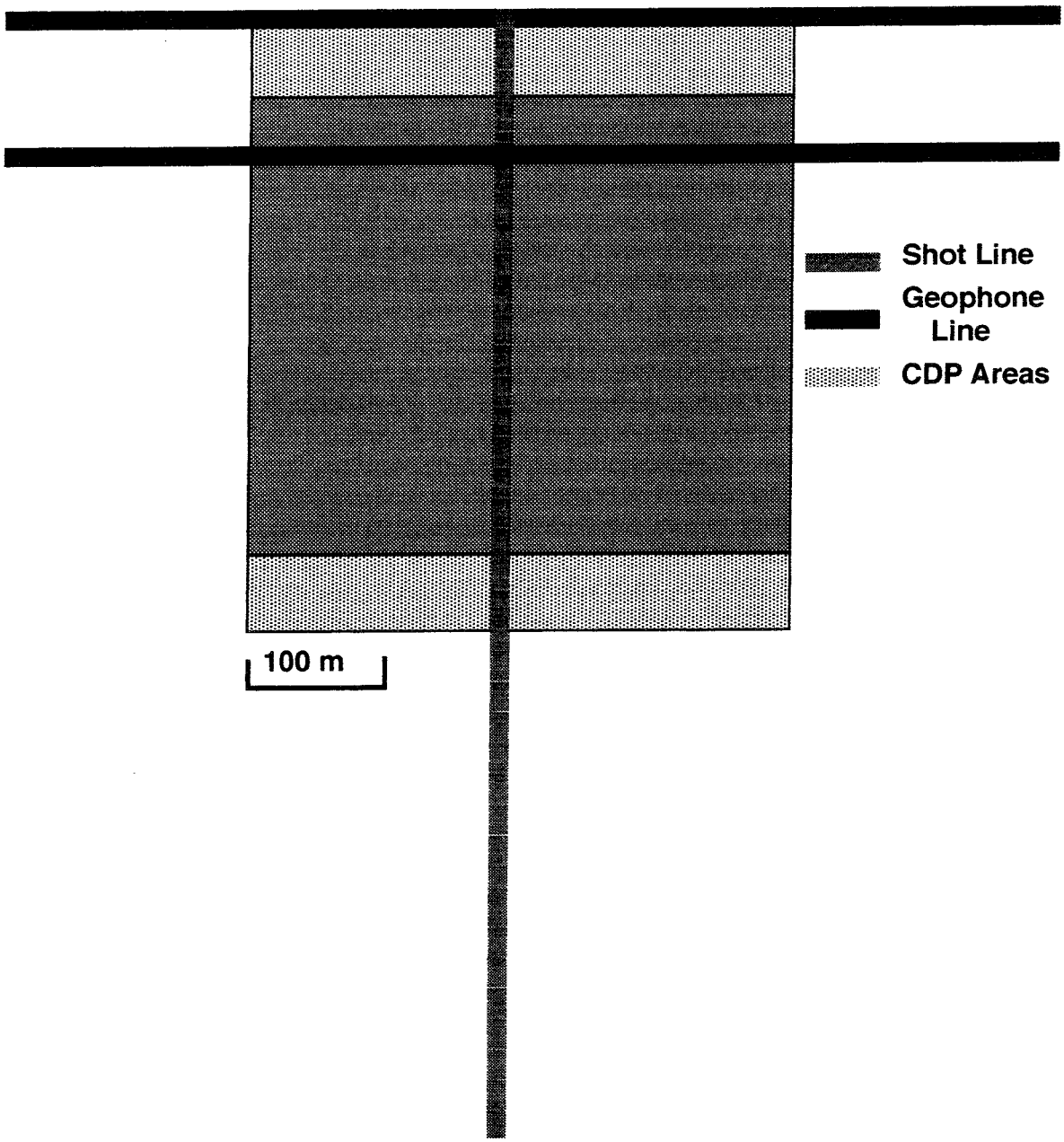

Figure 10-3 As Figure 10-2, but a second geophone line has been added resulting in increased coverage where the two areas overlap.

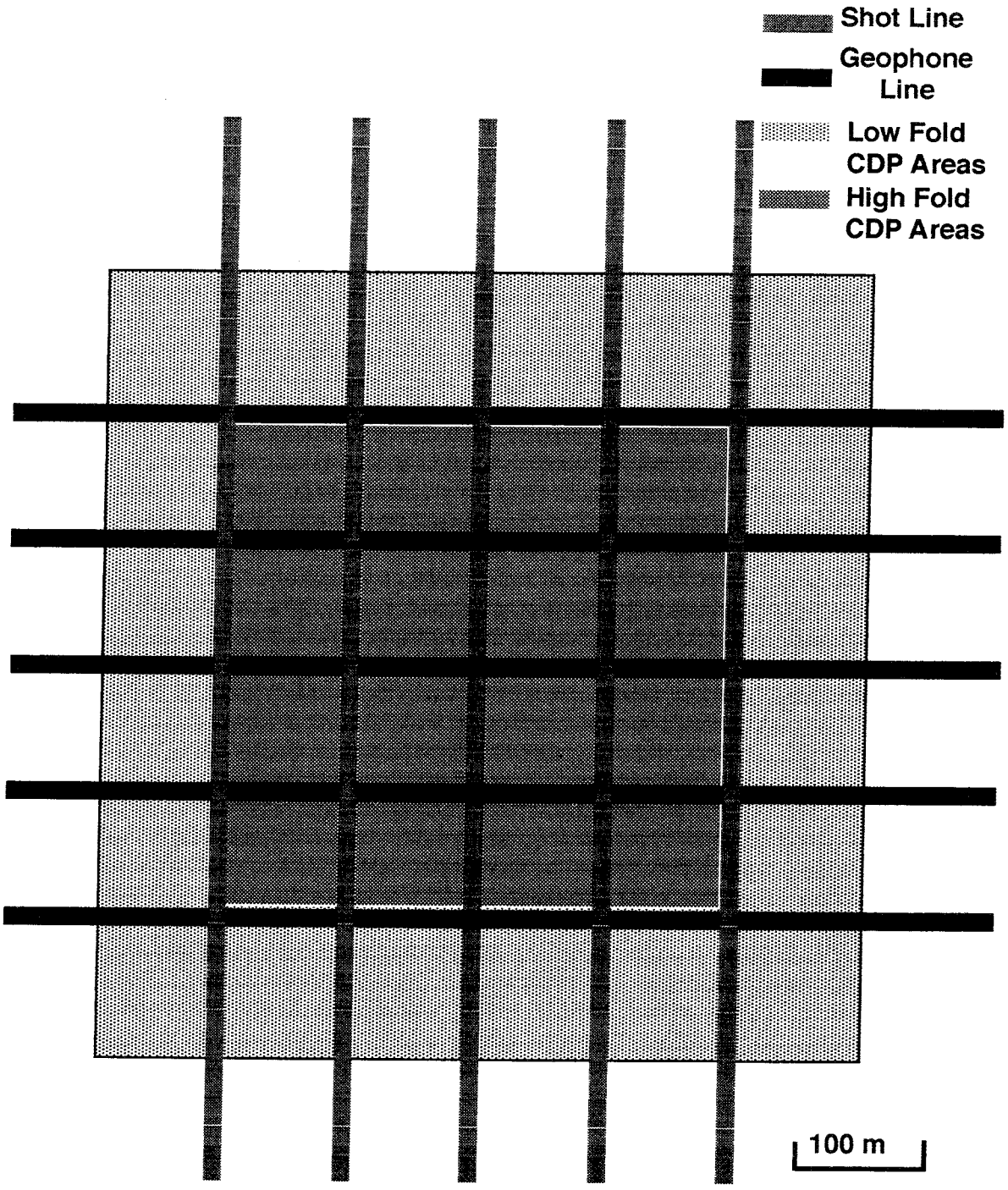

Figure 10-4 As Figure 10-3, but now there are 5 shot lines and 5 geophone lines. It data are recorded from each shot on all lines then the coverage will be as high as 25 in the central portions of the area under investigation.

10.5 POTENTIAL EXAMPLE FOR AN SKB STUDY SITE

10.5.1 Acquisition parameters

A realistic 3-D survey may consist of a 500x500 m square area where it is desired to acquire higher fold data. Five geophone lines spaced at 120 m with 50 geophones spaced at 20 m and five shot lines spaced at 120 m with 50 shotpoints spaced at 20 m is one possible field setup. This geometry would provide a 500x500 m square with a minimum of nine fold coverage using 10x10 m CDP bins. If 5x5 m CDP bins are desired (the horizontal resolution in Finnsjön) with the same coverage then the shot point and geophone point spacing must be decreased to 10 m resulting in twice as many shots having to be fired and twice as many geophones having to be deployed. For 10x10 m bins a total of 250 shotpoints need to be fired into 250 geophone points. For comparison, about 150 shots were fired into about 200 geophone points (with 60 active at any one time) at Finnsjön.

10.5.2 Time and cost considerations

Experience from Australia, Sweden, and Russia shows that it is possible to fire 50-100 shots in a day if the spread is stationary and loading of shotholes is done efficiently. With these production rates, the limiting factor in how long a survey will take will be the number of geophones which can be deployed at one time.

If only 50 geophone stations are available then each shot-line must be recorded 5 different times into five different geophone lines. This implies that data acquisition will take 25 days since it is unreasonable to expect to set up a geophone line and shoot 50 shots twice in one day. In addition one must be sure that the shotholes can be reused 5 times, once for each geophone line. Alternatively, 5 holes need to be drilled at each shotpoint, not an insignificant cost.

If 250 geophones can be deployed then the actual data collection should not take more than 3 days since no moves need to be made and the shotholes need only to be used once. An added advantage to this strategy is that shot variability will be less since shotholes do not need to be reused. Assuming that 250 geophones can be deployed then the basic cost for acquisition excluding the source can be kept nearly as low as for a 2-D survey. The main added cost be will be the additional shot lines.

10.6 BASIC PROCESSING STRATEGY

The quantity of data collected for the outlined survey would be on the order of 2000 samples per trace x 250 geophones x 250 shots or about 0.5 Gbyte. This quantity is fairly high, but easily manageable on a powerful work station. The data may be initially processed as a series of 2-D lines using 2-D packages. However, the acquisition geometry outlined above will allow full 3-D processing and interpretation to be applied to the data. Commercial packages are now available to process 3-D data. There are also packages which can be used for interpretation of 3-D data. The latter may be a more important consideration since visualization of the data set will become important as one goes from 2-D to 3-D.

11 PROPOSED APPLICATION OF SEISMIC REFLECTION SURVEYS AT SKB STUDY SITES

11.1 LIMITED 3-D SURVEY

The primary use of seismic reflection surveys are in the initial investigations of a potential repository site before any deep boreholes are drilled. The dimensions of the area from which information is required in the early stage of a site investigation are fairly large. It can be anticipated that the area of interest encompasses several square kilometers. To perform a full 3-D survey over this region would be prohibitively costly. A possible strategy to obtain limited 3-D information about the subsurface in such an area would be to survey two orthogonal profiles with a length of say 4 km. This would provide two crossing 2-D sections of geologic features. It is possible to obtain information on the dip and strike of reflectors by placing geophones along lines perpendicularly to the main survey line at regular intervals. These cross-lines can be relatively short (e.g. 230 m) and signals can be recorded as shots are fired along the main line. The separation between the cross-lines could tentatively be set to 500 m. The proposed configuration is illustrated in Figure 11-1.

Valuable additional information on anisotropy and velocity structure can could be obtained at negligible additional cost by putting 3-component geophones at three fixed locations along each main survey line. These geophones would record the signals generated by all shots along the line.

The addition of these cross-lines is expected to result in a marginal cost increase for data acquisition as shown in Section 11.2. It is considered sufficient to place the geophones for the cross-lines on the ground surface. Hence, no additional boreholes will be required. Integration of data from the cross-lines with data from the main line is expected to require additional processing which will increase processing costs. However, the proposed survey layout will provide information on dip and strike of reflectors along the main survey lines which should facilitate construction of a 3-D structural model of the site at a very early stage of the investigation. Given the moderate increase in cost, the availability of 3-D information should well motivate the effort.

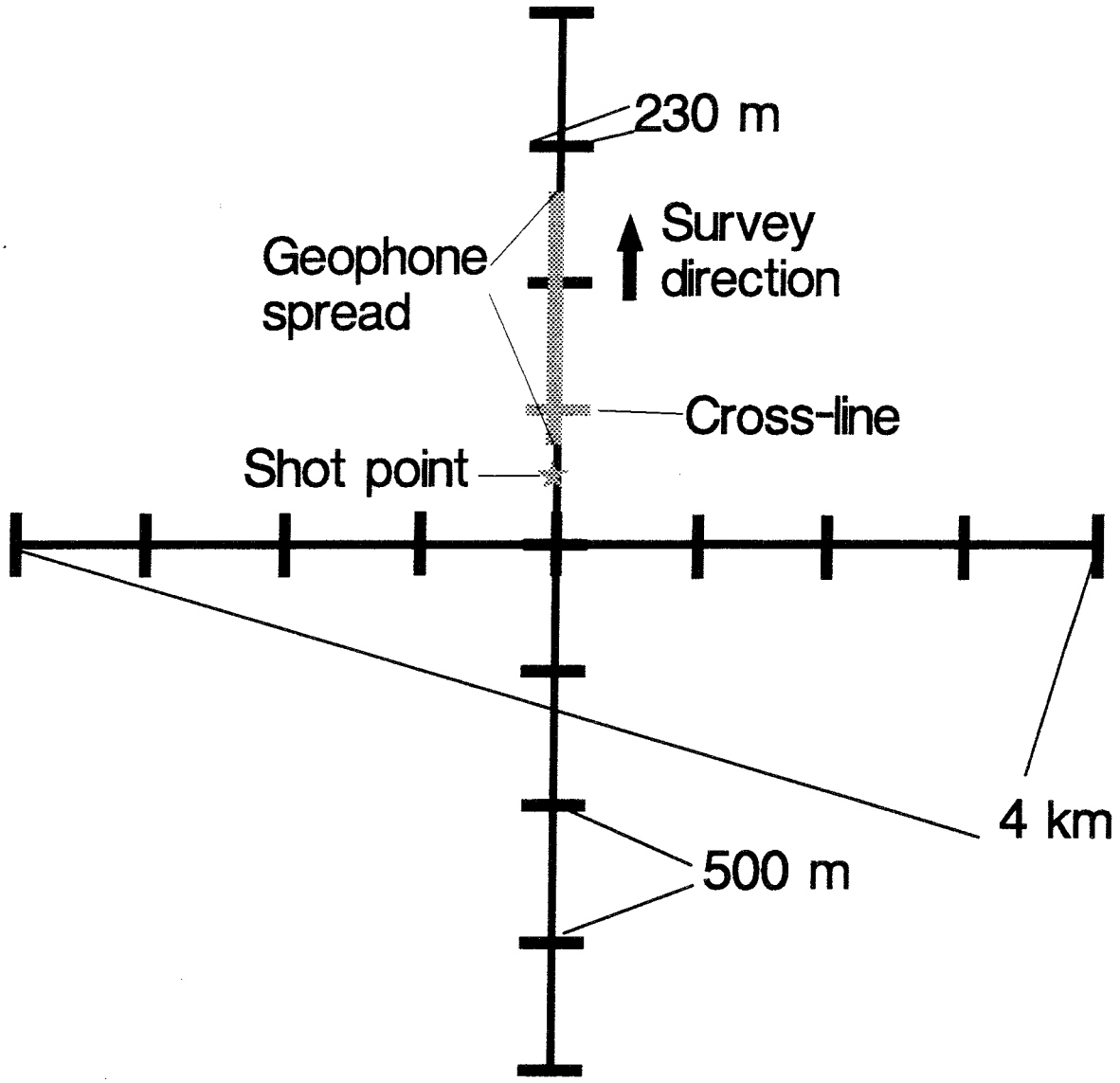

Figure 11-1 Proposed layout of survey lines for a seismic reflection survey at a potential deep repository site. Short cross-lines are included to provide 3-D information.

11.2 COST CONSIDERATIONS

The main cost items of a seismic reflection survey are identified as

- drilling
- data acquisition
- processing
- interpretation

The theoretical analysis and the experience from Finnsjön indicate that drilling is necessary if explosives sources are to be used. The drilling of shot holes is a comparatively costly and time consuming item in a seismic survey.

Experience from a test at Olkiluoto with a light drilling rig showed that the drill rig was suitable for testing but too slow for routine operations. For outcrops and shallow overburden drilling one hole took 30 - 40 minutes. Drilling through 10 m thick moraine and installing casing is much more time consuming.

With a heavier rig the drilling time can be reduced to 15-20 minutes but moving the rig to the next position will last another 15-20 minutes.

A feasibility/cost analysis for drilling has been done for two "typical cases" and a "worst case" under the following assumptions:

Case A: Conditions similar to Finnsjön, i.e. 40% outcrop, 30% overburden less than 1 m thick, 20% overburden with thickness between 1 m and 4 m and 10% deep troughs where the overburden can be up to 10 m.

Case B: Conditions similar to Klipperås, i.e. no outcrops, average overburden thickness 3 m - 4 m with an estimated 20% overburden thicker than 5 m and occasional troughs deeper than 10 m. A small part of the profile can be covered with water.

Case C: Area covered with approximately 10 m of moraine where about 30% consists of wetlands and peat bogs.

The cost calculations are based on drilling of shot and/or geophone holes to an average depth of 6 m below the ground surface. Under conditions described in case A, an average production rate of 10 holes per 8 hour shift is expected. This estimate includes time and cost for installing a plastic casing in the holes to protect them until they are used for the seismic survey. The average cost per hole is estimated to SEK 750.

For a 4 km long profile with a shot and geophone spacing of 10 m the total drilling cost for the three cases is estimated to:

Case A: Drilling time without measuring: 8 weeks
Estimated drilling costs (driller + rig) SEK 300 000.

Case B: Drilling time without measuring: 10 weeks
Estimated drilling costs (driller + rig) SEK 360 000.

Case C: Drilling time without measuring: 15 weeks
Estimated drilling costs (driller + rig) SEK 450 000.
(This estimate is based on the assumption that drilling is made during winter time when access to drilling on peat bogs should be reasonably simple. Surveys during summer time could be significantly more costly.)

It can be observed that the drilling cost is not very sensitive to the overburden conditions.

A 3-D survey as outlined in Section 10.5 would involve drilling of 250 shot and 250 geophone holes. Under the assumptions described in case A above, we estimate a production rate of 10 boreholes per working day. This would imply that 50 working days or 10 weeks were required to drill the 500 holes. The total cost for this is estimated to approximately SEK 400 000.

The next major cost item is data acquisition for which estimated costs have been tabulated in Table 11-1. Costs have been estimated for 1) a 4 km long profile with 10 m shot and geophone spacing, 2) a 4 km long profile with some short cross-lines (as described in Section 11.1) and 3) a 3-D survey as described in Section 10.5. The cost estimate is based on assumed commercial rates. The costs for an actual survey may of course differ considerably.

The estimated processing costs for the three cases are also listed in Table 11-1. These estimates are rough and indicate order of magnitude costs for processing and basic reporting of results. Within certain limits, processing costs are roughly proportional to the number of traces recorded.

The last cost item for a seismic survey is interpretation of results. We have not found it useful to estimate costs for this item as they may vary widely depending on geologic conditions, other data available, seismic data quality, as well as objective and scope of the interpretive effort.

Table 11-1 Estimated costs for data acquisition and processing for three different survey configurations.

Survey type	4 km profile	4 km with limited 3-D info	3-D survey 500x500 m
Data acquisition			
Duration	2 weeks	2 weeks	1 week
Surveying	60 kSEK	60 kSEK	45 kSEK
Equipment rental	100 kSEK	130 kSEK	250 kSEK
Geophones & explosives	80 kSEK	80 kSEK	140 kSEK
Mantime	160 kSEK	200 kSEK	80 kSEK
Transportation etc	50 kSEK	50 kSEK	50 kSEK
Total	450 kSEK	520 kSEK	565 kSEK
Processing	225 kSEK	300 kSEK	500 kSEK

12 CONCLUSIONS

12.1 RECOMMENDATIONS FOR SEISMIC SURVEYS IN CRYSTALLINE ROCK ENVIRONMENTS

The reprocessing of the Finnsjön data show that reflection seismics is a viable technique for mapping fracture zones in crystalline rock. The data acquisition procedures used at the Finnsjön survey were basically sound and could, with minor modifications, be applied at other sites. The results indicate that both sources and receivers in future surveys should be placed in boreholes a few meters below the ground surface.

Based on the analysis of the Finnsjön data and the theoretical analysis presented above the following conclusions can be drawn on how a seismic reflection survey is best performed in a crystalline rock environment.

Spread (shooting geometry)

End-on spread, possibly with reverse shooting, is the favored alternative. An asymmetric spread could also be considered (e.g. 30/70 %). The spacing of geophone and shot-points should be 5-10 m. An end-on spread has the advantage that the same borehole can be used for placing both geophones and shots below the ground surface. An asymmetric spread would require drilling of additional holes for the geophones, hence increasing the costs.

Source

The recommended source is dynamite charges detonated in shot-holes. Placing the source on the surface is considerably cheaper than drilling holes to the bedrock. This study shows that deeper shots give stronger signals arguing against the use of a surface source. In addition, the use of sources on the surface has so far given poor results.

Shots fired in bedrock below the water table give significantly higher frequency data than shots fired above bedrock. This observation favors the use of a downhole source. The best data quality will be obtained if the source is placed in the bedrock. However, sufficient data quality is obtained if the source is placed 3-6 m below the ground surface. Hence, in places with thick overburden it will not be necessary to drill to reach bedrock.

The most economical way to produce seismic signals is the use of explosives.

So far, the most efficient routine seems to be to drill the boreholes in advance. This requires that plastic casing is introduced in most boreholes to keep them open. Some general indications for the depth of the holes are:

a) In overburden thicker than 5 m: 2-3 m below the water table, at least half the depth to the bedrock.

b) In shallow overburden and outcrops: 2-3 m in the rock.

To obtain information from depths greater than 1.5 km a large shot (1-2 kg of dynamite) could be fired every 5th shot-point.

Geophones (receivers)

Geophones can be placed on the ground or in short boreholes reaching into the soil or into the bedrock. Placing geophones on the surface is of course cheaper than putting them in a borehole. If geophones are put on the surface, geophone groups can be used. However, the use of geophone groups can give problems with statics (surface layer variability). In general, vertical component geophones are considered sufficient even though 2- or 3-component geophones could provide additional information. However, valuable additional data could be acquired at negligible additional cost by putting 3-component geophones at, for example, three fixed locations along a survey line. It should be noted that 3-component geophones are only useful if placed in boreholes.

This study indicates that the highest data quality will be obtained with both sources and receivers placed in boreholes. Hence, it is recommended that vertical geophones placed in boreholes are used as receivers. If an end-on spread is used it is possible to use the same hole for both sources and receivers.

Data recording

The dynamic range of the recording system should be at least 16 bits. The recommended number of channels for a 10 m geophone spacing is 96. For this case, the minimum number of channels is 48. If a 5 m geophone spacing is used the number of channels should be greater than 96.

Survey line layout

Some form of three dimensional coverage is required. The cheapest way to obtain this is to use a single survey line with short cross-lines of geophones. For an initial survey at a study site it is recommended that two orthogonal survey lines, each approximately 4 km long, are used. These lines should include short cross-lines. A better coverage could be obtained by using a few parallel lines and one or two crossing lines.

It is possible to collect 3-D data over a limited area (500 m x 500 m) at a reasonable cost if a large amount of geophones can be deployed. A total of 250 shotpoints and geophone points will give good coverage.

Data processing

The results of the reprocessing of the Finnsjön data presented in this report have shown that adequate processing algorithms exist for identifying fracture zones in crystalline rock based on reflection seismic data. Intelligent application of the toolbox of processing algorithms available in the literature should suffice if data of adequate quality have been collected. This work has shown that pre-stack migration is not required to produce satisfactory results.

12.2 A SUGGESTED STRATEGY FOR SITE INVESTIGATIONS

The seismic site investigations should be seen as parts of an iterative process, where each stage should provide the grounds for planning the next one, while the knowledge of the site gains in resolution and complexity.

The investigations should start by surveying two perpendicular lines, crossing approximately in the center of the site. The length of each line is tentatively set to 4 km. Regional geology and airborne geophysics will provide the necessary information for positioning the lines in the best way possible for acquiring information on the major site structures.

A preliminary interpretation will be done with stacking and migration velocities estimated from the data itself, by velocity analyses. It is expected that the major structures of the site will be detected and a preliminary three dimensional model will be built. Most probably, at this stage, the structures will be represented as planes.

This model can then be used for selecting a smaller area, to be investigated by a 3-D layout. It is preferable that the 3-D survey is performed early in the investigation sequence, even if the full interpretation will not be possible until merging the results with data from borehole surveys. The processing of

the 3-D data will add confidence to the preliminary model and help in choosing the location for the first borehole. A 3-D survey is useful even if it is performed after the first borehole has been drilled at a site as the information obtained is likely to reduce the total number of boreholes needed to adequately characterize the site. The cost of a 3-D survey is of the same magnitude as the cost for a borehole with subsequent investigations.

Once a borehole is drilled, information on the site structures and properties of the rock mass can be obtained directly. Among the borehole investigations, VSP is of particular importance. First of all, it provides a velocity calibration of the seismic surface data which will increase accuracy and reliability in depth determinations along the seismic surface profiles. Second, correlation of VSP data with seismic surface data and information from the boreholes will provide knowledge on the geologic character of the seismic reflectors. Finally, the VSP data will provide information on the location and orientation of reflectors in a volume with a radius of several hundred meters around the borehole which is essential for building a structural model of the site. Each subsequent VSP survey in new boreholes at the site will add information on the location and orientation of structural features across the site. Eventually reliable data will exist for the entire site.

The sequence consisting of: 1) updating the 3-D model by reprocessing the seismic surface data, 2) drilling, and 3) VSP measurements could be repeated a number of times during the investigation of the repository site. It is reasonable to assume that this sequence will achieve an equally detailed description of the site structures, with less boreholes.

ACKNOWLEDGEMENT

Karl-Erik Almén, SKB, is thanked for his encouragement and support during the course of the project.

REFERENCES

Ahlbom, K., Tirén, S., 1991. Overview of geologic and geohydrologic conditions at the Finnsjön site and its surroundings. TR 91-08, SKB, Stockholm, Sweden.

Ahlbom, K., Andersson, J.-E., Andersson, P., Ittner, T., Ljunggren, C., Tirén, S., 1992. Finnsjön study site - Scope of activities and main results. TR 92-33, SKB, Stockholm, Sweden.

Blümling, P., Cosma, C., Korn, M., Gelbke, C., Cassel, B., 1990. Geophysical methods for the detection of discontinuities ahead of a tunnel face. TR 90-07, NAGRA, Wettingen, Switzerland.

Båth, M., 1985, Superficial granitic layering in shield areas. Tectonophysics, 118, 75-83.

Bäckblom, G., 1989. Guidelines for use of nomenclature on fracture zones and other topics. TPM 25-89-007, SKB, Stockholm, Sweden.

Cosma, C., Heikkinen, P., Pekonen, S., 1991. Improvement of high resolution seismics: Part I, Development of processing methods for VSP surveys; Part II, Piezoelectric signal transmitter for seismic measurements. Stripa Project Tr 91-13, SKB, Stockholm, Sweden.

Dahl-Jensen, T., Lindgren, J., 1987. Shallow reflection seismic investigation of fracture zones in the Finnsjö area, method evaluation. SKB TR 87-13, SKB, Stockholm, Sweden.

Ekman, L., Andersson, J.-E., andersson, P., Carlsten, S., Eriksson, C.-O., Gustafsson, E., Hansson, K., Stenberg, L., 1988. Documentation of borehole BFi02 within the Brändan area, Finnsjön study site. AR 89-21, SKB, Stockholm, Sweden.

Green, A. G., Mair, J. A., 1983. Subhorizontal fractures in a granitic pluton: Their detection and implications for radioactive waste disposal. Geophysics 48, 1428-1449.

Heikkinen, P., Cosma, C., Olsson, O., 1992. Processing of surface reflection data from Äspö. PR 25-93-04, SKB, Stockholm, Sweden.

Juhlin, C., 1990a. Evaluation of reprocessed seismic refraction data from Äspö. SKB PR 25-90-02, SKB, Stockholm, Sweden.

Juhlin, C., 1990b. Interpretation of the reflections in the Siljan Ring area based on results from the Gravberg-1 borehole. Tectonophysics, 173, 345-360.

Juhlin, C., 1990c. Seismic attenuation, shear wave anisotropy and some aspects of fracturing in the crystalline rock of the Siljan Ring area, central Sweden. PhD., University of Uppsala, Sweden.

Juhlin, C., Lindgren, J, Collini, B., 1991. Interpretation of seismic reflection and borehole data from Precambrian rock in the Dala Sandstone area, Central Sweden. First Break, 9, 24-36.

Kind, R., Odom, R. I., 1983. Improvements to layer matrix methods. J. Geophys., 53, 127-130.

Lambourne, A. N., Evans, B. J., & Hatherly, P. J., 1989, The application of the 3D seismic surveying technique to coal seam imaging - case histories from the Arckaringa and Sydney Basins. Exploration Geophysics, 20,137-141.

Loewenthal D., Wang C.J., Johnson O.G., and Juhlin C., 1991, High order finite difference modeling and reverse time migration, Explor. Geophys., 22, 533-546.

Milkerit, B., Reed, L., Cinq-Mars, A., 1992a. High frequency reflection seismic profiling at Les Mines Selaine, Quebec. *in* Current Research, Part E; Geological Survey of Canada, Paper 92-1E, 217-224.

Milkerit, B., Green, A., 1992b. Deep geometry of the Sudbury structure from seismic reflection profiling. Geology, 20, 807-811.

Milkerit, B., Adam, E., Barnes, A., Beaudry, C., Pinealut, R., Cinq-Mars, A., 1992c. An application of reflection seismology to mineral exploration in the Matagami area, Abitibi Belt, Quebec. *in* Current Research, Part E; Geological Survey of Canada, Paper 92-1C, 13-18.

Olsson, O., 1992. Reflections seismic profiling with a vibrator source on the Äspö Island. SKB PR 25-92-10, SKB, Stockholm, Sweden.

Plough, C., Klitten, K., 1989. Shallow reflection seismic profiles from Äspö, Sweden. SKB PR 25-89-02, SKB, Stockholm, Sweden.

SKB, 1992. RD&D Programme 92. SKB, Stockholm, Sweden.

Spencer, C., Thurlow, G., Wright, J., White, D., Carroll, P., Milkerit, B., Reed, L., A vibroseis reflection seismic survey at the Buchans Mine in central Newfoundland. Geophysics, 58, 154-166.

Stenberg, L., 1987. Detailed investigations of fracture zones in the Brändan area, Finnsjön study site. AR 87-27, SKB, Stockholm, Sweden.

Stenberg, L., Triumph, C.-A., 1990. Försök med reflektionsseismik i Slöinge, Halland. BeFo 203:1/90, SevBefo, Stockholm, Sweden.

Stewart, S. C., Evans, B. J., 1989, A case history of a cost effective 3D seismic survey over the Perth Basin, Western Australia. Exploration Geophysics. 20, 229-236.

Taner, M. T., & Koehler, F., 1981, Surface consistent corrections. Geophysics, 46(1), 1 7-22.

Urosevic, M., Evans, B. J., & Hatherly, P. J., 1992, Application of 3-D seismic methods to detection of subtle faults in coal seams. In 62nd Annual Society of Exploration Geophysicists Meeting Expanded Abstracts, . New Orleans: SEG.

Young, R. A., Stewart, S. C., Seman, M., & Evans, B. J., 1990, Fault plane reflection processing and 3D display: Moora, Western Australia. Tectonophysics, 173, 107-118.

APPENDICES

A STATIC CORRECTIONS USED BY UPPSALA UNIVERSITY

Below are plots of the geophone and shot point staic corrections used after the first pass of refraction statics. The remaining two passes resulted in only marginal differences. Time scale runs from -5 to +5 ms. Stations run from 0 to 256.

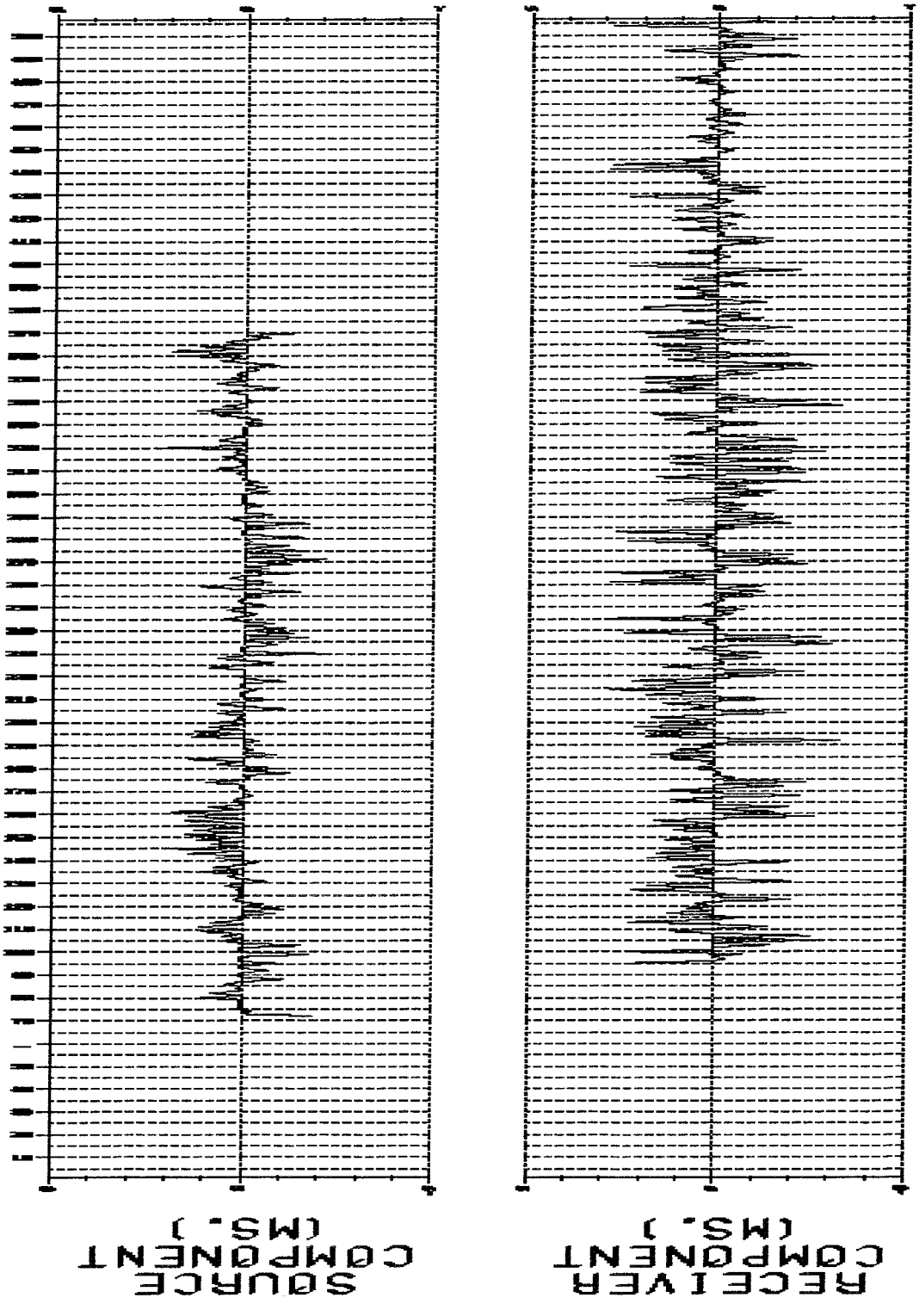

B VELOCITY FIELD USED BY UPPSALA UNIVERSITY

Below is a listing of the time velocity pairs used for stacking along the seismic line. The format is Shotpoint location, CDP location, number of pairs to follow, time, and velocity used.

```
/VELOCITY
 VEL  10 105 6 0,5000  60,5200  80,5300 160,5400 200,5700 400,7000
 VEL  30 145 4 0,5000  80,5400 220,5700 400,7000
 VEL  55 160 5 0,5000 110,5300 200,5700 300,5700 400,7000
 VEL  57 170 5 0,5000 110,5200 200,5700 300,5700 400,7000
 VEL  60 180 4 0,5000 110,5300 200,5700 400,7000
 VEL  70 200 4 0,5000 120,5300 200,5700 400,7000
 VEL  75 210 4 0,5100 100,5400 200,6000 400,7000
VEL 100 285 4 0,5200 160,5400 200,6500 500,7000
VEL 115 315 5 0,5300  70,5300 130,5700 200,6500 400,7000
VEL 121 330 4 0,5300 160,5400 200,6000 400,7000
VEL 138 360 5 0,5500 100,5500 160,5700 200,6000 400,7000
VEL 152 400 4 0,5500 120,6100 200,6500 400,7000
```

C SHOT-HOLE DATA

	A	B	C	D	E	F	G	H	I
1	File	Station	Peat	Till	Bedrock	Total dep	Tamped with		charge
2	Number	Number							depth
3									
4	1	36		0	2	2	water	2	2
5	2	37		0	3	3	water	2	3
6	3	40		0	3	3	water	2	3
7	4	41		0	2	2	water	2	2
8	6	40		0	3	3	water	2	2.5
9	7	42		0	2	2	water	2	2
10	8	43		0	2	2	water	2	2
11	9	44		0	2	2	water	2	2
12	10	45		0	2	2	water	2	2
13	11	46		2.9	0.2	3.1	water	2	2.5
14	12	47		3.1	0.2	3.3	water	2	3.3
15	14	49		2.3	0.7	3	water	2	3
16	16	51	0.4	0.9	0.7	2	water	2	2
17	17	52	0.4	0.5	1.1	2	water	2	2
18	18	53	0.3	1	0.7	2	water	2	2
19	19	54	0.2	0.2	2	2.4	water	2	2
20	20	55	0	0	2	2	water	2	2
21	21	56	0	0	3	3	water	2	3
22	23	58	0	0	2	2	water	2	3
23	24	59	0	0	2	2	water	2	2
24	25	60	0	0	2	2	water	2	2
25	26	61	0	0.3	1.65	1.95	water	2	1.5
26	27	63	0	0	3	3	water	2	3
27	29	64	0	0	2.05	2.05	water	2	2
28	30	65	0.4	1.3	0.3	2	water	2	2
29	31	66	0	0	2	2	water	2	2
30	32	67	0	0	2	2	water	2	2
31	33	68	0	0	2	2	water	2	2
32	34	69	0	0.2	1.8	2	water	2	1.5
33	35	70	0	0	2	2	water	2	2
34	36	71	0	0	2	2	water	2	1
35	37	72	0	0	2	2	water	2	1
36	38	73	0	0	2	2	water	2	2
37	39	74	0	0	2	2	water	2	1.5
38	40	75	0	0	2	2	sand/wat	1	2
39	41	76	0	0	2	2	water	2	1.5
40	42	77	0	0	2.05	2.05	water	2	1.5
41	43	78	0	0	2	2	water	2	2
42	44	79	0.7	0.55	0.75	2	water	2	2
43	45	80	0.2	0.5	2	2.7	water	2	2.5
44	46	81	0	0	2	2	water	2	1.5
45	47	82	0	0	2	2	water	2	1.5
46	48	83	0	1.2	0.8	2	water	2	1.5
47	49	84	0	0	2	2	water	2	1.5
48	50	85	0	0	2	2	water	2	2

	A	B	C	D	E	F	G	H	I
49	52	86	0	0	2	2	water	2	1.5
50	53	88	2	0.2	0.2	2.4	water	2	2
51	54	89	0	0.4	2	2.4	water	2	1.8
52	55	90	0.1	0.4	2	2.5	water	2	1.4
53	56	91	0	0	2	2	water	2	2
54	57	92	0	0	2	2	water	2	2
55	58	93	0.3	0	2	2.3	water	2	1.5
56	59	94	0.6	0.4	1.05	2.05	water	2	1
57	60	95	0.4	0.6	1	2	water	2	1.5
58	61	96	0.1	0	2	2.1	water	2	2
59	62	97	0	0	2	2	water	2	2
60	63	98	0.2	0	1.8	2	water	2	2
61	64	99	0	0	2	2	water	2	1.5
62	65	100	0.4	0	2	2.4	water	2	0.7
63	66	101	0.2	0.2	2	2.4	water	2	1
64	67	102	0	0	2	2	water	2	1.5
65	68	103	0	0	2	2	water	2	2
66	69	104	0.5	0.5	1	2	water	2	1.5
67	70	104	0.5	0.5	1	2	sand	0	2
68	72	107	0	0	2.05	2.05	sand	0	2
69	73	108	0	0	2	2	sand	0	2
70	74	109	0	0	2	2	sand	0	2
71	75	110	0.9	1.45	0.2	2.55	sand	0	2
72	76	111	0.4	0	2	2.4	sand	0	1.5
73	77	112	0.9	0.5	0.6	2	water	2	1.5
74	78	113	0.8	0.1	1.1	2	water	2	1.5
75	79	114	0.8	0.9	1.3	3	water	2	1.5
76	80	116	0.1	0.35	2	2.45	water	2	0.5
77	81	117	0.5	0.4	1.1	2	water	2	2
78	83	118	0.9	0.2	0.9	2	water	2	2
79	84	119	0.5	0.5	1	2	water	2	2
80	85	120	0	0	2	2	water	2	1.5
81	86	121	0	0	2	2	sand	0	2
82	87	122	0	0	2	2	sand	0	2
83	88	123	0.1	0.85	1.1	2.05	water	2	2
84	89	124	0	1.8	0.2	2	water	2	1.5
85	90	125	0.5	1.2	0.3	2	water	2	2
86	91	126	0.5	1.8	0.2	2.5	water	2	2.5
87	92	127	0.5	0.5	1.2	2.2	water	2	2
88	93	128	0	1	1.15	2.15	water	2	1
89	94	129	0	0.8	1.2	2	sand	0	2
90	95	130	0	0	2	2	sand	0	1.5
91	96	131	0	0.7	2	2.7	sand	0	2.5
92	97	132	0	0.5	1.5	2	sand	0	2
93	98	133	0	1.2	0.8	2	sand	0	2
94	99	134	0	3	0.5	3.5	sand	0	2.5
95	100	135	0	2.3	0.2	2.5	sand	0	2.5
96	101	136	0.1	0.8	1.1	2	sand	0	2

	A	B	C	D	E	F	G	H	I
97	102	137	0	0.9	1.1	2	sand/wat	1	2
98	103	138	0	0.8	1.2	2	sand/wat	1	1.5
99	104	139	0.9	1.7	0.2	2.8	sand/wat	1	2.5
100	105	140	0.9	1.1	0.2	2.2	water	2	2
101	106	141	0	0	2	2	sand	0	2
102	107	142	0.5	0.4	1.1	2	sand/wat	1	2
103	108	143	0	2	0.2	2.2	sand/wat	1	1.5
104	109	144	0.5	0.5	1	2	sand/wat	1	2
105	110	145	0.3	0.5	1.2	2	sand/wat	1	1.5
106	111	146	0.9	0.5	0.6	2	sand/wat	1	2
107	112	147	0.9	1.8	0.15	2.85	sand/wat	1	2
108	114	150	0.6	0	1.4	2	sand	0	2
109	115	151	0.3	0.5	1.2	2	sand	0	2
110	116	152	0.35	0.5	1.25	2.1	sand	0	1.5
111	118	153	0.3	0.7	1	2	sand	0	2
112	119	154	0.3	0.4	1.3	2	sand	0	2
113	120	155	0.3	1.2	0.5	2	sand	0	1.5
114	122	158	0	0	2	2	water	2	2
115	123	157	0.3	2.2		2.5	sand	0	1.5
116	125	160	0.4	0.6	1	2	sand	0	2
117	126	161	0.4	0.45	1.15	2	sand	0	2
118	127	162	0	0.2	2	2.2	sand	0	2.2
119	128	163	0	0	2	2	sand	0	1
120	129	164	0.35	0.4	1.25	2	sand	0	2
121	130	159	0.4	0.4	1.2	2	water	2	1.8
122	131	165	0.3	0.4	1.3	2	sand	0	2
123	132	166	0	0.3	2	2.3	sand	0	2
124	133	167	0	0	2	2	sand	0	2
125	134	168	0.8	0	1.2	2	sand	0	2
126	135	169	1	0.6	0.4	2	water	2	2
127	136	170	1.2	0.8	0.2	2.2	water	2	2
128	137	171	0.9	1.5	0.2	2.6	sand	0	2.5
129	138	172	0	0	2	2	sand	0	2
130	139	173	0	0	2	2	sand	0	2
131	140	174	0	0	2	2	sand	0	2
132	141	175	0	0	2	2	sand	0	2
133	142	176	0.7	0.3	1	2	water	2	2
134	143	177	0	0	2	2	sand/wat	1	1.4
135	144	178	0.2	0.4	1.4	2	sand	0	2
136	145	179	0	0	2	2	sand	0	1.5
137	146	180	0	0	2	2	water	2	1.75
138	147	181	0	0	2	2	sand	0	1.5
139	148	182	0	0	2	2	sand	0	1.75
140	149	183	0	0	2	2	sand	0	1.5
141	150	184	0	0	2	2	sand	0	2
142	151	185	0	0	2	2	sand	0	2

List of SKB reports

Annual Reports

1977-78
TR 121
KBS Technical Reports 1 – 120
Summaries
Stockholm, May 1979

1979
TR 79-28
The KBS Annual Report 1979
KBS Technical Reports 79-01 – 79-27
Summaries
Stockholm, March 1980

1980
TR 80-26
The KBS Annual Report 1980
KBS Technical Reports 80-01 – 80-25
Summaries
Stockholm, March 1981

1981
TR 81-17
The KBS Annual Report 1981
KBS Technical Reports 81-01 – 81-16
Summaries
Stockholm, April 1982

1982
TR 82-28
The KBS Annual Report 1982
KBS Technical Reports 82-01 – 82-27
Summaries
Stockholm, July 1983

1983
TR 83-77
The KBS Annual Report 1983
KBS Technical Reports 83-01 – 83-76
Summaries
Stockholm, June 1984

1984
TR 85-01
Annual Research and Development Report 1984
Including Summaries of Technical Reports Issued during 1984. (Technical Reports 84-01 – 84-19)
Stockholm, June 1985

1985
TR 85-20
Annual Research and Development Report 1985
Including Summaries of Technical Reports Issued during 1985. (Technical Reports 85-01 – 85-19)
Stockholm, May 1986

1986
TR 86-31
SKB Annual Report 1986
Including Summaries of Technical Reports Issued during 1986
Stockholm, May 1987

1987
TR 87-33
SKB Annual Report 1987
Including Summaries of Technical Reports Issued during 1987
Stockholm, May 1988

1988
TR 88-32
SKB Annual Report 1988
Including Summaries of Technical Reports Issued during 1988
Stockholm, May 1989

1989
TR 89-40
SKB Annual Report 1989
Including Summaries of Technical Reports Issued during 1989
Stockholm, May 1990

1990
TR 90-46
SKB Annual Report 1990
Including Summaries of Technical Reports Issued during 1990
Stockholm, May 1991

1991
TR 91-64
SKB Annual Report 1991
Including Summaries of Technical Reports Issued during 1991
Stockholm, April 1992

1992
TR 92-46
SKB Annual Report 1992
Including Summaries of Technical Reports Issued during 1992
Stockholm, May 1993

Technical Reports
List of SKB Technical Reports 1994

TR 94-01
Anaerobic oxidation of carbon steel in granitic groundwaters: A review of the relevant literature
N Platts, D J Blackwood, C C Naish
AEA Technology, UK
February 1994

TR 94-02
Time evolution of dissolved oxygen and redox conditions in a HLW repository
Paul Wersin, Kastriot Spahiu, Jordi Bruno
MBT Technología Ambiental, Cerdanyola, Spain
February 1994